



# CAPWAP-Based Correlations for Estimating the Static Axial Capacity of Open-Ended Steel Pipe Piles in Alaska



Authors:

Stephen E. Dickenson, Ph.D., P.E.

New Albion Geotechnical, Inc.

December 2012

Prepared For:

Alaska Department of Transportation & Public Facilities

Research, Development, and Technology Transfer

2301 Peger Road

Fairbanks, AK 99709-5399

FHWA-AK-RD-12-07

<b>REPORT DOCUMENTATION PAGE</b>			Form approved OMB No.	
Public reporting for this collection of information is estimated to average 1 hour per response, including the time for reviewing instructions, searching existing data sources, gathering and maintaining the data needed, and completing and reviewing the collection of information. Send comments regarding this burden estimate or any other aspect of this collection of information, including suggestion for reducing this burden to Washington Headquarters Services, Directorate for Information Operations and Reports, 1215 Jefferson Davis Highway, Suite 1204, Arlington, VA 22202-4302, and to the Office of Management and Budget, Paperwork Reduction Project (0704-1833), Washington, DC 20503				
1. AGENCY USE ONLY (LEAVE BLANK)  FHWA-AK-RD-12-07	2. REPORT DATE  December 2012	3. REPORT TYPE AND DATES COVERED  FINAL REPORT 8/12/2009 – 12/26/2012		
4. TITLE AND SUBTITLE CAPWAP-Based Correlations for Estimating the Static Axial Capacity of Open-Ended Steel Pipe Piles in Alaska			5. FUNDING NUMBERS  AKSAS #60616/T2-08-01 Federal # HPR-4000(69)	
6. AUTHOR(S) Stephen E. Dickenson, Ph.D., P.E.				
7. PERFORMING ORGANIZATION NAME(S) AND ADDRESS(ES) New Albion Geotechnical, Inc. 1625 O'Farrell Street, Reno, NV 89503			8. PERFORMING ORGANIZATION REPORT NUMBER	
9. SPONSORING/MONITORING AGENCY NAME(S) AND ADDRESS(ES)  State of Alaska, Alaska Dept. of Transportation and Public Facilities Research, Development and Technology Transfer 2301 Peger Rd Fairbanks, AK 99709-5399			10. SPONSORING/MONITORING AGENCY REPORT NUMBER  FHWA-AK-RD-12-07	
11. SUPPLEMENTARY NOTES  Performed in cooperation with the U.S. Department of Transportation, Federal Highway Administration.				
12a. DISTRIBUTION / AVAILABILITY STATEMENT			12b. DISTRIBUTION CODE	
13. ABSTRACT (Maximum 200 words)  CAPWAP analyses of open-ended steel pipe piles at 32 bridge sites in Alaska have been compiled with geotechnical and construction information for 12- to 48-inch diameter piles embedded in predominantly cohesionless soils to maximum depths of 161-feet. This database includes 68 piles, 33 of which tested at End of Initial Driving and Beginning of Restrike demonstrating time-effects on pile resistance. The CAPWAP analyses were used to develop empirical relationships for unit shaft and toe resistances at BOR. The CAPWAP-based unit shaft resistance demonstrates a depth-dependent trend, with values 1 to 3 days after EOID that are considerably less than estimates made using common static analyses. The toe resistance was found to be highly variable and dependent on both the prevalence of gravel and cobbles at the toe and pile diameter.  Class A Prediction involving 29 piles driven into deltaic deposits demonstrated very good agreement with CAPWAP results for 1 to 6 day BOR. The proposed method provided much more reliable estimates of pile resistance than widely-adopted static analyses and modifications for set-up are proposed. The method can be refined with new data, reducing uncertainties in computed pile resistance, pile lengths, and construction costs associated with field modifications of piles.				
14. KEYWORDS : Pile foundations (Pbpbfs), Axial loads (Smimb), Monitoring (Dmbm), Dynamic tests (Gbsd), Pile driving (Fcat)			15. NUMBER OF PAGES  92	16. PRICE CODE  N/A
17. SECURITY CLASSIFICATION OF REPORT  Unclassified	18. SECURITY CLASSIFICATION OF THIS PAGE  Unclassified	19. SECURITY CLASSIFICATION OF ABSTRACT  Unclassified	20. LIMITATION OF ABSTRACT  N/A	

# DISCLAIMER

## **Notice**

This document is disseminated under the sponsorship of the U.S. Department of Transportation in the interest of information exchange. The U.S. Government assumes no liability for the use of the information contained in this document.

The U.S. Government does not endorse products or manufacturers. Trademarks or manufacturers' names appear in this report only because they are considered essential to the objective of the document.

## **Quality Assurance Statement**

The Federal Highway Administration (FHWA) provides high-quality information to serve Government, industry, and the public in a manner that promotes public understanding. Standards and policies are used to ensure and maximize the quality, objectivity, utility, and integrity of its information. FHWA periodically reviews quality issues and adjusts its programs and processes to ensure continuous quality improvement.

## **Author's Disclaimer**

Opinions and conclusions expressed or implied in the report are those of the author. They are not necessarily those of the Alaska DOT&PF or funding agencies.

# SI\* (MODERN METRIC) CONVERSION FACTORS

## APPROXIMATE CONVERSIONS TO SI UNITS

Symbol	When You Know	Multiply By	To Find	Symbol
<b>LENGTH</b>				
in	inches	25.4	millimeters	mm
ft	feet	0.305	meters	m
yd	yards	0.914	meters	m
mi	miles	1.61	kilometers	km
<b>AREA</b>				
in <sup>2</sup>	square inches	645.2	square millimeters	mm <sup>2</sup>
ft <sup>2</sup>	square feet	0.093	square meters	m <sup>2</sup>
yd <sup>2</sup>	square yard	0.836	square meters	m <sup>2</sup>
ac	acres	0.405	hectares	ha
mi <sup>2</sup>	square miles	2.59	square kilometers	km <sup>2</sup>
<b>VOLUME</b>				
fl oz	fluid ounces	29.57	milliliters	mL
gal	gallons	3.785	liters	L
ft <sup>3</sup>	cubic feet	0.028	cubic meters	m <sup>3</sup>
yd <sup>3</sup>	cubic yards	0.765	cubic meters	m <sup>3</sup>

NOTE: volumes greater than 1000 L shall be shown in m<sup>3</sup>

<b>MASS</b>				
oz	ounces	28.35	grams	g
lb	pounds	0.454	kilograms	kg
T	short tons (2000 lb)	0.907	megagrams (or "metric ton")	Mg (or "t")
<b>TEMPERATURE (exact degrees)</b>				
°F	Fahrenheit	5 (F-32)/9 or (F-32)/1.8	Celsius	°C
<b>ILLUMINATION</b>				
fc	foot-candles	10.76	lux	lx
fl	foot-Lamberts	3.426	candela/m <sup>2</sup>	cd/m <sup>2</sup>
<b>FORCE and PRESSURE or STRESS</b>				
lbf	poundforce	4.45	newtons	N
lbf/in <sup>2</sup>	poundforce per square inch	6.89	kilopascals	kPa

## APPROXIMATE CONVERSIONS FROM SI UNITS

Symbol	When You Know	Multiply By	To Find	Symbol
<b>LENGTH</b>				
mm	millimeters	0.039	inches	in
m	meters	3.28	feet	ft
m	meters	1.09	yards	yd
km	kilometers	0.621	miles	mi
<b>AREA</b>				
mm <sup>2</sup>	square millimeters	0.0016	square inches	in <sup>2</sup>
m <sup>2</sup>	square meters	10.764	square feet	ft <sup>2</sup>
m <sup>2</sup>	square meters	1.195	square yards	yd <sup>2</sup>
ha	hectares	2.47	acres	ac
km <sup>2</sup>	square kilometers	0.386	square miles	mi <sup>2</sup>
<b>VOLUME</b>				
mL	milliliters	0.034	fluid ounces	fl oz
L	liters	0.264	gallons	gal
m <sup>3</sup>	cubic meters	35.314	cubic feet	ft <sup>3</sup>
m <sup>3</sup>	cubic meters	1.307	cubic yards	yd <sup>3</sup>
<b>MASS</b>				
g	grams	0.035	ounces	oz
kg	kilograms	2.202	pounds	lb
Mg (or "t")	megagrams (or "metric ton")	1.103	short tons (2000 lb)	T
<b>TEMPERATURE (exact degrees)</b>				
°C	Celsius	1.8C+32	Fahrenheit	°F
<b>ILLUMINATION</b>				
lx	lux	0.0929	foot-candles	fc
cd/m <sup>2</sup>	candela/m <sup>2</sup>	0.2919	foot-Lamberts	fl
<b>FORCE and PRESSURE or STRESS</b>				
N	newtons	0.225	poundforce	lbf
kPa	kilopascals	0.145	poundforce per square inch	lbf/in <sup>2</sup>

\*SI is the symbol for the International System of Units. Appropriate rounding should be made to comply with Section 4 of ASTM E380.  
(Revised March 2003)

## ACKNOWLEDGEMENTS

The compilation of the numerous project files for the PDA/CAPWAP database developed in this investigation required significant contributions by several individuals. Also, the interpretation of geologic conditions, review of construction records, incorporation of direct project-specific observations and experience, and other pertinent aspects of the field performance of the pile foundations during driving benefitted from insights provided by engineers and engineering geologists with the ADOT&PF and Robert Miner Dynamic Testing, Inc. The principal investigator (PI) wishes to thank the following individuals for their tremendous contributions throughout the execution of this project:

David Hemstreet, P.E., State Foundation Engineer, ADOT&PF  
David Stanley, C.P.G., Chief Engineering Geologist, ADOT&PF  
Bruce Brunette, P.E., Regional Materials Engineer, ADOT&PF  
Jeremy Stephens, P.E., ADOT&PF

The vast majority of the PDA data and CAPWAP analyses results compiled in this project were obtained and produced by Bert Miner, P.E., of Robert Miner Dynamic Testing, Inc., Manchester, WA. The extensive collection of PDA data and CAPWAP analyses on the Hyder Causeway Trestle project was obtained and prepared by Andrew Banas, of Robert Miner Dynamic Testing, Inc. Mr. Miner generously shared technical materials from his personal library in support of the project and the PI greatly benefitted from insightful discussions pertaining to the interpretation of the dynamic pile load test data compiled in this investigation. The PI is very grateful to Mr. Miner and Mr. Banas for their support and contributions to the project.

The PI also appreciates the contributions made to the Hyder Causeway Trestle case study by Doug Schwarm of Atlas Geotechnical Services, Santa Cruz, CA.

A debt of gratitude is noted for Angela Parsons, P.E., Research Engineer (ADOT&PF) for her valuable efforts with project coordination and administration, and to Mr. Clint Alder, P.E., Chief of Research, Development and Technology Transfer, for his support of project implementation and dissemination of the research findings.

*Report cover photograph courtesy of Bruce Brunette (ADOT&PF). The photograph was taken in March 2007 at the Indian River Bridge (#865), Sitka Sawmill Creek Rehabilitation Project.*

# TABLE OF CONTENTS

ACKNOWLEDGEMENTS.....	iv
TABLE OF CONTENTS.....	v
FIGURES.....	vii
TABLES .....	viii
EXECUTIVE SUMMARY .....	ix
1.0 PROBLEM STATEMENT .....	1
2.0 DEVELOPMENT OF AN EMPIRICAL METHOD FOR ESTIMATING STATIC AXIAL PILE CAPACITY.....	3
2.1 SYNTHESIS OF THE RESULTS OF CAPWAP ANALYSES .....	4
2.1.1 <i>Utilization of CAPWAP Analyses for Unit Shaft Resistance</i> .....	7
2.1.2 <i>Utilization of CAPWAP Analyses for Unit Toe Resistance</i> .....	12
2.2 CONSIDERATIONS FOR A CAPWAP-BASED, EMPIRICAL PROCEDURE FOR ESTIMATING PILE RESISTANCE.....	16
3.0 STATIC ANALYSIS METHODS FOR SINGLE PILES .....	18
3.1 STEP BY STEP PROCEDURE FOR THE PROPOSED CAPWAP-BASED METHOD.....	19
3.1.1 <i>Site Characterization, Soil Classification, and Review of In Situ Penetrometer Data</i> .....	19
3.1.2 <i>Estimation of Shaft and Toe Resistance</i> .....	21
3.2 PILE RESISTANCE ESTIMATED BY THE EFFECTIVE STRESS METHOD.....	28
4.0 CORRELATIONS BETWEEN STATIC CAPACITY OBTAINED FROM CAPWAP AND SELECTED DYNAMIC FORMULAS.....	32
4.1 BACKGROUND AND METHODS .....	32
4.2 APPLICATION OF DYNAMIC FORMULAS AND COMPARISON TO CAPWAP.....	39
4.3 RECOMMENDATIONS .....	40
5.0 EXAMPLE APPLICATION FOR DEEP FOUNDATION ANALYSIS .....	47
5.1 INTRODUCTION TO THE CASE STUDY AND CLASS A PREDICTION .....	47
5.2 SITE INVESTIGATION AND PRELIMINARY FOUNDATION DESIGN AT HYDER.....	47
5.3 ESTIMATION OF AXIAL ULTIMATE BEARING RESISTANCE FOR PILES AT THE HYDER PROJECT SITE .....	50
5.4 COMPARISON OF ESTIMATED SOIL RESISTANCE AND CAPWAP ANALYSES AT HYDER.....	60
5.4.1 <i>Shaft Resistance</i> .....	61
5.4.2 <i>Toe Resistance</i> .....	62
5.5 TIME-DEPENDENT SHAFT RESISTANCE AND SOIL SET-UP FACTORS .....	62
5.6 CONCLUSIONS PERTAINING TO THE CASE STUDY AT HYDER.....	63

6.0	RECOMMENDATIONS FOR FUTURE RESEARCH.....	68
7.0	REFERENCES .....	70
APPENDIX A:	PDA Database:.. .....	74
Appendix A:	.....	75
APPENDIX B:	PDA Database Revisions link.....	92
PDA Database Revisions	December 23, 2012.....	92

## FIGURES

Figure 2-1	Example of graphical output from CAPWAP analysis showing the distribution of shaft resistance with pile embedment .....	6
Figure 2-2	Normalized unit shaft resistance versus pile-soil segment from CAPWAP for two, 42-inch diameter pipe piles embedded in predominately sandy silt with gravel .....	9
Figure 2-3	Normalized unit shaft resistance versus pile-soil segment from CAPWAP for all of the 42-inch diameter pipe piles embedded in predominately cohesionless, young, lightly-overconsolidated soils.....	10
Figure 2-4	Comparison of unit shaft resistance (F/L) computations using a static formula ( $\beta$ -Method) and the CAPWAP-Based Method for three project sites .....	11
Figure 3-1	Trend of stress-normalized unit shaft resistance ( $f_s/\sigma_v'$ ) versus depth for Site Class 1 soils .....	24
Figure 3-2	Chart for estimating $\beta$ coefficient as a function of soil type and $\phi'$ value.....	30
Figure 3-3	Chart for estimating $N_t$ coefficient as a function of soil type and $\phi'$ value .....	30
Figure 3-4	Observed ultimate base resistance of open-ended steel pipe piles plugged with sand .....	31
Figure 4-1	Chart for application of the Janbu method for estimating pile capacity in sand.....	35
Figure 4-2	Nominal pile bearing resistance estimated using the Case Method versus that estimated with CAPWAP .....	37
Figure 4-3	Histograms for comparison between the results of the Case Method and CAPWAP analysis at End of Driving and Beginning of Restrike.....	38
Figure 4-4	Nominal pile bearing resistance estimated using the EN Method versus that estimated with CAPWAP .....	41
Figure 4-5	Nominal pile bearing resistance estimated using the Janbu Method versus that estimated with CAPWAP .....	41
Figure 4-6	Nominal pile bearing resistance estimated using the Gates Equation versus that estimated with CAPWAP .....	42
Figure 4-7	Nominal pile bearing resistance estimated using the WSDOT Equation versus that estimated with CAPWAP .....	42
Figure 4-8	Histograms for comparison between the results of the Engineering News Method and CAPWAP analysis at End of Driving and Beginning of Restrike.....	43
Figure 4-9	Histograms for comparison between the results of the Janbu Method and CAPWAP analysis at End of Driving and Beginning of Restrike.....	44
Figure 4-10	Histograms for comparison between the results of the Gates Equation and CAPWAP analysis at End of Driving and Beginning of Restrike.....	45
Figure 4-11	Histograms for comparison between the results of the WSDOT Equation and CAPWAP analysis at End of Driving and Beginning of Restrike.....	46
Figure 5-1	Hyder Causeway Trestle and Harbor Island .....	49
Figure 5-2	Construction on the Hyder Causeway Trestle project .....	49
Figure 5-3	Aerial image showing the Salmon River delta and Hyder Causeway Trestle .....	52
Figure 5-4	Trend of corrected SPT penetration resistance, $(N_1)_{60}$ , versus elevation .....	53
Figure 5-5	Trend of Friction Penetrometer resistance versus depth.....	55

## FIGURES

Figure 5-6	Trends of cumulative shaft resistance with embedment depth for a 24-inch diameter steel pipe pile .....	57
Figure 5-7	Trends of stress-normalized unit shaft resistance with pile embedment depth for dynamic load tests (BOR) on 3 piles at the Gustavus Causeway Trestle project and the proposed CAPWAP-Based method .....	58
Figure 5-8	Comparison of computed trends in total shaft resistance with embedment depth with the results of CAPWAP analyses for 16 piles tested for BOR conditions ...	65
Figure 5-9	Comparison of computed trends in total shaft resistance with embedment depth with the results of CAPWAP analyses for 12 piles tested for BOR conditions at two time intervals .....	66
Figure 5-10	Trends of cumulative shaft resistance with embedment depth for a 24-inch Diameter steel pipe pile .....	67

## TABLES

Table 2-1	Example of CAPWAP results for a steel pipe pile .....	7
Table 2-2	Unit Toe Resistance based on CAPWAP Analysis .....	14
Table 3-1	Approximate Range of $\beta$ and $N_t$ Coefficients .....	29
Table 4-1	Dynamic methods for evaluating pile capacity: advantages, disadvantages, and comments .....	33

## EXECUTIVE SUMMARY

High strain dynamic testing of 68 piles performed at 32 project sites in Alaska has provided the basis for modifying existing procedures for estimating the static axial capacity of open-ended steel pipe piles in predominantly cohesionless soils. Holocene deposits of glacial outwash, stream alluvium, deltaic lobes, and intertidal soils have been found on numerous projects to be problematic due to the interlayered nature of the deposits and for the low axial capacities that are often exhibited with open-ended pipe piles. Dynamic load testing and analysis are commonly required by the Alaska Department of Transportation & Public Facilities (ADOT&PF) during construction to confirm the axial capacity of piles in the sensitive and difficult soils found in the geologic environments previously listed. Dynamic driving analyses performed at the End of Initial Driving (EOID) are often supplemented with additional testing performed, in general, one to five days later (Beginning of Restrike, BOR) in order to assess time-dependent aspects of pile resistance and confirm axial capacity.

A dynamic load test database has been compiled for 68 cases provided by the ADOT&PF. Trends in the statewide data have been evaluated to enhance existing practice-oriented methods for estimating the static axial capacity of open-ended steel pipe piles in deposits common along streams and in coastal regions of Alaska. The following site- and project-specific data have been compiled and tabulated in the database: site location, geologic conditions, pile characteristics, hammer and driving system, driving resistance, Pile Driving Analyzer (PDA) data, results of analysis from the Case Pile Wave Analysis Program (CAPWAP) and Case Method, and correlations between the CAPWAP-derived capacity and the results of four common dynamic formulae (Engineering News, Janbu Method, Gates equation, and the Washington State Department of Transportation equation).

The extensive collection of dynamic load test data from ADOT&PF projects has facilitated the development of CAPWAP-based correlations for static axial capacity. It would be advantageous to establish empirical relationships for axial pile capacity on the basis of static load test data; however, the lack of static data from ADOT&PF projects necessitates a reliance on the dynamic load test database. Two practice-oriented methods making use of the database are provided in this report: (i) the “CAPWAP-Based Method” wherein unit shaft resistance ( $f_s$ ) and toe resistance ( $q_t$ ) are estimated from average trends of the CAPWAP results for the 68 piles in the database, and (ii) the Effective Stress Method (Fellenius, 1996, Hannigan et al, 1997, 2006) with recommendations for selecting the input soil parameters ( $\phi'$ ,  $\beta$ ,  $N_t$ ), and limiting values for  $f_s$  and  $q_t$  for the soil conditions that prevail in the database. This investigation highlights the uncertainty inherent in pile capacity estimation procedures applied to cohesionless soils in Alaska. Procedures are proposed for refining capacity estimates computed during initial analysis using static methods and during construction using dynamic formulas. The proposed methods have been developed for predominantly cohesionless soil deposits in Alaska and provide correlation to the static axial capacity of open-ended steel pipe piles derived from dynamic analysis performed, therefore, inherently reflect the same limitations that may be associated with CAPWAP estimates of resistance for the pipe piles making up the database (diameters of 12 to 48 inches, embedment lengths of 23 to 161 feet, median time between EOID to BOR of 46 hours).

CAPWAP results at BOR are used to confirm the design capacity for the pile (ultimate bearing resistance · LRF soil resistance factor) has been achieved. In the “problem” soils commonly encountered in Alaska, the results of the CAPWAP analyses at BOR for open-ended pipe piles are often considerably less than estimates made using static analysis procedures. Therefore, a primary goal of the investigation was the development of a static analysis procedure that would yield soil resistances (shaft and toe) that are equivalent to the CAPWAP results at BOR. The empirical CAPWAP-Based procedure developed in this investigation provides estimates of shaft and toe resistance for the conditions and construction sequence that existed for the projects making up the database. As previously noted, the time constraints associated with the construction sequence on most projects, many at remote sites, limits the length of time between EOID and BOR; therefore, full set-up may not have been achieved. This situation can result in computed shaft resistance that is systematically lower than the static, long-term resistance. Guidelines are provided for adjusting the soil resistance estimates to account for soil set-up.

The proposed procedure has been applied in a step-by-step manner for a Class A prediction in order to demonstrate the application of the method, and to highlight the strengths and limitations of the CAPWAP-based correlations on a project-specific basis. The Hyder Causeway Trestle project in the southern coastal region of Alaska provided a very timely and worthwhile application for the proposed procedures. The geotechnical site investigation and preliminary pile bearing resistance estimates were made in 2008, with construction commencing after the first draft of this project report was completed and the pile resistance estimate was presented. The Hyder Causeway project, presented in Chapter 5 of this report, provided the most comprehensive collection of CAPWAP results obtained to date on a ADOT&PF project. The project involved 24-inch diameter closed-ended steel pipe piles driven in deltaic deposits of sand with gravel and silt to depths ranging from roughly 90 feet to 160 feet. PDA monitoring was carried out on 29 piles providing BOR data for all piles, with 12 piles evaluated during a second BOR test 1 to 4 weeks after the first BOR test. The time between EOID and BOR was as much as 48 days. Overall, the CAPWAP-based correlations provided very good agreement with the project-specific CAPWAP results at the Hyder Causeway project for BOR tests performed 1 to 5 days after EOID, which is consistent with the data from which the empirical relationship was based. The extensive pile testing program at Hyder highlighted the inherent variability of pile resistance at a single project site, provided a thorough case study for possible refinements to axial capacity estimation in coastal Alaska, and facilitated the development of a soil set-up factor for the sandy deposits at the site.

## 1.0 PROBLEM STATEMENT

Estimation of static axial capacity for the steel H-sections and open-ended pipe piles most commonly used by the ADOT&PF involves significant uncertainty due to the prevalent soil types and interlayered nature of the stream deposits, glacial outwash, and glacial till common on ADOT&PF bridge projects. Problematic soils include gravels and cobbles that preclude the use of standard in situ testing tools for correlation with engineering parameters used in deep foundation design, and silt-rich deposits (commonly referred to as “*Intermediate*” or “*Transitional*” soils) for which the engineering properties may be alternatively sand-like or clay-like. The often inter-bedded nature of the soil deposits routinely encountered at bridge sites in Alaska compounds the uncertainty associated with computed pile capacity. The potential difficulties associated with these soils for pile design have been addressed in numerous technical references, including a notable paper by Gerwick (2004) who observed the following regarding pile capacity in deposits of glacial outwash in Alaska:

*“Deep beds of gravel and cobbles of near-uniform size have been encountered in Alaskan fjords such as Whittier, Alaska and in the Inland Passage. High driving resistance was expected. However, steel piling, both H-piles and 4-ft diameter open-ended steel tubular piles developed surprisingly low resistance in skin friction. The uniform, rounded stones have apparently acted like roller bearings.”*

In addition to anomalously low skin friction, issues related to the dynamic and static behavior of the soil plug in gravelly soils complicates estimation of unit toe resistance due to the following; arching and patterns of stress adjacent to the pile toe, possible slipping of the plug during driving and dynamic monitoring, and yielding of the plug under static loads. These factors have been found to be functions of pile diameter, soil particle size distribution, and in the case of the dynamic behavior the size of the hammer and driving resistance. Issues associated with open-ended pipe piles in cohesionless soils have been addressed in the literature (e.g., Hannigan et al, 1997, Paik et al, 2003).

The difficulties associated with assessing skin friction and end bearing of open-ended pipe piles in inter-bedded silty and gravelly soils results in significant variability when estimating the pile length required to achieve the specified axial resistance. Limitations in the application of common methods of static analysis such as the Meyerhoff and Norlund Methods used in the FHWA program DRIVEN (Mathias and Cribbs, 1998) have been noted for open-ended pipe piles and H-piles in cohesionless soils. Over-prediction of pile capacity using the static capacity methods can result in costly pile modification during construction involving splices, internal plates, or welding shoes at the pile tips in the field to increase the cross sectional area and achieve design capacity (Bhushan, 2004).

In light of the large uncertainty in capacity estimation using static analysis methods for open-ended pipe piles in cohesionless soils, confirmation of the axial pile capacity is required by the ADOT&PF during construction. Static load tests are not practicable for most projects in Alaska due to the cost as well as the remote nature of the sites. Therefore, high strain dynamic load testing using Pile Driving Analyzer (PDA) monitoring, and CAPWAP analysis is routinely employed by the ADOT&PF to evaluate the axial capacity of piles during construction. The use of PDA data and CAPWAP analyses on numerous ADOT&PF projects has demonstrated clear limitations in the following aspects of axial capacity analyses using static methods for open-ended pipe piles in silty and gravelly soils.

1. Static methods tend to significantly over-predict unit skin friction in gravelly soils. This is especially pronounced in gravel deposits composed of greater than roughly 35% by weight sand and silt, wherein the behavior of the gravel is likely dominated by the engineering properties of the matrix (i.e., sand and silt).
2. Examination of the CAPWAP analyses demonstrates a depth-dependency on the mobilized unit skin friction ( $f_s$ ) indicating the influence of geostatic stresses on the soil-pile behavior.
3. Ultimate toe resistance ( $R_t$ ) is unreliably modeled in static analysis using the common assumptions of: (a) only the steel cross section area at the pile toe, or (b) the full cross section of the pile assuming a rigid soil plug and the unit toe resistance ( $q_t$ ) computed using Toe Bearing Capacity Coefficient ( $N_t$ ) based on drained friction values ( $\phi'$ ). Guidelines such as those presented by API (1993) recommend that toe resistance be estimated as the sum of the bearing pressure acting over the pile annulus and the interior shaft resistance provided by the soil plug. It has been recommended that the interior unit shaft friction be computed as  $\frac{1}{2}$  of the exterior unit shaft friction to account for soil disturbance during driving (Hannigan et al, 1997, 2006; Merrill et al, 1999); however, well-instrumented field investigations have shown the inner unit shaft resistance can exceed the outer unit shaft resistance for piles in sand (Paik et al, 2003). These results highlight the uncertainty associated with estimating the contribution of the soil plug to toe resistance. Soil-pile interaction involving gravel and cobbles for piles ranging in diameter from 12-inch to 48-inch compounds these uncertainties due to size effects.
4. Dividing the CAPWAP computed toe resistance by the full cross sectional area of the pile provides an "equivalent unit toe resistance." This simple quotient implicitly accounts for complex aspects of plug development; however, it must be acknowledged that dynamic plug behavior varies from the static behavior and this has been found to be a function of the following: soil type, pile diameter, hammer size, and blow count (Merrill et al, 1999, Rausche et al, 2009). Plug "slippage" during driving can yield toe resistance values based on CAPWAP that are lower bound values of the static soil resistance. These limitations notwithstanding, this simplified approach has been found to provide useful bounds on toe resistance and can be used to calibrate the  $N_t$  values used in static analysis formulations. The resulting nominal toe resistance computed using the equivalent unit toe resistance has been found to result in much larger estimates than those based on the steel cross section assumption, and less than the estimates made based on a rigid soil plug and full cross section area of the pile.

The application of dynamic load monitoring using PDA and subsequent CAPWAP analysis on ADOT&PF projects has been extremely useful for illustrating trends in the unit shaft resistance and toe resistance of open-ended steel pipe piles in the cohesionless soils common to glacial outwash, fluvial environments, and glacial till. The CAPWAP results, supplemented with standard of practice static analysis methods adjusted for common soil conditions in Alaska, provide a substantially improved procedure for estimating the axial capacity of steel pipe piles in the state. The development of an empirical method based on a large base of CAPWAP analyses from ADOT&PF projects is described as follows and the step-by-step procedure for applying the proposed method is provided.

## 2.0 DEVELOPMENT OF AN EMPIRICAL METHOD FOR ESTIMATING STATIC AXIAL PILE CAPACITY

The primary objectives of this investigation were to: (1) develop an enhanced method based on PDA data and CAPWAP analyses for estimating the axial capacity of pipe piles prior to construction, and (2) develop trends between the results of resistance estimates made using dynamic formulas and CAPWAP analyses that may be used in the field to estimate the nominal pile resistance at the time of driving using project-specific pile driving records. The latter effort included plotting trends in the results of four commonly used dynamic formulas for estimating static axial capacity relative to CAPWAP analyses so that pile driving records can be easily applied in the field using one or more of the dynamic methods, with the resulting capacity estimate converted to an equivalent CAPWAP-based capacity prior to PDA testing. The proposed relationships are considered very useful for obtaining equivalent CAPWAP-based capacities, but are not intended to be used in lieu of project-specific PDA measurements and CAPWAP analyses.

A database has been established for ADOT&PF projects including 68 piles at 32 sites in order to: develop the resistance estimation method based on CAPWAP analyses for projects located throughout the State of Alaska, and to enhance practice-oriented static analysis methods for deep foundation applications involving open-ended steel pipe piles in cohesionless soils. The projects included pile diameters from 12-inch to 48-inch, pile embedment lengths ranging from roughly 23-foot to 160-foot, a variety of geologic conditions, pile driving equipment with maximum rated energies ranging from 28 to 246 kip-ft, and varying driving behavior with final penetration resistances ranging from 7 to 360 blows per foot. As the first step in this effort, a spreadsheet archive was developed that provides pertinent data regarding the following project-specific information:

- Project location and specifics
- General geologic conditions
- Penetration resistance at the elevation of the pile toe from the ADOT&PF Friction Penetrometer
- Pile parameters
- Characteristics of the driving system
- Driving data at the End of Initial Driving (EOID), Beginning of Restrike (BOR), and End of Second Driving (EOD2)
- The length of time between EOID and BOR
- Computed results from CAPWAP analyses and the simplified Case Method, both using the PDA data
- Results of capacity estimates made using four dynamic formulas, with figures showing trends of the capacity estimates for the four dynamic formulas plotted against the capacity obtained by CAPWAP

The majority of the case studies making up the database involve piles embedded in coarse-grained, cohesionless soils, and non-plastic to low-plasticity silt. Only six of the 68 piles were driven into deposits that included clayey soils along more than 30 percent of the embedded pile length. The empirical relations derived from this PDA/CAPWAP data set are, therefore,

applicable for, and limited to, open-ended steel pipe piles in predominantly cohesionless, coarse-grained soils and silt-rich soils with low plasticity (very generally defined herein as Plasticity Index less than 12). In addition, the proposed correlations provide pile resistance estimates that are intended to match the CAPWAP results on which the procedures are based. No attempt was made to adjust the CAPWAP results, as submitted to the ADOT&PF, for possible project-specific factors that might contribute to differences between the dynamic method and long-term static resistance.

## 2.1 SYNTHESIS OF THE RESULTS OF CAPWAP ANALYSES

The monitoring of piles during driving using High Strain Dynamic Testing (HSDT) techniques and subsequent analysis using the signal matching techniques implemented in the model CAPWAP are routinely employed on ADOT&PF projects for determination of axial pile resistance. Thorough coverage of pile monitoring, modeling, and applications of PDA and CAPWAP have been well addressed in the technical literature (e.g., Rausche et al, 2008, 2009, 2010) and will not be repeated in this report. In addition, several very worthwhile papers addressing collections of case studies and observed correlation between the results of HSDT and static load tests are pertinent to the efforts presented in this report (e.g., Fellenius and Altaee, 2002, Likins and Rausche, 2004, Morgano et al, 2008). The following explanation provides key aspects of the data compilation and use of CAPWAP output. This is provided to highlight the strengths and inherent limitations of the methods proposed.

The CAPWAP results for ADOT&PF projects have been used to establish ranges of applicable unit shaft resistance ( $f_s$ ) and unit toe resistance ( $q_t$ ) for the conditions represented in the database. The following conditions and parameters were evaluated for their influence on the back-calculated values of both  $f_s$  and  $q_t$  using the CAPWAP output:

- Prevalent soil type(s) along the pile
- General geologic environment and post-depositional history, most importantly stress-history
- Pile diameter
- Depth increment and corresponding vertical effective stress
- Driving resistance (blow count/set) at EOID, BOR, or EOD2
- Shaft and toe quake at EOID, BOR, or EOD2
- Compressive stress in the pile and average energy imparted during driving at EOID, BOR, or EOD2

The CAPWAP output is routinely presented in tabular form, an example of which is provided in Table 2-1. The pile is modeled as a series of solid segments connected by springs, with viscous dampers (*dashpots*) providing velocity-dependent forces along the pile. For the CAPWAP analyses compiled in this study the individual pile-soil segments in the models were usually 6 to 7 feet long. Using the signal matching techniques previously alluded to the CAPWAP model provides the shaft resistance along each of the pile segments, leading to the distribution of shaft resistance with depth.

The shaft resistance along each pile-soil segment is expressed in two forms: (i) resistance per unit length of pile segment ( $F/L$ ), and (ii) resistance per unit area of pile ( $F/L^2$ ). The computed pile resistance mobilized along the pile segment is first converted to a “Unit Resistance (Depth)” by dividing the computed shaft resistance along the segment by its length. The length-normalized unit resistance is then converted to a “Unit Resistance (Area)” dividing by the outside circumference of the pile to yield the shaft resistance ( $f_s$ ). The summary plots of shaft resistance and toe resistance, pile load versus displacement, and matching of the measured and computed force time histories for the data in Table 2-1 are provided in Figure 2-1. The unit shaft resistances ( $f_s$ ) provided in the CAPWAP output summary tables have been used directly in the development of the CAPWAP-based pile resistance procedures.

The unit toe resistance is also provided in the CAPWAP output (Table 2-1). The computed toe resistance is divided by the cross sectional area of the pile toe providing the unit toe resistance. In Table 2-1 the toe resistance (260 kips) has been divided by the pile cross sectional area assuming no soil plug (0.50 inch wall thickness) resulting in a unit toe resistance of 1,015 kip/ft<sup>2</sup>. This is an extremely large unit toe resistance for an open-ended pipe pile in cohesionless soil, demonstrating that the total cross sectional area of the pile (assumed plugged condition) should be used to compute the unit toe resistance. A limiting value for the unit toe resistance of roughly 105 kip/ft<sup>2</sup> has been recommended due to soil plug formation and the long-term behavior of the plug under static load (Hannigan et al, 1997). For comparison, the unit toe resistance using the toe area of the plugged pile and the data provided in Table 2-1 is 83 kip/ft<sup>2</sup>. The pile in this example was driven into soils described as “*silty sandy gravel containing occasional cobbles and boulders.*” The unit toe resistance of 83 kip/ft<sup>2</sup> should be viewed as an “equivalent” static value due to the following considerations:

1. The toe resistance is computed on the basis of dynamic load test data and does not account for long-term plug behavior associated with soil creep and possible time-dependent changes in soil stresses adjacent to the pile toe.
2. There is inherently more scatter in CAPWAP estimates of toe resistance than shaft resistance relative to static load tests due to the influence of the soil-pile displacement needed to mobilize the full end bearing, the importance of toe quake, and aspects of dynamic plug behavior such as plug slip (Rausche et al, 2008).
3. The influence of potentially small pile motions near the toe, the very short time interval between waves arriving from the pile toe and the adjacent lower portions of the pile, and the computational procedure in CAPWAP all limit the resolution of shaft and toe resistance adjacent to the pile toe. For this reason, the estimates of toe resistance and shaft resistance along the lower 1 or 2 pile-soil segments in the model can be variable (Miner, 2012).

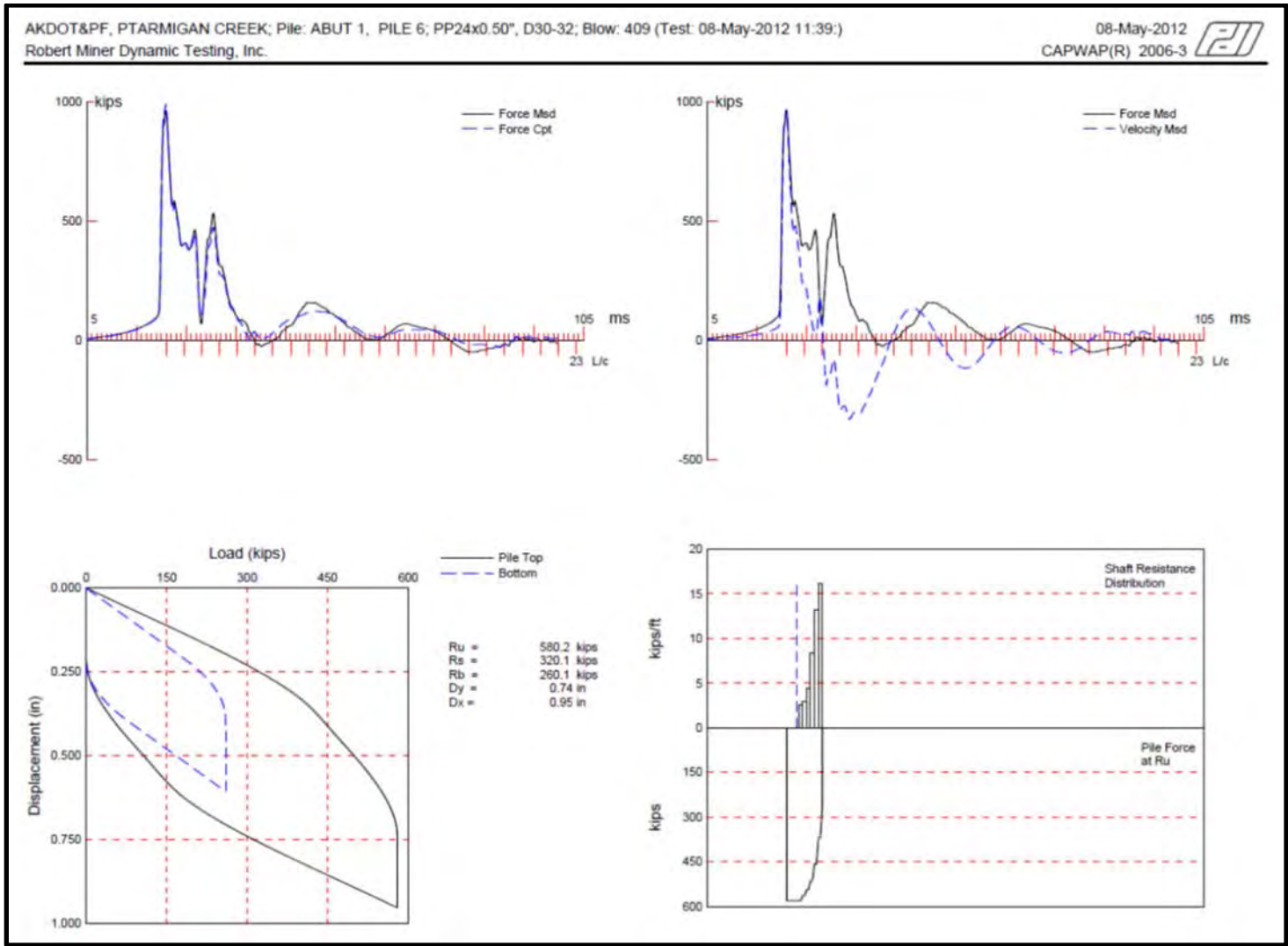


Figure 2-1: Example of graphical output from CAPWAP analysis showing the distribution of shaft resistance with pile embedment (from Robert Miner Dynamic Testing, ADOT&PF Project at Ptarmigan Creek, 2012).

**Table 2-1: Example of CAPWAP results for a steel pipe pile (from Robert Miner Dynamic Testing, ADOT&PF Project at Ptarmigan Creek, 2012).**

AKDOT&PF, PTARMIGAN CREEK; Pile: ABUT 1, PILE 6						Test: 08-May-2012 11:39:		
PP24x0.50", D30-32; Blow: 409						CAPWAP (R) 2006-3		
Robert Miner Dynamic Testing, Inc.						OP: RMDT		
CAPWAP SUMMARY RESULTS								
Total CAPWAP Capacity:			580.2;	along Shaft	320.1;	at Toe	260.1	kips
Soil Sgmt No.	Dist. Below Gages ft	Depth Below Grade ft	Ru kips	Force in Pile kips	Sum of Ru kips	Unit Resist. (Depth) kips/ft	Unit Resist. (Area) ksf	Smith Damping Factor s/ft
				580.2				
1	26.8	8.5	17.5	562.7	17.5	2.06	0.33	0.120
2	33.5	15.2	19.7	543.0	37.2	2.94	0.47	0.120
3	40.2	21.9	29.5	513.5	66.7	4.40	0.70	0.120
4	46.9	28.6	56.5	457.0	123.2	8.43	1.34	0.120
5	53.6	35.3	88.6	368.4	211.8	13.22	2.10	0.120
6	60.3	42.0	108.3	260.1	320.1	16.16	2.57	0.120
Avg. Shaft			53.4			7.62	1.21	0.120
Toe			260.1				1015.02	0.080

The “equivalent” unit toe resistance (toe resistance/total cross sectional area of the pile toe) was computed for all of the cases in the database. This is intended to provide practical ranges of the CAPWAP-derived unit toe resistance for a variety of geologic conditions, pile sizes, and pile lengths. While differences in the dynamic test results and long-term static behavior are acknowledged, the unit toe resistances provided in the database should be supplemented with estimates made using static formulations to bracket the range of reasonable values for a given application.

### 2.1.1 Utilization of CAPWAP Analyses for Unit Shaft Resistance

The distribution of unit shaft resistance was evaluated for each of the piles in the database using the CAPWAP output. Trends with depth were plotted for the shaft resistance at BOR only in order to develop a procedure that more closely provides the long-term, static resistance. The length of time between initial pile driving and load testing has been demonstrated to be very important in glacial deposits (Fellenius et al, 1989, Tweedie et al, 2009), particularly in silt- and clay-rich till deposits due to soil set-up. Similar observations have been made regarding the time-dependent nature of shaft resistance estimated from dynamic tests (i.e., time between EOID and BOR tests) on piles in sandy silt, sands, and gravels (Merrill et al, 1999, Morgano et al, 2008). Soil set-up factors have been proposed by numerous investigators (e.g., Axelsson, 2002, Hannigan et al, 1997, 2006, Lee et al, 2010) with values ranging from 1.0 to 2.0 in cohesionless soils.

The relationships developed in this investigation for unit shaft resistance were based on pile driving data at BOR to allow for either soil set-up or relaxation after driving. The time between EOID and BOR for all of the cases in the database ranged between 8 and 520 hours (mean 37 hours, median 46 hours). The relatively short time interval between EIOD and BOR for several of the piles in the database suggests that full set-up was not achieved for these cases, thus providing lower computed unit shaft resistance relative to long-term static values.

An example of the trends of unit shaft resistance with depth for two piles at the same project site is provided in Figure 2-2. The unit shaft resistance has been divided by the vertical effective stress at the mid-elevation of each pile segment to yield a stress-normalized value ( $f_s/\sigma'_v$ ). Normalizing the unit shaft resistance by vertical effective stress was useful for making more direct comparisons of the trends from the numerous sites in the database. The trends in Figure 2-2 demonstrate the variability in computed unit skin friction that can occur with piles in similar soils at the same site. The pile segments modeled in CAPWAP are roughly 6.6 feet long, providing the conversion to depth.

The trends in normalized unit shaft resistance for 17 cases involving 42-inch to 48-inch diameter piles are provided in Figure 2-3. The legend provides the database ID number for each pile. The collection of CAPWAP-based unit shaft resistances covers sites with Holocene deposits (fluvial, lacustrine, estuarine, coastal near-shore) that are inferred to be normally- to lightly-overconsolidated, therefore, excludes deposits that are highly-overconsolidated due to glacial loading and subsequent un-loading. The soil deposits represented in the figure are predominantly cohesionless silts, sands, and gravels, with several cobble layers (general soil profiles are provided in the database file). The scatter in the plot is primarily due to the variability in the soil profiles (soils types, layering, stress history) and to a lesser degree construction-related factors such as the time between EOID and BOR. The unit shaft resistances in the top pile segment and bottom one or two pile segments demonstrate additional variability due to CAPWAP modeling constraints. It is noted in CAPWAP data reports that “*A portion of the soil resistance calculated on an individual soil segment in a CAPWAP analysis can usually be shifted up or down the shaft one soil segment without significantly altering the (computed signal) match quality.*” For this reason, the variation in unit shaft resistance in the soil segment immediately above the pile toe should be tempered by the influence of toe resistance and modeling constraints in the analytical result.

A mean trend in the unit shaft resistance has been provided that effectively averages out the site-specific variables from the various projects. A depth- or stress-dependency is evident in the mean trend for the normalized unit shaft resistance. The variability in the unit shaft resistance from the various sites is also apparent. Although a statistical analysis was not performed due to the small sample set (17 cases), the mean trend provides a “global” average that is broadly applicable and when applied with bounds of  $\pm 0.15$  captures the majority of the cases at all depths.

The distributions of unit shaft resistance computed using CAPWAP results and the Effective Stress ( $\beta$ ) method were prepared for all of the piles in the database. Comparison of the two methods highlighted systematic differences in the computed values and provided guidance on the selection of soil parameters in the Effective Stress Method that would provide the greatest agreement between the two procedures. Three cases are provided in Figure 2-4 that illustrate the variability in unit shaft resistance (F/L) between CAPWAP analyses and the Effective Stress method. The Effective Stress method was applied using lower-bound values of  $\beta$  for all soil layers, consistent with overall trends provided for Holocene fluvial, lacustrine, and alluvial soils. A limiting unit shaft resistance of 1.9 kip/ft<sup>2</sup> was applied in the development of the plots.

The three cases provide comparisons between the trends of unit shaft resistance with depth for the CAPWAP analysis and Effective Stress method. Integrating the area under the trend line at a specified depth provides the cumulative shaft resistance, therefore, from a practical perspective the most appropriate comparison between the methods would focus on the relative areas under

the respective trend lines and not necessarily on the variability in the trends over depth. From this perspective, the two methods are in very good agreement to a pile embedment depth of roughly 100 feet at Bridge 656. The Effective Stress method is found to provide significantly greater estimates for cumulative shaft resistance for Bridges 1308 and 597 relative to the CAPWAP analyses. The practical significance of these trends is two-fold: (i) if CAPWAP analyses are used during construction as the method of confirming pile resistance then reliance on the Effective Stress method without adjustments for regional soils or pile type would yield an over-prediction of resistance, and (ii) the required pile length will be much greater than assumed in initial analysis and design. It is noted that that PDA data at Bridge 597 was obtained during a pile restrike only 9 hours after end-of-initial driving; therefore, it is highly likely that excess pore pressures generated during driving had not completely dissipated, and that negligible set-up had occurred at the time leading to an artificially low estimate of unit shaft resistance.

The tendency toward general over-prediction of unit shaft resistance by the Effective Stress method in the soils making up the majority of the PDA database highlighted the benefits of developing an empirical CAPWAP-based procedure for initial estimation the shaft resistance.

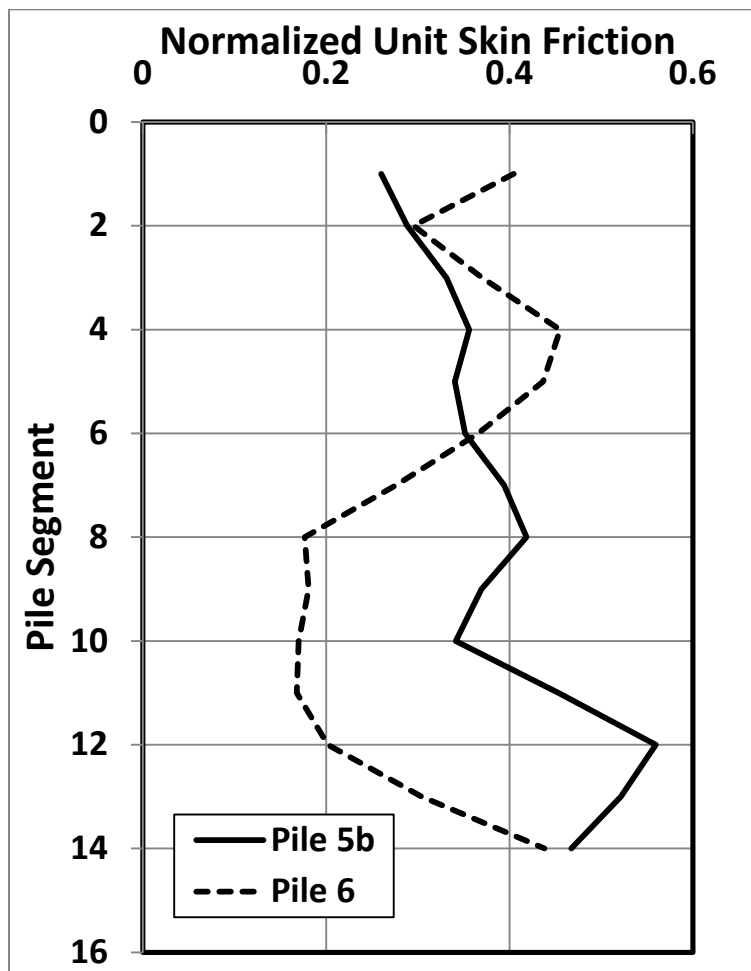


**Figure 2-2:** Normalized unit shaft resistance versus pile-soil segment from CAPWAP for two, 42-inch diameter pipe piles embedded in predominantly sandy silt with gravel (Bridge 210).

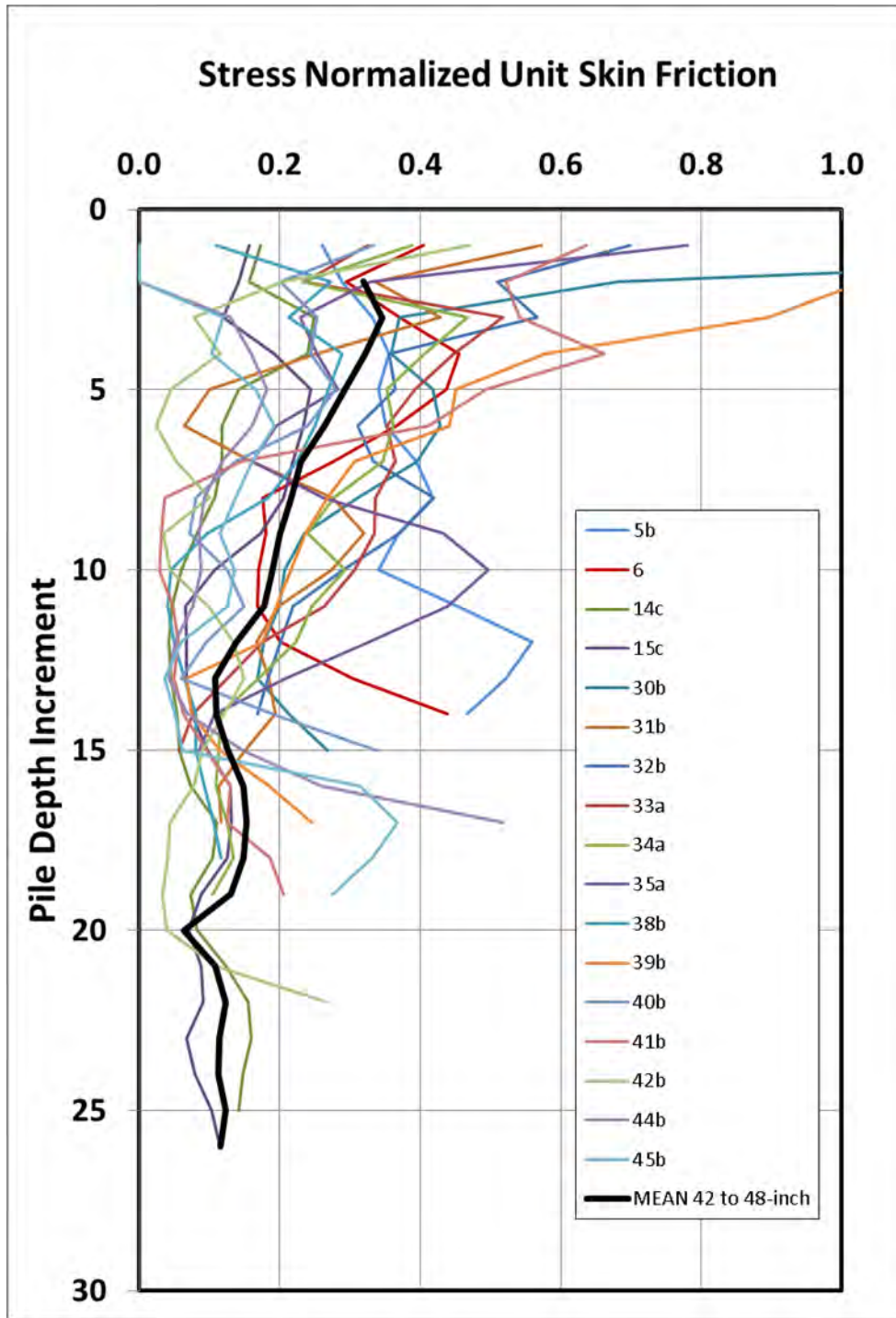


**Figure 2-3:** Normalized unit shaft resistance versus pile-soil segment from CAPWAP for all of the 42-inch to 48-inch diameter pipe piles embedded in predominantly cohesionless, young, lightly-overconsolidated soils. The legend provides the pile identification numbers from the database.

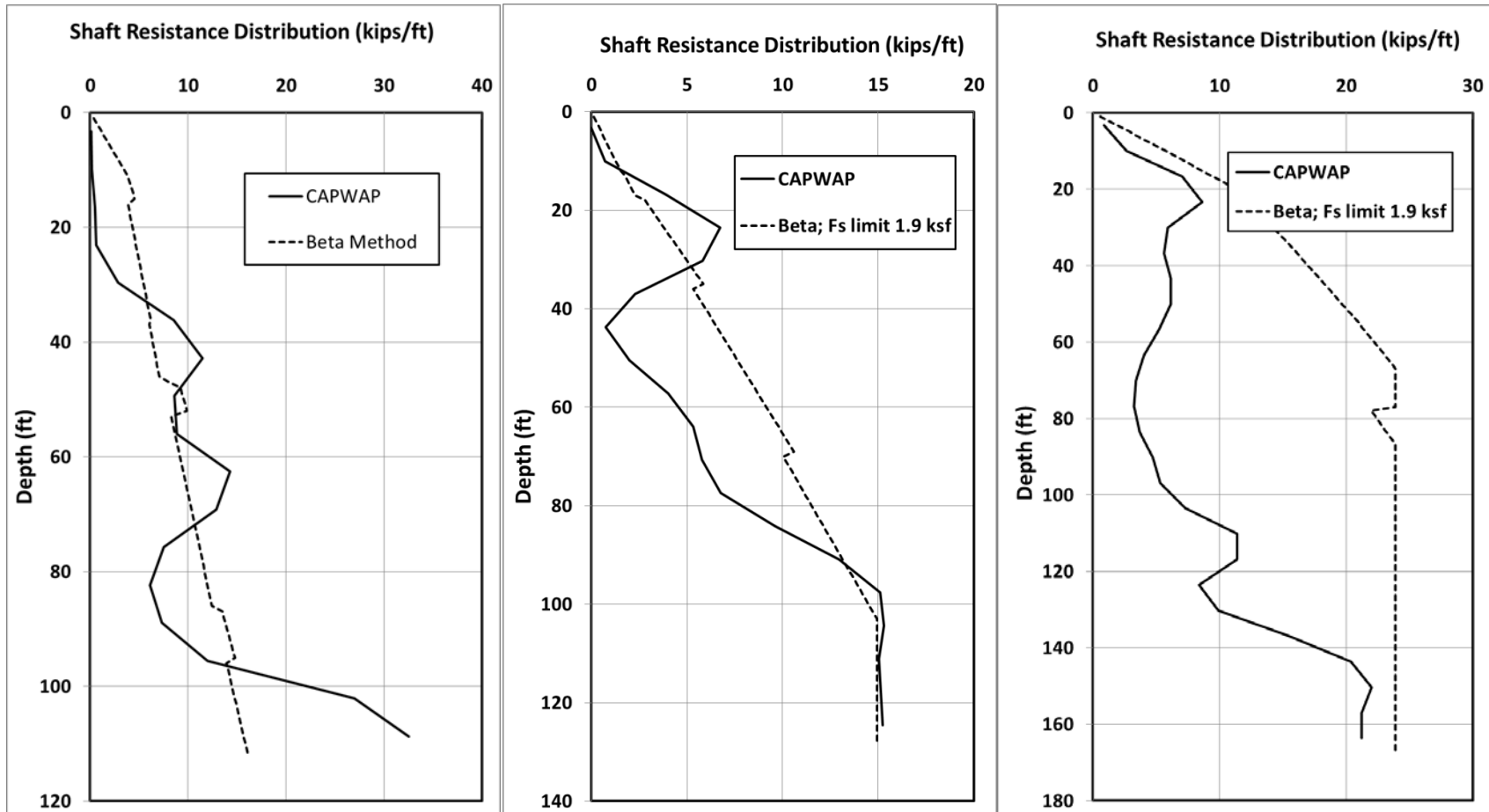


Figure 2-4: Comparison of unit shaft resistance (F/L) computations using a static formula ( $\beta$ -Method) and the CAPWAP-Based Method for three project sites. From left: Bridge 656, Bridge 1308, and Bridge 597.

### 2.1.2 Utilization of CAPWAP Analyses for Unit Toe Resistance

The unit toe resistance was evaluated using PDA data from EIOD, BOR, and EOD2 data, with consideration of the driving resistance and toe quake in each instance. In many cases the toe capacity estimated by CAPWAP was greater at EIOD. This may have been due to the effects of dilation adjacent to the pile toe during initial driving and subsequent relaxation prior to BOR, or the failure to mobilize full toe resistance during BOR, which could be inferred for cases where the driving resistance at BOR was greater than roughly 96 to 120 blows/ft (Allen, 2005, Merrill et al, 1999, Rausche et al, 2010). The equivalent unit toe resistance was based on the greater of the resistances computed by CAPWAP for EIOD, BOR, or EOD2 conditions.

The mobilized toe resistance for open-ended pipe piles reflects the formation and behavior of a soil plug within the pile. Rausche and others (2009) state that piles may experience: (a) coring or no plugging, (b) have a fully plugged end bearing (the end bearing is then transferred in full magnitude to the inside of the pile), or (c) have a slipping plug, (i.e., partial end bearing which is causing inside pipe friction). They follow with the observation that, for piles of diameter greater than roughly 24 inches, the inertia of the soil mass inside the pile often prevents full plugging. This situation may apply to all but 7 of the piles in the database (i.e., those with diameters less than 24 inches).

No construction records, measurements, or observations were available regarding plug formation for the cases in the database. The formation of a soil plug for most cases can be inferred on the basis of general observations for plug development as functions of the pile diameter, depth of pile embedment, and soil type. Hannigan and others (1997) provide general ranges for the initiation of plugging in medium dense to dense sands at pile penetration (B) to pile diameter (D) ratios of 20 to 30, and 20 in dense sands. The B/D values exceeded 20 in all but 10 of the cases in the database. In the absence of project-specific information on the cases in the database, the simplifying assumption of a slipping plug was made and the unit toe resistance values were computed as the nominal toe resistance computed with CAPWAP divided by the toe area of the plugged pile (i.e., full cross sectional area of the pile). It is acknowledged that this approximation does not account for important differences between dynamic and static plug behavior.

A final cautionary note is commonly provided with the results of CAPWAP analyses (as prepared by Goble Rausche Likins & Associates, Inc.):

*“Larger diameter open-ended pipe piles may behave differently under dynamic and static loading conditions. Under dynamic loads soil inside the pile may slip and produce internal friction while under static loads the plug may move with the pile, thereby creating end bearing over the full pile cross section. As a result both friction and end bearing components may be different under static and dynamic conditions.”*

The unit toe resistance values for all of the cases in the database are provided in Table 2-2. These values should be interpreted as approximate, or “equivalent,” unit toe resistances ( $q_t$ ) for the reasons previously addressed. Pertinent aspects of each case are provided and include the following: pile diameter and embedment length, site geology at the pile toe, set at end of driving, computed toe quake from the CAPWAP analysis, approximate ADOT Friction Penetrometer driving resistance over 2 pile diameters beneath to pile toe, and the equivalent unit toe resistance for each case in the PDA database. Examination of the unit toe resistance yields the following general observations:

1. Relatively high values for  $q_t$  are indicated for piles end bearing on rock; however, the lithology and degree of weathering has a significant influence on the applicable range of values. From a practical perspective, this observation may be of limited utility as piles driven into rock generally achieved required resistance within a small length of embedment into the rock.
2. There is a pronounced influence of pile diameter on the computed values of  $q_t$ , supporting the observations of Rausche and others (2009) pertaining to dynamic plug behavior in piles over 24 inches in diameter. The  $q_t$  values in the larger diameter piles (42 to 48-inch) are overall very low despite large embedment depths. This supports the use of the pile cross sectional area of an unplugged pile for bracketing the capacity estimates of toe resistance.
3. The toe resistance computed with CAPWAP must be interpreted with respect to the permanent set during the driving interval of interest. A set of greater than approximately 0.1 inch/blow is required in order to mobilize full end bearing in soil (Merrill et al, 1999, Rausche et al, 2008, 2009). At lower values, the toe resistance may not be fully mobilized leading to lower bound unit resistance estimates.
4. The stress history of the deposit has a pronounced influence on the toe resistance, with heavily-overconsolidated soils (e.g., glacial till) providing much larger  $q_t$  values in comparable soil types and depths than lightly-overconsolidated soils.
5. The  $q_t$  values were only weakly related to the penetration resistance measured at the elevation of the pile toe using the ADOT&PF Friction Penetrometer. This was particularly true with the longer piles and due in part to the fact that the friction penetrometer resistance includes all side friction along the full length of the rods.
6. No clear trend of  $q_t$  with depth or vertical effective stress is evident in the database, when accounting for similar site geology and stress history. While this may reflect the small data sets for specific soil types, this observation is pertinent when evaluating the effectiveness of additional pile embedment for toe resistance in vertically uniform soils.
7. The influence of gravel and cobbles on  $q_t$  is interpreted to be a function of the following: the percentage of sand and silt in the soil matrix, and very importantly the diameter of the pile. No clear trend was evident with the presence of gravel and cobbles on the toe resistance of the 42 to 48 inch diameter piles.
8. In the absence of a multi-parameter regression analysis of the CAPWAP results to develop a formulation for unit toe resistance as a function of key parameters (e.g., pile diameter, embedment length, soil type and stress history), it is recommended that for project-specific applications a range of representative  $q_t$  values be prescribed based on the data in Table 2-2. The lower- and upper-bound values for  $q_t$  should be selected from the table for cases involving similar pile configuration, soil type, and embedment depth. The uncertainty in the computed toe resistance should be acknowledged when presenting the results of capacity analyses, with parallel trends with depth plotted to highlight the best-estimate range of pile capacity.
9. The toe resistance computed using this CAPWAP-based “equivalent” unit toe resistance approach should be checked against field data in similar geologic settings and the results of estimates made using well-calibrated static formulation procedures (e.g., Effective Stress method, Norlund method as implemented in DRIVEN, etc.).

**Table 2-2: Unit Toe Resistance based on CAPWAP Analyses.**

Pile ID	Pile Diameter (in)	Pile Embedment (ft)	Soil/Rock at Pile Toe	Set (in/blow)	Toe Quake (in)	ADOT Penetrometer (blows/ft)	Unit Toe Resistance (kip/ft <sup>2</sup> )
<b>Pile Diameter: 12 to 24 inches</b>							
1	12.75	26	n/a	1.71	1.2	n/a	22.6
2	18.00	30	n/a	1.00	0.60	n/a	6.2
3	12.75	23	n/a	0.30	0.30	n/a	157.9
8b	18	116	silty sandy gravel	0.25	0.20	65	101.9
20a	24	33	gravelly silt/silty gravel	0.10	0.33	110	54.1
21a	24	33	gravelly silt/silty gravel	n/a	0.33	200	92.3
22	24	79	bedrock/boulder (?)	0.11	0.28	>600	267.4
23	24	79	bedrock/boulder (?)	0.11	0.23	>600	248.3
59a	18	30	silty gravel with sand	0.29	0.40	n/a	130.2
60b	18	30	silty gravel with sand	0.33	0.30	n/a	124.5
61	18	30	silty gravel with sand	0.13	0.20	n/a	237.7
62	18	30	silty gravel with sand	0.30	0.40	n/a	141.5
63	24	63	medium sand	0.12	0.06	30	11.1
64	24	82	medium sand	0.40	0.33	60	14.3
65	24	90	medium sand	0.20	0.34	70	38.5
<b>Pile Diameter: 30 to 36 inches</b>							
7a	36	145	sandy silt/silty sand	0.10	0.19	500	56.6
9	30	59	gravel w/ cobbles	0.04	0.12	>600	158.9
10a	30	56	gravel w/ cobbles	0.52	0.32	>600	109
11	30	55	gravel w/ cobbles	0.12	0.30	>600	224.1
16b	36	64.5	clayey silt w/ gravel	0.11	0.10	n/a	72.9
17b	36	70	clayey silt/clay w/ gravel	n/a	0.24	n/a	32.5
18	30	90.5	sand to sandy silt	0.13	0.24	>600	50.9
19a	30	112	sandy silt	0.04	0.12	>600	63.2
24b	36	89.6	interlensed sand to silt	0.21	0.12	>600	21.2
29a	30	128	argillite/siltstone bedrock	0.07	0.05	>600	81.5
36	30	94	sandy silt/silty sand	0.33	0.09	120	8.1
37	30	94	sandy silt/silty sand	0.33	0.13	120	16.3
46	36	98	weathered mica schist	0.21	0.24	n/a	52.3
47	36	112	weathered mica schist	0.11	0.14	n/a	48.1
48	36	52	weathered mica schist	0.25	0.33	n/a	150
49	36	71	weathered mica schist	0.06	0.05	n/a	66.5
50	36	53	weathered mica schist	0.19	0.32	n/a	162.7

Pile ID	Pile Diameter (in)	Pile Embedment (ft)	Soil/Rock at Pile Toe	Set (in/blow)	Toe Quake (in)	ADOT Penetrometer (blows/ft)	Unit Toe Resistance (kip/ft <sup>2</sup> )
51	36	79	weathered mica schist	0.26	0.18	n/a	83.5
52	36	79	weathered mica schist	0.25	0.20	n/a	77.8
53	36	58	frozen sandy gravel	0.17	0.37	n/a	134.4
54b	36	67	weathered mica schist	0.03	0.26	n/a	155.6
57	36	57	silty gravel with sand	0.13	0.14	>600	90.5
58a	36	58	silty gravel with sand	0.15	0.20	>600	90.5
<b>Pile Diameter: 42 to 48 inches</b>							
4	42	97	sandy silt	0.08	0.10	n/a	31.2
5a	42	96	sandy silt w/ gravel	0.07	0.10	>600	43.7
6	42	94	sandy silt w/ gravel	0.05	0.12	>600	34.3
12	48	166	silty sand	0.11	0.16	210	9.5
13	48	107	silty sand w/ gravel & cobbles	0.27	0.23	70	30.2
14c	48	167	silty sand w/ gravel & cobbles	0.13	0.19	115	15.1
15c	48	170	silty sand w/ gravel lenses	0.13	0.17	110	15.9
25c	48	114	sandy silty gravel	0.06	0.2	>600	11.9
26	48	108	silty sandy gravel	0.20	0.25	150	15.9
28	48	122	silty sandy gravel	0.24	0.27	70	24.7
30b	48	99	interlayered sand to silt	0.24	0.26	160	23.9
31a	48	113	fine to medium sand	0.19	0.15	130	27.9
32b	48	91	interlayered sand to silt	0.40	0.2	70	15.1
33b	48	106	sand and silty sand	0.35	0.2	140	11.9
34a	48	128	silt and sandy silt	0.17	0.16	450	24.3
35b	48	106	sandy silt/silty sand	0.32	0.14	300	10.4
38b	48	119	sandy silt/silty sand	0.14	0.09	n/a	5.6
39a	42	120	sand and gravelly sand	0.13	0.09	140	41.6
40a	48	102	silty sand w/ gravel	0.23	0.15	250	15.6
41a	48	129	Siltstone (?)	0.14	0.19	n/a	23.9
42a	42	147	greywacke	0.05	0.08	n/a	160.1
44c	42	116	sand	0.07	0.122	n/a	57.2
45a	42	124	sand to silty sand	0.04	0.182	400	58.2
55a	42	60	silty sand to sandy silt	0.21	0.15	>600	31.2
56b	42	60	sandy gravel to sand	n/a	0.18	>600	21.8

## 2.2 CONSIDERATIONS FOR A CAPWAP-BASED, EMPIRICAL PROCEDURE FOR ESTIMATING PILE RESISTANCE

The preparation of the ADOT&PF driven pile database and evaluation of CAPWAP results has facilitated the development of the proposed procedures for estimating the static axial capacity of open-ended steel pipe piles. While it would have been preferable to base semi-empirical formulations on pile capacities obtained from static load tests, the absence of such data for ADOT&PF projects necessitated the use of dynamic testing data as the basis for the proposed procedures. The correlations provided in this report are entirely based on the dynamic PDA data and CAPWAP analyses, and are, therefore, subject to the same limitations associated with the interpretation of dynamic testing results (Paikowsky et al, 2004). These potential limitations should be viewed relative to the uncertainties associated with the application of static analysis methods (e.g., Hannigan et al, 1997, 2006). These limitations have been widely acknowledged by geotechnical practitioners in the State of Alaska. Several of the primary advantages and limitations of the proposed CAPWAP-based method are provided as follows.

### Advantages

- The proposed procedures provide guidance for estimating the axial capacity of open-ended steel pipe piles of various diameter based on dynamic load test data from numerous sites.
- The proposed procedures provide estimates of equivalent CAPWAP-derived axial capacity, which is currently the basis for ADOT&PF assessment of the load carrying capacity of piles.
- The trends of  $f_s$  and  $q_t$  derived from the collection of CAPWAP analyses at numerous sites demonstrate the uncertainty inherent in dynamic analysis of axial pile capacity and allow for reasonable ranges of values to be estimated. It is anticipated that this will yield enhanced estimates for required pile length and help to identify situations where variations in required pile length may be expected in advance of pile procurement and construction.
- The development of straightforward correlations between CAPWAP results and the axial capacities computed using standard dynamic formulations provides field engineers with practice-oriented tools to more reliably estimate pile capacity real-time using pile driving records.

### Limitations

- The procedures presented in this report are based on CAPWAP analyses and, therefore, subject to the same uncertainties and possible limitations that are inherent in HSDT and wave matching analyses for open-ended steel pipe piles (Rausche et al, 2008, 2010).
- The procedures are most readily applicable at sites with soil deposits that are similar to those that are prevalent in the database, specifically young soils in the following depositional environments: streams, deltas, estuaries, lakes, and near-shore coastal settings. It is inferred on the basis of the geologic history of many of these sites that the soils are normally- to slightly-overconsolidated. A sub-set of the database included sites in Anchorage where the deposits are highly-overconsolidated, dense, and stiff. The resulting relationships for  $f_s$  and  $q_t$  in the Anchorage area are significantly different from those developed for the former group of soil deposits.

- No field data was available on the depth to the soil plug at the end of driving, therefore, it was not possible to reliably estimate the internal shaft resistance using static methods.
- The median time between EOID and BOR was 46 hours for the projects reviewed in this investigation. AASHTO (2009) recommends required wait times before restrrike based on the predominant soil type: 1 day for piles in clean sands, 2 days for silty sands, 3 to 5 days for sandy silts, and 7 days for clays. These trends have been confirmed in several recent research reports and pile load test databases (Paikowsky et al, 2004, Smith et al, 2011). Most of the piles in this database were driven in silty sands and sandy silts, or gravel deposits in which the engineering behavior is inferred to be matrix-controlled (sands and silts), therefore, the recommended time between EOID and BOR is roughly 48 to 120 hours. It is possible that additional capacity due to set-up could have been observed in many of the cases.
- The results of CAPWAP analyses on 29 piles on the Hyder Causeway Trestle project highlight aspects of soil set-up that are not explicitly accounted for with the proposed CAPWAP-based relationship, a consideration that is particularly important for shaft resistance in sensitive soils. Dynamic pile testing data from the Hyder project provides approximate trends in shaft resistance with time after EOID. This site-specific trend, supplemented with data from projects in similar soils, can be used to adjust the empirical CAPWAP-based shaft resistance proposed herein for long-term, static capacity.

### 3.0 STATIC ANALYSIS METHODS FOR SINGLE PILES

The CAPWAP analyses performed at 32 project sites in Alaska have provided the basis for modifying existing procedures for estimating the static axial capacity of open-ended steel pipe piles in predominantly cohesionless soils. Two practice-oriented methods making use of the database are proposed in this report: (i) the “CAPWAP-Based Method” wherein  $f_s$  and  $q_t$  are estimated from average trends of the PDA/CAPWAP results for the 68 piles in the database, and (ii) the Effective Stress Method (Fellenius, 1996, Hannigan et al, 1997, 2006) with empirically-based recommendations for selecting the input soil parameters ( $\phi'$ ,  $\beta$ ) and limiting values for  $f_s$  and  $q_t$ . The two methods are very similar in their application with minor differences based on the relationship to the PDA database. As the name implies, the “CAPWAP-Based Method” is based entirely on the Alaskan data and is intended to bracket the likely range of pile capacity for pipe piles in similar soil deposits. The Effective Stress Method, which has been widely adopted by state departments of transportation, is also outlined and provided as a check on the results of the proposed CAPWAP-Based Method. Minor modifications to the Effective Stress Method as presented by Fellenius (1996) and Hannigan and others (1997, 2006) are recommended based on trends from the PDA database.

Of the static methods for axial pile capacity presented in the FHWA manual Design and Construction of Driven Pile Foundations (Hannigan et al, 1997, 2006) the Effective Stress Method was selected for application in this investigation due to the ease of use in spreadsheets and commonly used engineering calculation software. The development of empirically-based  $\beta$ -coefficients reflecting the CAPWAP results in the cohesionless soils making up the database is advantageous in that it eliminates the need to estimate  $\phi'$  in soils containing appreciable gravel and/or cobbles based on in situ data. The presence of these coarse soils precludes the use of the CPT and makes the Standard Penetration Test an unreliable indicator of engineering behavior. The CPT and SPT are the in situ tests most commonly used as the basis for many of the correlations for estimating  $\phi'$  and static pile capacity estimation methods (e.g., Meyerhoff, Laboratoire des Pons at Chaussees (LPC), and Nottingham and Schmertmann). In the absence of this data, judgment based on local experience is necessary to estimate the geotechnical parameters for pile design. Guidance is provided on the range of friction values found to provide the best agreement between the Effective Stress Method and the CAPWAP results.

Step by step procedures are provided for both methods as follows. The procedure is intended to provide a straightforward method for the collection and interpretation of geotechnical data, the estimation of axial pile capacity, and very importantly to highlight the uncertainty in the capacity estimate. The step by step procedures are not intended to short circuit the engineering judgment required on a project-specific basis, and it must be noted that iteration may be required and/or sensitivity analyses performed to establish the most representative estimate of pile capacity. Emphasis should be placed on bracketing the likely range of required pile design output (e.g., estimated capacity versus pile embedment, minimum required pile embedment) and the application of the procedures outlined herein provide a straightforward, practice-oriented approach for these analyses.

### 3.1 STEP BY STEP PROCEDURE FOR THE PROPOSED CAPWAP-BASED METHOD

The following procedures highlight aspects of the process associated with synthesizing site-specific geologic and geotechnical data for deep foundation design, make use of regional experience with dynamic pile testing, and bracket estimates for pile capacity in the soil types represented in the PDA database. Site- and project-specific requirements may require additional steps or assumptions not specifically addressed herein. Therefore, these procedures should be viewed as providing general guidance for pile capacity estimation.

#### 3.1.1 Site Characterization, Soil Classification, and Review of In Situ Penetrometer Data

The geologic and geotechnical investigations should follow the procedures provided in ADOT&PF guides and manuals (2007a, b). The ADOT&PF Alaska Geological Field Investigations Guide (2007a) identifies deposits of gravel, cobbles, loose cohesionless soils, and very dense glacial soils as potentially problematic geologic conditions and recommends that “*special consideration and care must be taken when selecting the proper sampling equipment, obtaining the sample, and evaluating the performance of problematic geologic conditions.*” This is directly applicable for the locations and geologic conditions experienced at many of the bridge crossings examined in the database.

#### **STEP 1: Classify the soil deposits based on the depositional environment and post-depositional stress history.**

The majority of the cases in the database involve piles driven into Holocene, alluvial and fluvial deposits that are inferred based on penetrometer data to be normally- to lightly-overconsolidated along much of the pile length. These soils are well represented in the database. Alternatively, dense glacial till is represented by only a small subset of the projects evaluated. The trends in  $f_s$  and  $q_t$  were found to be significantly affected by the depositional environment and stress history. These factors are very generally separated into two categories of soil deposits:

##### Class 1: Young, Normally- to Lightly-Overconsolidated Alluvial/Fluvial Soils

- Stream deposits (channel, levee, overbank, floodplain)
- Lacustrine deposits (deltaic, lake bottom)
- Near-shore bay deposits (estuarine, deltaic, bay floor)
- Other alluvial deposits

##### Class 2: Highly-overconsolidated, Dense Soils

- Dense glacial till
- Soils overconsolidated by glacial loading or removal of significant soil overburden

It is recommended that input from project geologists and/or engineering geologists on the geologic history of the soil deposits be provided to determine the simple site classification, or to refine the classification on a layer by layer basis.

**STEP 2: Review the boring logs to establish soil layers and the location of the groundwater table.**

Develop the soil profile interpreted from available boring logs, in situ testing, and geophysical exploration. Soil layers consisting of coarse gravel, cobbles, and boulders should be highlighted. The penetration resistances obtained from the Standard Penetration Test (SPT) and/or ADOT&PF Friction Penetrometer should be plotted versus elevation; however, the results must be interpreted with consideration of the influence of the coarse particles on the penetration resistance.

**STEP 3: Review particle gradation analyses.**

Particle size distributions are necessary for evaluating the likely influence of coarse-grained soils on the engineering properties of the deposits. This is especially useful for identifying gravelly soils in which the engineering behavior and properties are controlled by the silty and sandy matrix. For example, many of the soils classified in this investigation were listed in boring logs as “silty sandy gravel.” In numerous instances the gravel comprised between 50% and 60% by weight of the total soil, therefore, it seems likely the behavior of the soil was governed by the silty sand matrix. Selection of the engineering parameters used in deep foundation analysis should account for the interaction of the coarse particles with the matrix.

**STEP 4: Compute the Vertical Effective Stress versus Depth.**

This computation should reflect soil stratigraphy, sub-layering, changes in density inferred from penetrometer results, and local groundwater levels. It is anticipated the pile capacity computation procedure will be executed using a spreadsheet or other engineering computation software, therefore, the soil deposits will be modeled in 1 to 5-foot thick layers or sub-layers along the pile length. This will facilitate very straightforward and efficient computations involving vertical effective stress (e.g.,  $(N_1)_{60}$ , unit shaft resistance, unit toe resistance).

**STEP 5: Develop plots of SPT  $(N_1)_{60}$  versus Depth in soils that do not contain appreciable gravel or cobbles.**

Correct the field SPT values for effective overburden pressure and hammer energy. Judgment must be used when interpreting SPT N-values in soil containing gravel. Anomalously high SPT N-values in gravelly-deposits should be deemed unreliable and omitted from consideration when estimating engineering parameters. The influence of gravel on the SPT N-values can be assessed by comparison with supplementary data from adjacent locations (e.g., ADOT&PF Friction Penetrometer, Shear Wave Velocity).

**STEP 6: Review the trends of ADOT&PF Friction Penetrometer with Depth.**

The trend of penetration resistance with depth using the ADOT&PF Friction Penetrometer provides a useful index of soil stiffness that can be used for initial and very general classification of the site for deep foundation applications. The ADOT&PF penetrometer resistance reflects both the tip resistance and the cumulative skin friction mobilized along the penetrometer and rods. This precludes a simple correlation of tip resistance with soil bearing resistance; however, the trend of penetration resistance with depth has been found to be correlated (albeit weakly) with both  $f_s$  and  $q_t$ . The utilization of ADOT&PF penetrometer data for screening with respect to shaft resistance is provided in Step 7.

### 3.1.2 Estimation of Shaft and Toe Resistance

The ultimate bearing capacity of a single pile is the sum of the shaft and toe resistance ( $Q_u = R_s + R_t$ ) mobilized along the pile. It is commonly assumed the shaft resistance and toe bearing resistance can be determined independently and the nominal ultimate values are mobilized concurrently. This assumption should be assessed on a case by case basis with consideration of the relative pile-soil displacement required to mobilize both the shaft resistance and toe resistance. The  $f_s$  and  $q_t$  values provided in this section are based on CAPWAP analyses that account for the soil resistances mobilized at computed shaft and toe quakes, thus the relative contributions of  $R_s$  and  $R_t$  are implicitly accounted for.

#### **STEP 7: Estimation of the Stress-Normalized Unit Shaft Resistance ( $f_s/\sigma_v'$ ).**

The recommended procedure for estimating the variation of unit skin friction with depth along a pile involves several interrelated steps as follows.

1. Establish the general Site Class (Class 1: young, NC to lightly-overconsolidated alluvial and fluvial soils, or Class 2 highly-overconsolidated, dense soil deposits) based on the local geologic information and knowledge of the stress history of the soils.
2. Screen for the potential of very low unit skin friction using site-specific in situ data (CPT, SPT, or ADOT&PF Friction Penetrometer).
3. Estimate the unit shaft resistance at the depth of interest using the CAPWAP-Based relationships.
4. Compare the results computed using the CAPWAP-Based relationships with the Effective Stress Method outlined in Section 3.2 of this report.
5. Compare the results with CAPWAP analyses obtained in similar geologic settings and soils. Refer to the database for relevant cases that help to bracket the likely range of unit shaft resistance.

#### Screening for the Potential of Low Unit Shaft Resistance in Site Class 1 Soils

The potential for very low unit shaft resistance mobilized along pipe piles in cohesionless soils is well documented in the technical literature. Low shaft resistance was observed in many of the cases documented in the database. For Site Class 1 conditions screening for possible trends in unit shaft resistance with depth includes the review of the ADOT&PF Friction Penetrometer logs and SPT N-values. It is again noted that SPT N-values in soils with gravel and cobbles are deemed to be unreliable, and considerable assessment of the data and judgment is required if this data is used as an indicator of possible unit shaft resistance. It is important to consider several projects in the database that had the lowest unit shaft resistances determined by CAPWAP exhibited SPT N-values that were large due to the influence of the split spoon sampler size and the gravel and cobbles in the soil deposits. At these sites the ADOT&PF Friction Penetrometer often indicated a low penetration resistance and it is recommended that both sources of data must be critically evaluated.

Trends in unit shaft resistance, and recommended modeling procedures can be very generally related to the ADOT&PF Friction Penetrometer blow count as follows:

1. If  $N_{ADOT} \leq 0.80z + 5$ , the unit shaft resistance is likely to be very low with stress-normalized unit shaft resistance ( $f_s/\sigma_v'$ ) values as low as 0.10 to 0.15. The resulting unit shaft resistance in these very loose soils is substantially lower than estimated using either the CAPWAP-Based Method or Effective Stress Method using published ranges for the  $\beta$ -coefficient.
2. If  $N_{ADOT}$  is between roughly  $0.8z + 5$  and  $1.8z + 5$ , then the unit shaft resistance is well modeled using the proposed CAPWAP-Based Method.
3. If  $N_{ADOT} \geq 1.4z + 5$ , then the Effective Stress Method (Section 3.2) has been found to provide reasonable results when using lower bound values for the  $\beta$ -coefficient.

where;

$N_{ADOT}$  is the penetration resistance at the depth of interest (bl/ft), and  
 $z$  is the depth of interest (ft)

The overlap in approximate ranges of  $N_{ADOT}$  for cases (2) and (3) is intentional and highlights the general nature of this screening criterion.

Similar guidelines based on the SPT  $(N_1)_{60}$  values are proposed:

1. Very low unit shaft resistance is anticipated when  $(N_1)_{60} < 5$  bl/ft, with low values commonly observed in silt-rich and sandy soils with normalized penetration resistance less than 10 bl/ft/.
2. Overall, good agreement between average CAPWAP trends and the Effective Stress Method using lower-bound  $\beta$ -values was observed when  $12 \leq (N_1)_{60} \leq 20$  bl/ft.
3. No correlation was observed in soils with predominantly gravel-sized particles due to the negative influence of the sampler/particle diameter ratio on the SPT penetration resistance (i.e. artificially high N-values). This was demonstrated in several cases where low unit shaft resistance was indicated by CAPWAP analyses in gravelly soil deposits having relatively high SPT penetration resistances ( $(N_1)_{60} > 25$  to 30).

These recommendations are intended for preliminary screening purposes only and it must be acknowledged that significant variability was observed in the database. These simple screening tools are intended to provide suitably conservative guidelines for pile capacity estimation.

#### Estimating the Unit Shaft Resistance in Site Class 1 Soils

In deposits of low- to moderate-plasticity silt, silty sand, sand, and gravels interpreted to be matrix-controlled in engineering behavior, the unit shaft resistance at any depth along a pile can be estimated from the trend in stress-normalized unit shaft resistance ( $f_s/\sigma_v'$ ) illustrated in Figure 3-1. Multiplying the stress-normalized unit shaft resistance by the vertical effective stress at the mid-point of the layer of interest yields the unit shaft resistance at that depth. This process is completed for each sub-layer along the embedded pile length and provides the initial estimate of  $f_s$ .

The trend provided in Figure 3-1 was developed from CAPWAP data on over 20 piles in Site Class 1 soil deposits with different layering. The trend is, therefore, an “average” or homogenization of the unique stratigraphy at each of the sites. This may be significant if site-specific geologic history and geotechnical data indicate distinct soil layering that warrants the use of the simplified CAPWAP-Based Method in some soil layers and alternative methods (Effective Stress  $\beta$  Method, or higher- or lower-bound  $f_s$  values based on experience). Applying the CAPWAP-Based method for  $f_s$  in some layers and not in others requires judgment as the empirical method implicitly accounts for a degree of vertical variability in the soil deposits.

In order to bracket the likely range of  $f_s$  values with depth it is recommended that as many as three trends be developed and plotted: (i)  $f_s$  computed using the CAPWAP-Based Method (Figure 3-1), (ii) potentially lower  $f_s$  estimated for very loose soils if indicated based on the screening criteria previously addressed, and (iii)  $f_s$  computed from the Effective Stress Method (Section 3.2). These three trends provide a reasonable range of the unit shaft resistance versus depth and facilitate the use of a weighted-average approach for the selection of  $f_s$  in each soil layer or sub-layer.

#### Estimating the Unit Shaft Resistance in Site Class 2 Soils

A small subset of the PDA database featured sites in Anchorage that are not located along streams or bodies of water. The soil deposits consist of very dense sands and gravels, with occasional layers of very stiff to hard clays and silts. These are interpreted to be heavily-overconsolidated soils and they exhibit unit shaft resistance that is significantly greater than the trends provided by the Site Class 1 soil deposits. Back-calculating unit shaft resistance from CAPWAP analyses provides stress-normalized values ( $f_s/\sigma_v'$ ) ranging from 0.75 to 2.5, with most of the intervals well above 1.0. No reliable trend was observed, partially due to the small data set and large variability in the  $f_s$  values. A very crude, first approximation could be developed using  $f_s/\sigma_v'$  values of 0.8 to 1.0 in the upper 60 feet of the soil profile. No PDA data was obtained at greater depth at these sites due to the strength of the soils and adequate axial capacity gained at relatively shallow depths.

It is recommended in Site Class 2 soil deposits that this very approximate estimate of shaft resistance be supplemented with the Effective Stress method using upper-bound values for the  $\beta$ -coefficient. The use of upper-bound  $\beta$  values still provided estimates for shaft resistance that were lower than the CAPWAP-derived  $f_s$  values for all of the cases evaluated in this investigation.

The use of  $f_s/\sigma_v'$  values greater than 1.0 to 1.2 should be made with caution and tempered by local experience in similar soil deposits.

#### Estimating the Unit Shaft Resistance in Cohesive Soils

Very few cohesive deposits involving moderate- to high-plasticity silts, clays, and organic-rich soils were represented in the database. For this reason no modifications to existing procedures for estimating unit shaft resistance have been developed in this investigation. The Alpha and Beta Methods are recommended for cohesive soils, and the procedures are well presented by Hannigan and others (1997, 2006).

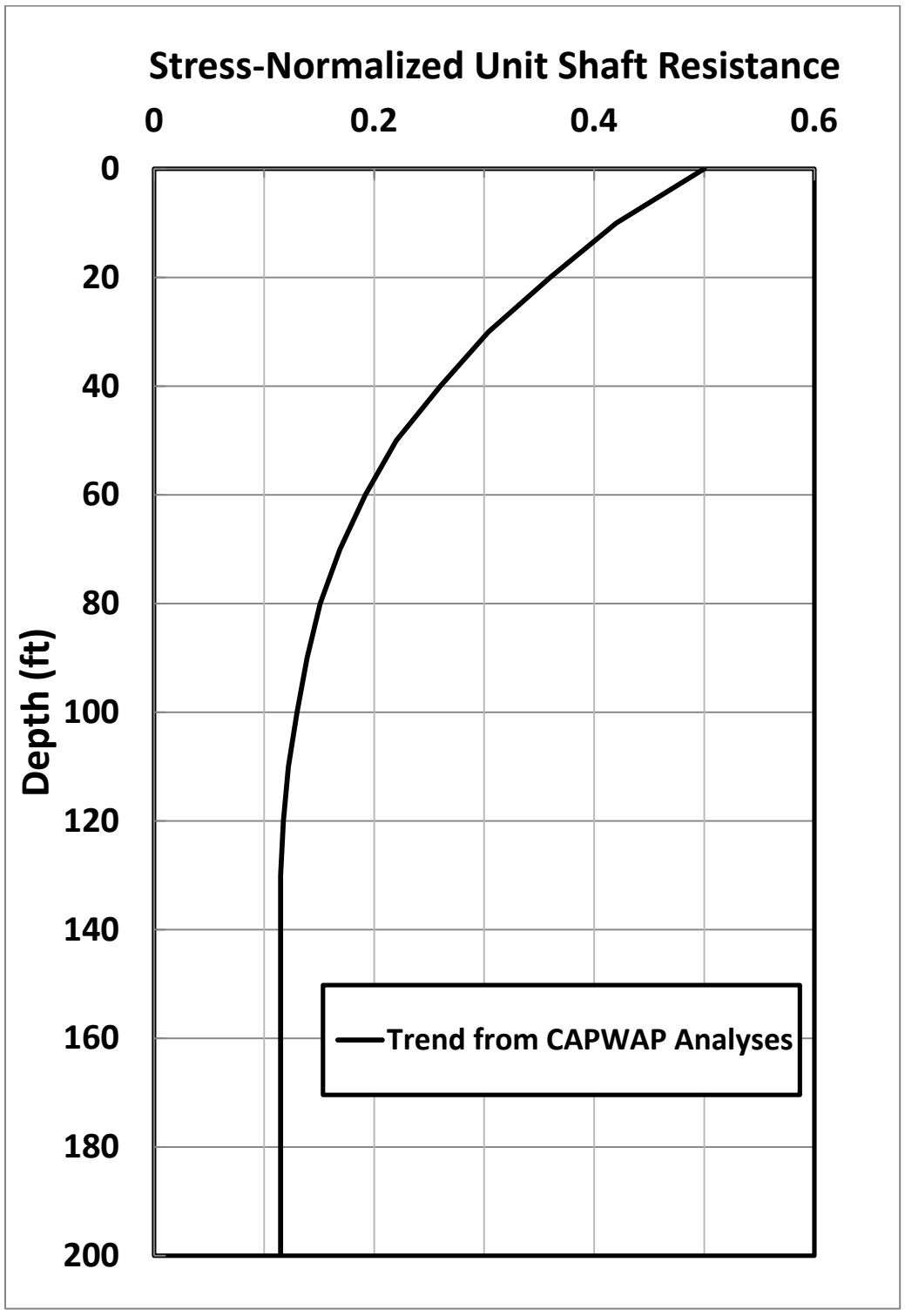


Figure 3-1: Trend of stress-normalized unit shaft resistance ( $f_s/\sigma_v'$ ) versus depth for Site Class 1 soils.

**STEP 8: Compute the Unit Shaft Resistance ( $f_s$ ) for each soil layer.**

The unit shaft resistance in each soil layer or sub-layer is computed as;

$$f_s \text{ (kips/ft}^2\text{)} = (f_s / \sigma_v') \cdot \sigma_v' \quad (3-1)$$

where;

$(f_s / \sigma_v')$  is the stress-normalized unit shaft resistance obtained from Figure 3-1, or selected based on local experience, and  
 $\sigma_v'$  is the vertical effective stress at the depth of interest (kips/ft<sup>2</sup>)

In the absence of local data a maximum, limiting unit skin friction in the range of 1.5 to 1.9 kips/ft<sup>2</sup> is recommended based on trends in the database. This recommendation is supported by Meyerhoff (1976, in Hannigan et al, 1997) who proposed a limiting  $f_s$  value of 2.0 kips/ft<sup>2</sup>.

**STEP 9: Compute the cumulative shaft resistance ( $R_s$ ) for the pile embedment of interest.**

Compute the shaft resistance in each soil sub-layer and the ultimate shaft resistance ( $R_s$ ) from the sum of the shaft resistance in each sub-layer. This is computed as;

$$R_s \text{ (kips)} = \Sigma(f_s \cdot \pi \cdot d \cdot L) \quad (3-2)$$

where;

$f_s$  is the unit shaft resistance (kips/ft<sup>2</sup>)  
 $d$  is the pile diameter (ft), and  
 $L$  is the pile length (ft) under consideration (full length or thickness of sub-layer)

This formulation applies for the shaft resistance mobilized along the exterior surface of the pile only. Aspects of internal shaft resistance for cases in which a soil plug is not anticipated are addressed in STEP 12.

**STEP 10: Compute the unit toe resistance ( $q_t$ ).**

Two methods are recommended for bracketing the range of unit toe resistance. The first follows well established procedures outlined by Hannigan and others (1997, 2006). The unit toe resistance at the depth of interest is computed as;

$$q_t \text{ (kips/ft}^2\text{)} = N_t \cdot \sigma_v' \quad (3-3)$$

where;

$N_t$  is the Toe Bearing capacity coefficient, and  
 $\sigma_v'$  is the vertical effective stress (kips/ft<sup>2</sup>) at the pile toe

Again, local experience should be used in the selection of the  $N_t$  coefficient. In the absence of local experience, the information in Table 3-1 and Figure 3-3 provides a useful range of values.

As a supplement to the estimation made using the Effective Stress Method, the range of “equivalent” unit toe resistance values computed from CAPWAP analyses in the database can be estimated from Table 2-2. Given the pile diameter and soil conditions within approximately two to four times the pile diameters of the toe, the equivalent unit toe resistance  $[(q_t)_{eq}]$  can be selected.

### **STEP 11: Compute the ultimate toe resistance ( $R_t$ ).**

The ultimate toe resistance is computed as;

$$R_t \text{ (kips)} = q_t \cdot A_t \quad (3-4)$$

where;

$q_t$  is the unit toe resistance (kips/ft<sup>2</sup>), and  
 $A_t$  is the cross sectional area of the pile toe (ft<sup>2</sup>)

It is important to note that experience in Alaska demonstrates significant differences between the estimates of  $R_t$  made using static methods and the computational results from CAPWAP. A portion of this discrepancy is due to the assumptions made concerning soil plug development and the appropriate cross sectional area to be used (i.e., cross sectional area of the pile walls versus the total cross sectional area of the pile toe assuming a rigid soil plug). The CAPWAP data in the database demonstrates the ultimate toe resistance is intermediate between these two scenarios. Use of the total cross sectional area of the pile and  $N_t$ -values provided in the technical literature commonly results in toe resistance estimates that are unreasonably large, and this approach should be tempered by regional experience. The majority of the CAPWAP results in the database suggest the use of common  $N_t$  values should be avoided for open-ended pipe piles with the toe bearing in cohesionless soil, unless a limiting value of  $q_t$  is defined.

The uncertainty associated in  $R_t$  computed using the Effective Stress Method, as well as other static methods, is great enough that it should be viewed as a preliminary method of estimation only. Bracketing the range of “equivalent” unit toe resistance from the compiled CAPWAP results (Table 2-2) is recommended and the following formulation applied;

$$R_t \text{ (kips)} = (q_t)_{eq} \cdot A_t \quad (3-5)$$

Utilization of the “equivalent” unit toe resistance requires that the full cross sectional area of the pile toe be used. The values of likely minimum and maximum unit toe resistance should be established with consideration of the following: pile diameter, soil type adjacent to the pile toe, potential for matrix controlled soil behavior, depth of embedment and plug development. The case history data in Table 2-2 provides guidance on reasonable ranges of unit toe resistance back-calculated from CAPWAP analyses.

### **STEP 12: Consideration of plug development.**

Plugging of open-ended pipe piles has been well addressed in the technical literature (e.g., Hannigan et al, 1997, 2006, Paik et al, 2003). Approximate guidelines for the depth at which a soil plug may form have been proposed for various soil types (e.g., pile embedment/pile diameter ratios of 20 to 35), and procedures developed for estimating the interior shaft resistance for non-plugged sections and toe resistance for plugged sections. Recommended procedures and considerations for computing the capacity of piles with plugged condition and unplugged condition are provided in Section 9.10.5 of Hannigan and others (1997, 2006).

Limiting maximum values of  $q_t$  have been recommended, in large part to account for the static behavior of the plug. Plug behavior reflects complex aspects of arching, yielding of the plug under load, and pile movement relative to soil at the pile toe. It should not be assumed the soil plug will develop a toe resistance equivalent to that of a solid end pile. It has been proposed

(Tomlinson, 1995) that this is due to the relatively large movement of the pile toe required to induce arching in soil adjacent to the toe, at which point the cumulative interior skin friction may be sufficient to induce passive failure in the soil mass beneath the pile toe. The relative pile movement required to mobilize full plug resistance is proportional to the pile diameter, therefore, the toe resistance provided by the soil plug is related to the pile diameter. This soil-pile behavior may have contributed to the general trend in the database for a decrease in the average “equivalent” unit toe resistance with increasing pile diameter in cohesionless soils.

Limiting values of toe resistance can be estimated from Figure 3-4. In most cases the piles on which the plot is based were driven into dense or very dense sands and it was demonstrated that failure occurred by yielding of the plug as opposed to bearing failure on the soils beneath the pile toe (Tomlinson, 1995). It is interesting to note that toe resistance estimates based on the API formulation would have dramatically overestimated the measured end bearing in most of the cases documented. The data in Figure 3-4 supports a limiting sand plug resistance in the range of 63 to 105 kips/ft<sup>2</sup>. The value of 105 kips/ft<sup>2</sup> has been recommended by Hannigan and others (1997, 2006).

It is recommended for applications involving piles driven to embedment depths greater than 20 to 35 times the pile diameter that the plugged condition be assumed and that the toe resistance be evaluated by:

1. Bracket the range of reasonable  $(q_t)_{eq}$  values from the database (Table 2-2) based on the pile diameter, soil type and stiffness at the pile toe, and the depth of embedment.
2. Perform a check of the results of (1) using the Effective Stress method and lower bound values of  $N_t$ .
3. Compare the results of (1) and (2) against limiting unit toe resistance values in similar soils based on local experience, or the trends provided in Figure 3-4.

**STEP 13: Compute the ultimate bearing resistance ( $Q_u$ ).**

The ultimate, or nominal unfactored, bearing resistance is computed as the sum of the shaft resistance and the toe resistance;

$$Q_u = R_s + R_t \quad (3-6)$$

**STEP 14: Adjust the ultimate bearing resistance using the appropriate Resistance Factor ( $\phi_r$ ).**

$$Q_{adj} = Q_u \cdot \phi_r \quad (3-7)$$

where;

$\phi_r$  is the Resistance Factor applied to static analysis formulations, or modified based on local data and experience.

### 3.2 PILE RESISTANCE ESTIMATED BY THE EFFECTIVE STRESS METHOD

The CAPWAP-Based Method previously outlined has been developed from a large base of data obtained in Alaska; however, conditions may arise where site- and project-specific aspects of deep foundation design will differ from those conditions on which the method is based. In these situations it is recommended that pile capacity estimates be supplemented with a well-calibrated method that has been widely used in similar deep foundation applications. As a check on the results of the proposed CAPWAP-Based Method it is recommended the Effective Stress Method also be applied for axial capacity estimates. Applications involving the Effective Stress Method are well presented in Fellenius (1996) and Hannigan et al (1997, 2006). The method requires estimation of the drained angle of internal friction for each soil layer, from which  $f_s$  and  $q_t$  are estimated. The method is easily implemented in spreadsheets and engineering calculation software, thus widely used in practice. Region-specific correlations have been developed for the soil parameters and a similar procedure has been adopted in this investigation. The step by step procedures are very similar to those presented in Section 3.1 and they have been well presented by Hannigan and others (1997, 2006). Minor modifications to the soil parameters are recommended based on the comparison of results by this method with the CAPWAP database.

Steps 1 through 6 are exactly the same as outlined in Section 3.1 for the CAPWAP-Based Method and are not repeated. Modifications to the soil parameters and coefficients used in the Effective Stress Method in order to achieve shaft resistance and toe resistance consistent with the CAPWAP-Based Method are provided as follows (modified after Hannigan et al, 1997, Section 9.7.1.3).

#### **STEP 7: Considerations for establishing the $\beta$ -coefficient for each soil layer.**

Regional experience should be reviewed prior to selecting the  $\beta$ -coefficients applied in the evaluation. The CAPWAP-Based Method synthesizes this experience for applications in Alaska. On projects involving conditions that differ from the database (e.g., geologic setting, soils, pile sizes, pile driving equipment) the  $\beta$ -coefficient for each layer can be estimated from Table 3-1. The table has been slightly modified from that presented by Hannigan and others (1997) with the addition of a Soil Type for sandy silt/silty sand, and intermediate values of  $\phi'$ ,  $\beta$ , and  $N_t$ .

The coefficients  $\beta$  and  $N_t$  can be selected from Table 3-1 based on general soil type or the  $\phi'$  angle of the soil. This introduces uncertainties for gravelly soils that are not routinely tested for  $\phi'$  and in which the SPT N-values are unreliable. The range of  $\phi'$  values for gravels provided in the table are largely based on work presented prior to 1970. Subsequent investigations have highlighted the stress-dependent nature of  $\phi'$  for sands and gravels (e.g., Charles and Watts 1980, Duncan et al, 1989, Duncan 2004, and Terzaghi, Peck, and Mesri 1996 [reproduced in AASHTO 2009]); however, these improved methods of estimating  $\phi'$  for gravels should not be used for selecting  $\beta$  as the coefficients in Table 3-1 are largely empirical and related to the earlier methods for estimating  $\phi'$ . The stress-dependent  $\phi'$  values for gravel tend to be greater than the older, more general estimates, and lead to significantly overestimated shaft resistance. This trend was observed in many of the cases evaluated in the database.

As previously addressed the nature of the matrix components of predominantly gravel and cobble soils has a significant influence on the engineering behavior of the soil. This is especially relevant when selecting the representative Soil Type and  $\phi'$  value for gravelly soils. For gravelly soils with greater than roughly 25% by weight sand and silt, it is recommended that parallel analyses be performed: one using gravel parameters, and one using sand parameters. This will help to bracket the likely range of pile capacity with depth and highlight the uncertainty inherent with the Effective Stress Method in these gravelly soils.

The lower bound  $\phi'$  angle in Table 3-1 is recommended for Class 1 soils and the upper bound  $\phi'$  angle for Class 2 soils based on comparison of shaft resistances computed with the Effective Stress Method and the CAPWAP-Based Method. Intermediate values of  $\beta$  can be obtained from Figure 3.2.

**STEP 8: Compute the Unit Shaft Resistance ( $f_s$ ) for each soil layer.**

The unit shaft resistance is computed as;

$$f_s \text{ (kips/ft}^2\text{)} = \beta \cdot \sigma_v' \quad (3-8)$$

where;

$\beta$  is the Beta Coefficient obtained from Table 3-1, Figure 3-2, or selected based on local experience, and

$\sigma_v'$  is the vertical effective stress at the depth of interest (kips/ft<sup>2</sup>)

In the absence of local data a maximum, limiting unit skin friction in the range of 1.5 to 1.9 kips/ft<sup>2</sup> is recommended based on trends in the PDA database. This recommendation is supported by Meyerhoff (1976, in Hannigan et al, 1997) who proposed a limiting  $f_s$  value of 2.0 kips/ft<sup>2</sup>.

Steps 9 through 14 follow the same procedures outlined in Section 3.1 and follow the general step by step process presented by Hannigan and others (1997, 2006), and, therefore, they are not repeated herein.

**Table 3-1: Approximate Range of  $\beta$  and  $N_t$  Coefficients  
(modified after Fellenius, 1991, in Fellenius 1996, and Hannigan et al, 1997).**

Soil Type	$\phi'$ (degrees)	$\beta$	$N_t$
Clay	25 – 30	0.23 – 0.40	3 – 30
Silt with PI > 5	28 – 34	0.27 – 0.50	20 – 40
Sandy Silt/Silty Sand	30 – 36	0.28 – 0.52	25 – 70
Sand	32 – 40	0.30 – 0.60	30 – 150
Gravel	35 – 45	0.35 – 0.80	60 - 300

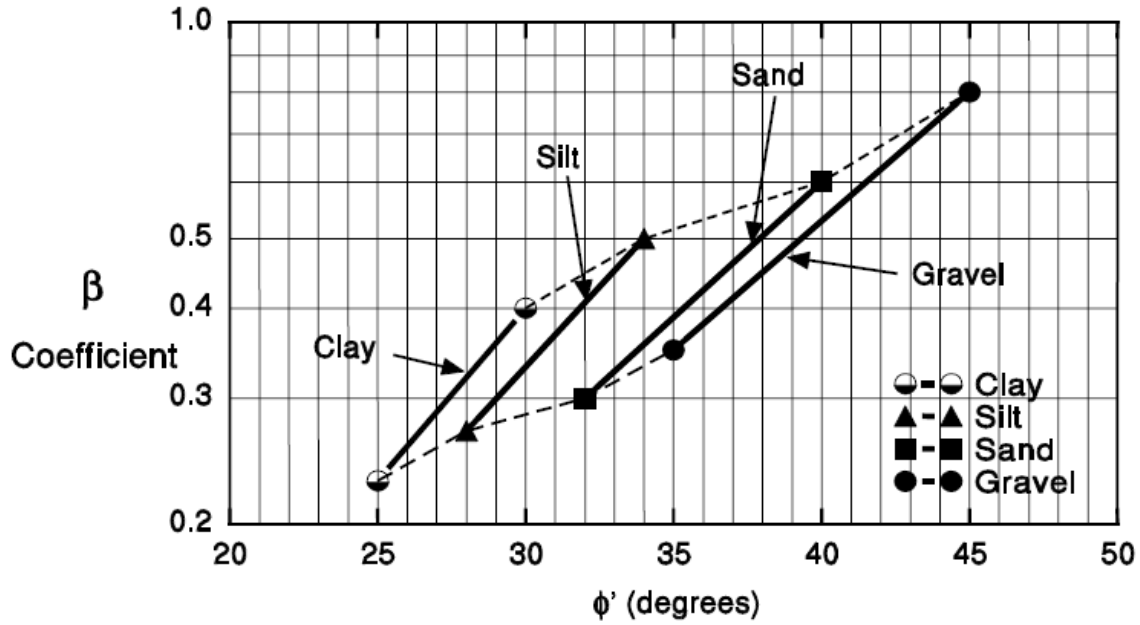


Figure 3-2: Chart for estimating  $\beta$  coefficient as a function of soil type and  $\phi'$  value (after Fellenius 1991, in Hannigan et al, 2006).

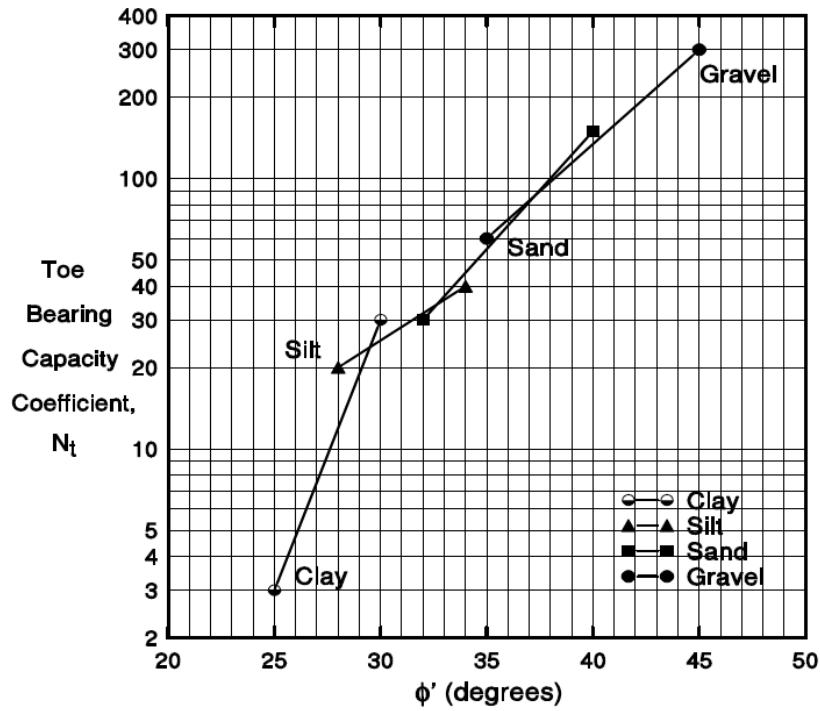


Figure 3-3: Chart for estimating the  $N_t$  coefficient as a function of soil type and  $\phi'$  value (after Fellenius 1991, in Hannigan et al, 2006).

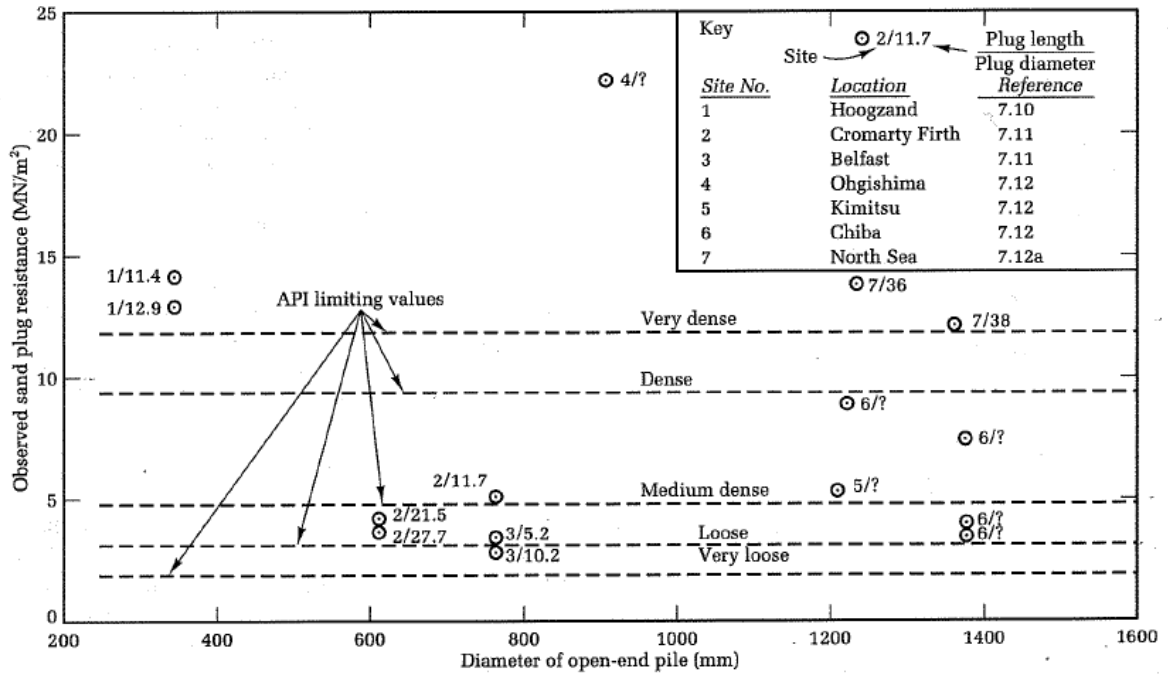


Figure 3-4: Observed ultimate base resistance of open-ended steel pipe piles plugged with sand (Tomlinson, 1995).

## **4.0 CORRELATIONS BETWEEN STATIC CAPACITY OBTAINED FROM CAPWAP AND SELECTED DYNAMIC FORMULAS**

### **4.1 BACKGROUND AND METHODS**

Trends in the static capacity estimates made using CAPWAP and the results of four commonly used dynamic formulas have been developed from the database with the goal of providing a practice-oriented method for estimating total soil resistance equivalent to CAPWAP analyses during pile driving. The dynamic formulas are advantageous in that they provide simple and straightforward capacity estimates in the field during construction. The dynamic formulas make use of site-specific pile driving data and provide approximate confirmation of capacity based on driving resistance and hammer energy; however, several of the methods have been demonstrated to provide large scatter (standard deviation) in capacity estimates as well as trends that are divergent from load test data at larger capacity (Fragazy et al, 1989, Hannigan et al, 1997b, Paikowsky et al, 2004, Allen, 2005). The trends provided in this chapter serve two purposes for foundation designers: (1) highlighting the range of uncertainty associated with each of the dynamic formulas when compared to CAPWAP analyses, and (2) provide a framework for adjusting the results of dynamic formulations to obtain “equivalent” CAPWAP results. While the correlations provide improved estimates of pile capacity during construction they should not be used in lieu of project-specific PDA monitoring and CAPWAP analysis.

The development and application of dynamic formulas analyses, PDA, and CAPWAP are well addressed in foundation engineering textbooks, design manuals, and other technical literature (e.g., Bowles 1996, Poulos and Davis, 1980, Prakash and Sharma, 1990, Tomlinson, 1995) and will not be summarized in this report. In addition, very worthwhile, practice-oriented papers and reports covering this background, as well as the strengths and limitations of the methods, have been presented by Hannigan and others (1997b), Paikowsky and others (2004), and Rausch and others (1985). Valuable insight on the use of these dynamic methods is provided by Paikowsky and others (2004), and reproduced in Table 4-1. The calibration of the dynamic formulas using region-specific data and local experience has been highly recommended in all of these comprehensive investigations. The database has been used to identify trends in the axial capacities computed with four widely-used dynamic formulas, providing refined estimates for applications involving open-ended steel pipe piles in similar soil deposits.

**Table 4-1: Dynamic methods for evaluating pile capacity: advantages, disadvantages, and comments (Paikowsky et al, 2004).**

Category	Method	Advantages	Disadvantages	Comment
Design Stage	WEAP (Smith, 1960, Goble et al., 1976)	- Equipment Match - Drivability Study - Structural Stresses	- Non unique Analysis - Performance sensitive to field conditions	- Required for Construction - Required Evaluation for capacity predictions
Dynamic Equations	ENR (Wellington, 1892)	- Sound Principles - Common use	- Unreliable	- Needs to be examined without a built in FS.
	Gates (Gates, 1957)	- Empirical - Common use	- Depends on original database	- Found to be more reliable than other equations
	FHWA version of Gates Eqn. (FHWA, 1988)	- Correction based on additional data	- Depends on database	- Was found to be reliable
Dynamic Measurements	Signal Matching (e.g. CAPWAP) (Goble et al., 1970)	- Solid principle of matching calculations to measurements by imposing msd. B.C.	- Stationary soil forces - Expensive - Requires time	- Office Method - Found reliable at BOR
	Case Method (Goble et al., 1970, Rausche et al., 1975)	- Simplified Analysis - Field Method	- Requires local calibration - Presumed dependency of soil conditions found baseless	- Was found reliable with local calibration - How to obtain national or international calibration?
	Energy Approach (Paikowsky, 1982, Paikowsky et al., 1994)	- Simplified Analysis - Field Method	- Shows long-term capacity which may not be present at EOD	- Ideal for construction

NOTES: ENR = Engineering News Record; FS = Factor of Safety; BOR = Beginning of Restrike; EOD = End of Driving.

The trends in direct comparisons of the results of dynamic formulas with CAPWAP analyses provide useful adjustment factors for future project-specific applications. As applied in the field the procedure may include: (i) collecting the pile driving records for EOID conditions, (ii) computing the static axial capacity of the pile using the dynamic method(s) of choice, then (iii) adjusting the results of the dynamic formulas to an equivalent CAPWAP capacity. It is recommended that two or three dynamic formulas be applied with judgment-based weighting factors in order to obtain a representative average axial capacity. The trends observed using CAPWAP and dynamic formulas for BOR conditions are also illustrated in this chapter.

This procedure does not account for the differences between capacities obtained by CAPWAP and static load tests, as has been quantified in other investigations (Fragazy et al, 1989, Paikowsky et al, 2004, Allen, 2005, Smith et al, 2011). It would be preferable to compare the results of the dynamic formulas to static load test data; however, the lack of readily available static load test data in the public domain for open-ended steel pipe piles in Alaska precludes this more direct assessment. An attempt was made to establish the ratio of CAPWAP capacity to static load test capacity from data presented in the extensive databases previously cited, but an insufficient number of cases for open-ended steel pipe piles with diameters of interest (36 to 48 inches) in cohesionless soils were presented to provide a meaningful value. For this reason, the correlations from the Alaska PDA database focus only on CAPWAP-based capacities. Adjustments made to the CAPWAP capacities to yield predictions for an equivalent static load test will require judgment involving the influence of key factors such as: time between End of Initial Driving (EOID) and Beginning of Restrike (BOR), soil types and density, Area Ratio (embedded surface area/area of pile tip), and the toe and shaft quakes at BOR compared to the soil-pile displacement required to mobilize full toe and shaft resistances. A thorough assessment of these factors for the development of capacity estimates representative of static load testing was outside the scope of this investigation.

The four dynamic methods used for comparison in this investigation are:

### 1. Engineering News (EN) Formula.

$$Q_{all} = \frac{2WH}{S+0.1\left(\frac{Wd}{W}\right)} \quad (4-1)$$

where;

- $Q_{all}$ : Allowable pile load in pounds  
W: Weight of the striking parts of the hammer in pounds  
H: Height of fall in feet  
 $W_d$ : Driven weights including pile in pounds  
Notes: This formulation is used when the driven weights are larger than the striking weights. A slightly modified formulation is applied when the striking weights exceed the driven weights (Prakash and Sharma, 1990)  
The ultimate nominal capacity is computed as:  $(Q)_{ult} = \text{Factor of Safety} \cdot (Q)_{all}$

### 2. Janbu Equation for Piles in Sand (1956).

$$Q_{ult} = \frac{WH}{k_u \Delta s} \quad (4-2)$$

where;

- $Q_{ult}$ : Ultimate bearing capacity  
W: Weight of the hammer  
H: Height of fall of the hammer  
 $k_u$ : dimensionless correlation parameter that is obtained graphically (Figure 4-1)  
 $\Delta s$ : average permanent set per blow at the end of driving  
Note: An example is provided in Figure 4-1 for the application of the Janbu method

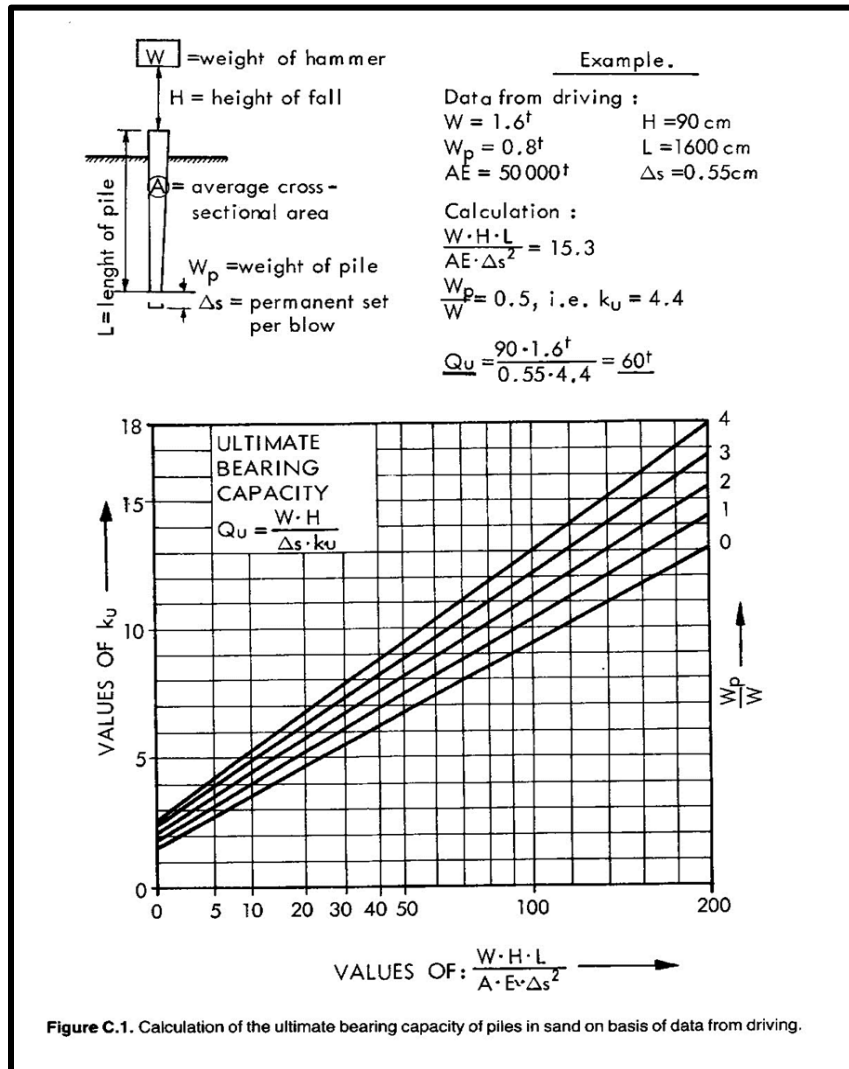


**Figure 4-1: Chart for application of the Janbu method for estimating pile capacity in sand (Janbu, 1956; figure from Bruun, 1981).**

**3. FHWA Gates Equation (as adopted by the Oregon Department of Transportation).**

$$R_u = [1.60\sqrt{E} \log(10N) - 100] \quad (4-3)$$

where;

- $R_u$ : Ultimate pile bearing capacity (kips)
- $E$ : Hammer energy (foot-pounds) at the ram stroke observed in the field. This is computed as  $W \cdot H$
- $W$ : Weight (pounds) of striking parts of hammer
- $H$ : Height of fall (feet) of the ram measured or computed (e.g., from saximeter readings) during pile driving in the field
- $\log(10N)$ : Logarithm to the base 10 of the quantity  $10 \cdot N$
- $N$ : Number of hammer blows per inch at final penetration

#### 4. WSDOT Equation (Allen, 2005, 2007).

$$R_n = 6.6 \cdot F_{eff} \cdot E \cdot \ln(10N) \quad (4-4)$$

where;

- R<sub>n</sub>: Ultimate, or nominal, bearing resistance mobilized during driving in kips
- F<sub>eff</sub>: Hammer efficiency factor
- E: Developed energy of pile hammer, equal to W · H, in foot-pounds
- ln(10N): Natural logarithm of the quantity 10 · N
- N: Number of hammer blows per inch (originally defined as the average penetration resistance in blows/in for the last 4 inches of driving [2005])

These methods were selected on the basis of one or more of the following criteria: (i) familiarity in practice, (ii) noted accuracy in investigations involving large collections of static pile load test data, and/or (iii) recent development and demonstrated applications on highway transportation projects. The estimated axial pile capacities using each of the four methods for the cases in the database are plotted against the analytical CAPWAP results for both EOID and BOR conditions. The final driving resistances (*blow/count* or *set* as required by the specific method), hammer specifications, and ram stroke at the end of driving were obtained in almost all cases from the dynamic testing reports and have been tabulated in the database. Additional data was obtained from the ADOT&PF field pile driving records.

For the sake of initial comparison, the capacities estimated using the simplified Case Method (RMX) are plotted against the CAPWAP results. Both of these methods make use of the PDA data, yet differ in the approximations and assumptions made regarding aspects of soil and pile behavior. The comparison of the computed results for both methods is provided in Figure 4-2. The figure demonstrates the influence of the modeling procedures on the computed pile capacity using the same PDA data. As anticipated, the agreement between the two methods is generally very good with most of the Case Method estimates falling within roughly ±20% of the CAPWAP results. The frequency distribution of the ratio of the capacity estimate made by the Case Method to the CAPWAP analysis for both EOID or EOD2 and BOR are provided in Figure 4-3. The histograms of these ratios are plotted to evaluate whether the data is log-normally distributed and assess possible skew in the trends. The expected good agreement between the methods is indicated by the relatively small standard deviation.

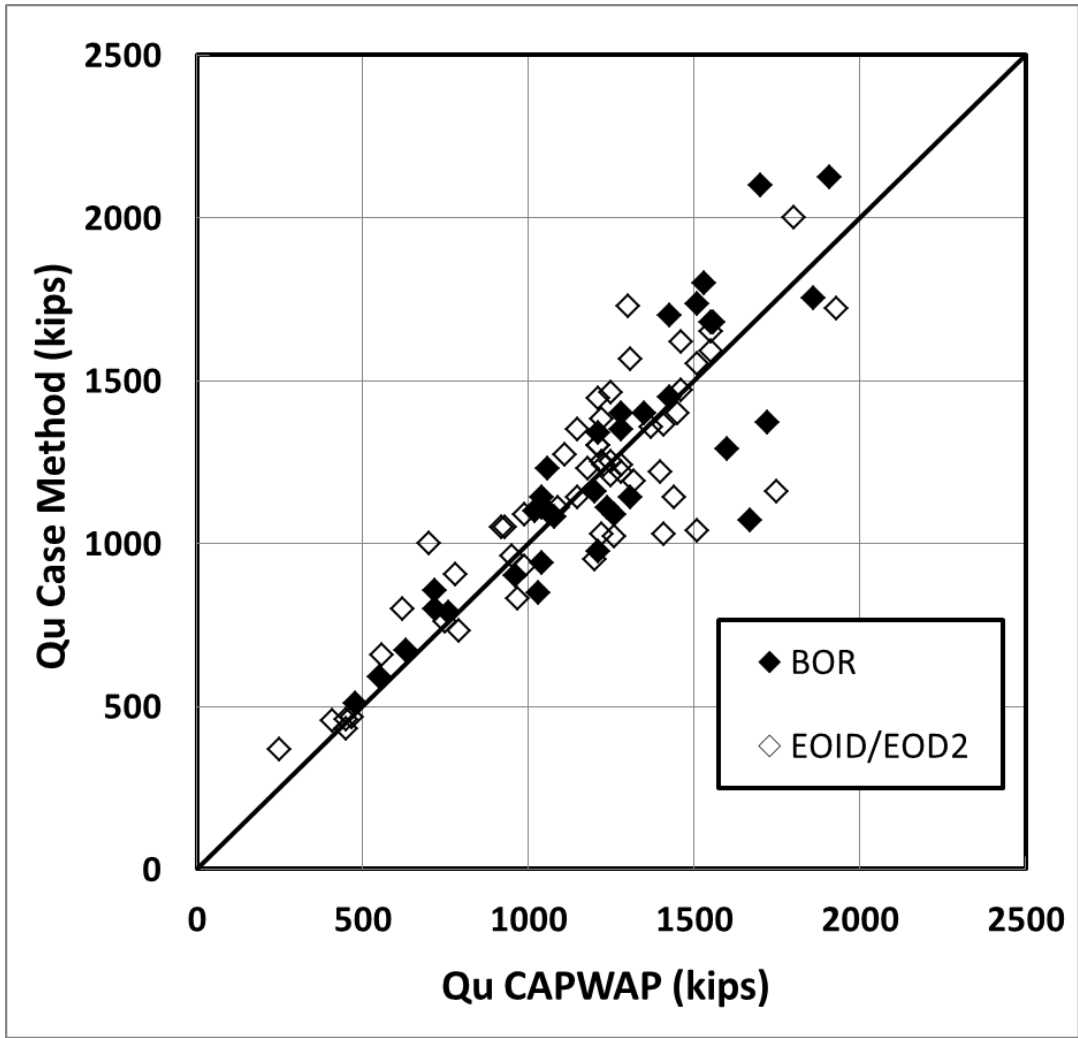


Figure 4-2: Nominal pile bearing resistance estimated using the Case Method versus that estimated with CAPWAP.

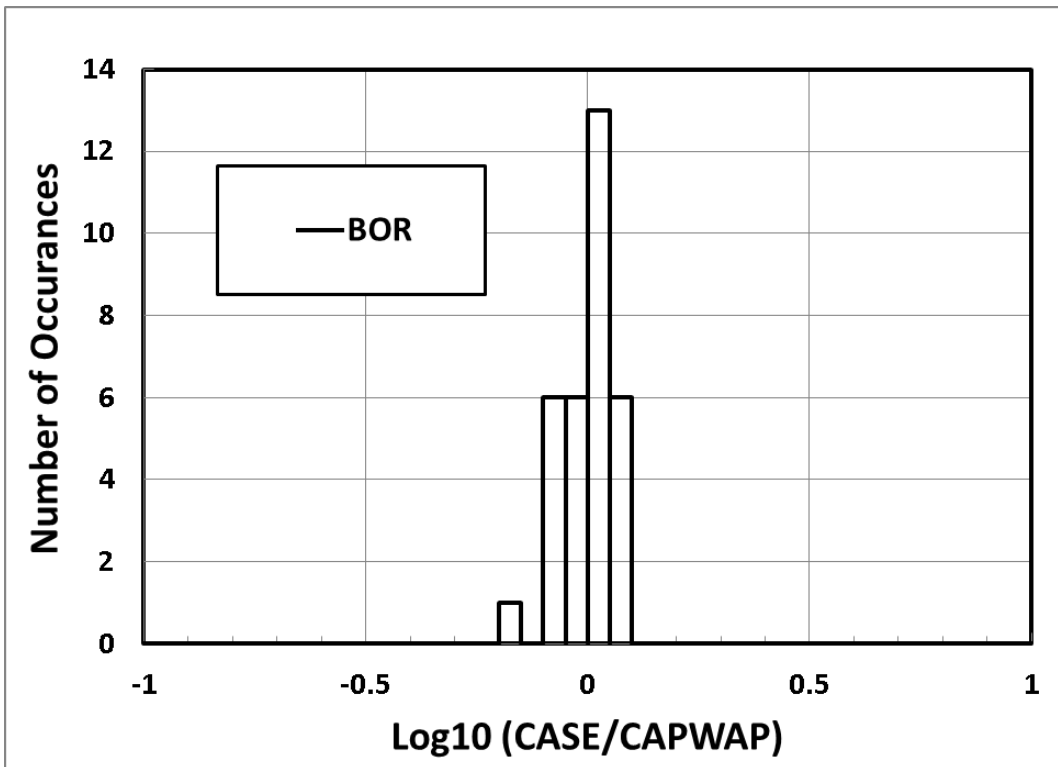
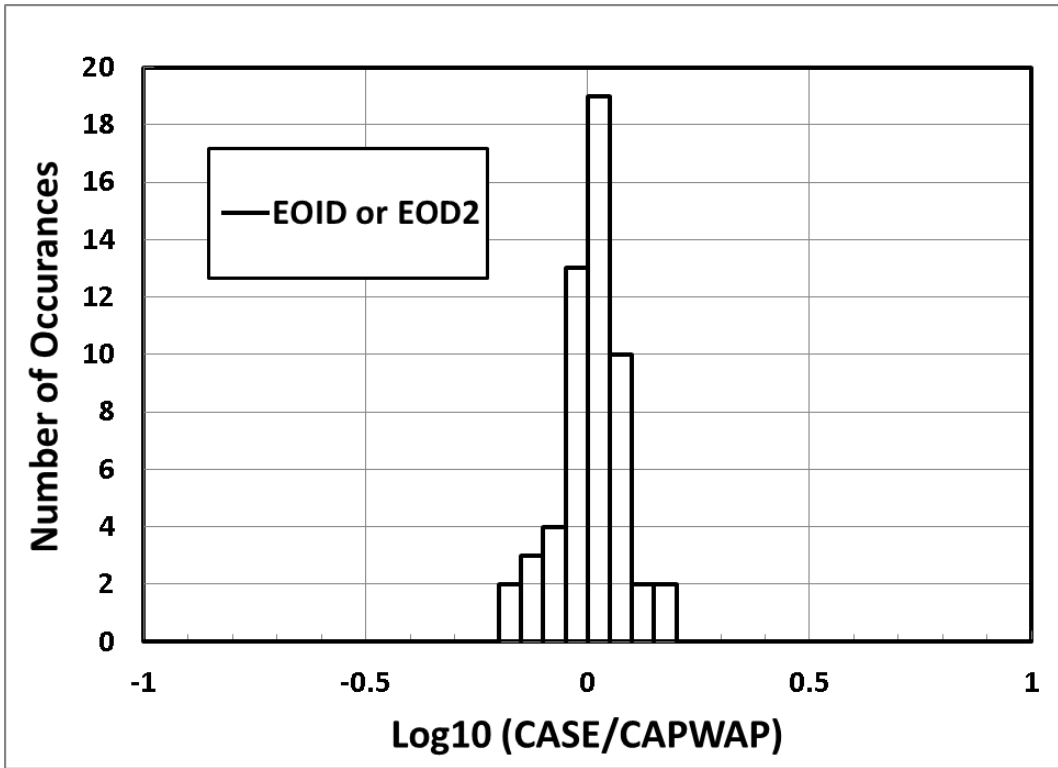


Figure 4-3: Histograms for comparison between the results of the Case Method and CAPWAP analysis at End of Driving and Beginning of Restrike.

The variability and applicability of the four dynamic formulas selected herein should be made with the trends in Figures 4-2 and 4-3 in mind. The simple dynamic methods should not be expected to provide capacity estimates that compare as favorably to CAPWAP as the results of the Case Method.

#### **4.2 APPLICATION OF DYNAMIC FORMULAS AND COMPARISON TO CAPWAP**

The trends in the ultimate soil resistance based on the four dynamic formulas relative to CAPWAP analyses are provided in Figures 4-4 to 4-11, and briefly addressed as follows.

Engineering News Method - The results of the Engineering News Method are plotted in Figures 4-4 and 4-8. The figures provide the comparison between the nominal capacity obtained by CAPWAP and the nominal capacity computed using the EN formula. A safety factor of 2.25 was used to adjust the allowable capacity provided by the EN Method to the nominal value. The value of 2.25 was selected to provide a reasonable overall trend between the two dynamic methods. The large variability in the capacity estimates relative to CAPWAP is evident. This variability has been noted in many investigations. The strengths and limitations of the EN Method have been well covered in the technical literature, and it has been gradually replaced over the past 20 years due to the large uncertainty and potentially unconservative capacity estimates that can be obtained. Figure 4-8 illustrates the relatively large variability in the capacity estimates using the EN Method. While the results could be adjusted by changing the factor of safety to yield a mean axial capacity that compared very favorably to CAPWAP, the scatter in the estimates would remain, with similarly large standard deviations.

Janbu Method – The Janbu Method has been adopted worldwide and provides benefits over the EN Method for piles in sand. The trends (Figures 4-5 and 4-9) demonstrate a much better correlation to the CAPWAP results, with BOR data providing somewhat closer estimate than the EOID data. In both cases the estimates are generally within 25% to 30% of the CAPWAP estimates.

Gates Equation – The Gates equation, as revised in Hannigan and others (1997), provided very consistent results when compared with CAPWAP. The standard deviation was the smallest of the four methods used in this investigation; however, the Gates equation demonstrates a pronounced trend in under-prediction of nominal capacity relative to CAPWAP (Figures 4-6 and 4-10). Remarkably similar trends have been demonstrated in comparisons of capacity estimates based on the Gates equation with static load tests (Fragazy et al, 1989, Allen, 2005). In light of the small variability exhibited using the Gates equation, this method is recommended for ADOT&PF projects with the nominal capacity adjusted to reflect the trend illustrated in Figure 4-6 to yield an equivalent CAPWAP capacity estimate.

WSDOT Equation – The Washington State Department of Transportation (WSDOT) developed a pile driving formula as a part of a larger investigation focused on calibrating LRFD factors for static axial capacity estimation (Allen, 2005, 2007). As with the Gates equation, the WSDOT formulation provided very consistent estimates and also exhibited a pronounced trend with increasing capacity (Figures 4-7 and 4-11). The WSDOT equation tended to slightly over-predict the capacity relative to CAPWAP. This method is also recommended using the same adjustment procedures outlined for the Gates equation.

### 4.3 RECOMMENDATIONS

Of the four dynamic formulas evaluated in this investigation, the Janbu, Gates, and WSDOT methods provide static axial capacity estimates for pipe piles that, when adjusted for average trends, are recommended for practice-oriented estimates of CAPWAP capacity. The EN Method is not recommended for use on ADOT&PF projects. Given the simplicity of the three dynamic formulas all three methods are recommended for use in the field, with the final capacity estimate based on a weighted average of the three methods. Statistical evaluation of the data trends and reliability analyses were outside the scope of this project, therefore, the relative weighting factors have not been developed. In the absence of more rigorous statistical analyses it is recommended that a weighting factor of 0.33 be applied to the adjusted ultimate resistance estimate made by each method thereby providing equal weighting and the mean value. On projects for which no PDA monitoring is available the trends in the EOID data presented in this chapter will be the most applicable, therefore, adjustments should be applied for the trends developed for EOID data. Restrike is usually carried out with the benefit of PDA instrumentation thus eliminating the need to rely on the simplified dynamic formulas for capacity estimation. The BOR trends were examined to identify possible systematic differences in the capacity estimates.

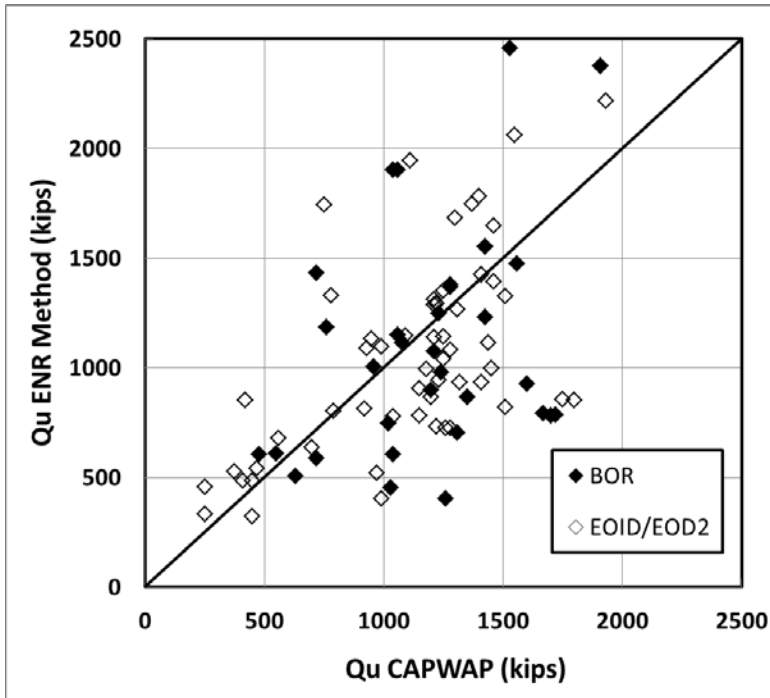


Figure 4-4: Nominal pile bearing resistance estimated using the EN Method versus that estimated with CAPWAP.

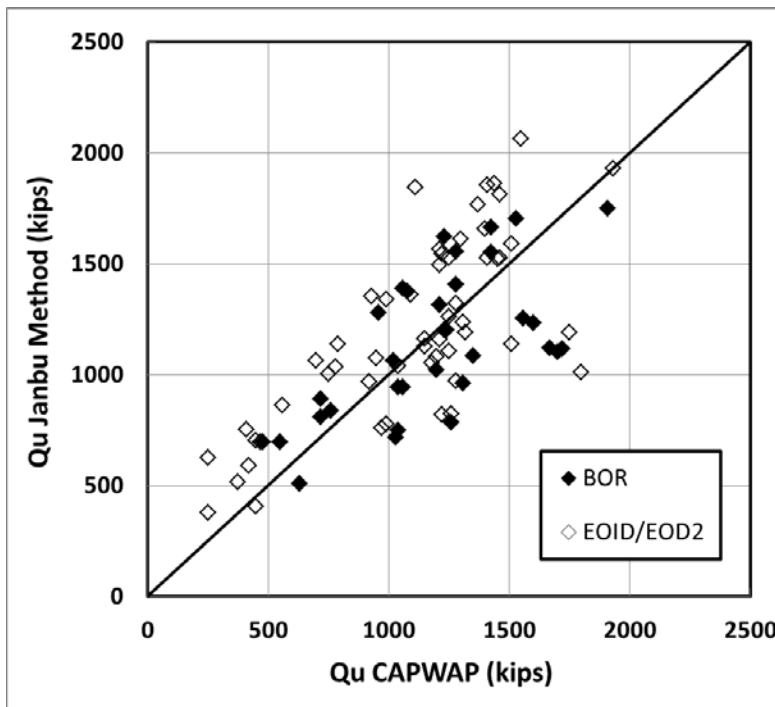


Figure 4-5: Nominal pile bearing resistance estimated using the Janbu Method versus that estimated with CAPWAP.

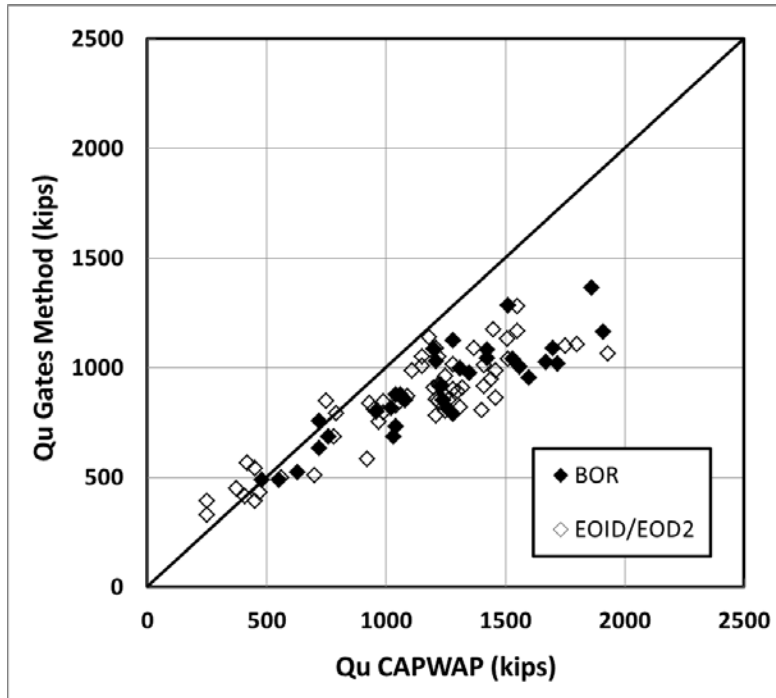


Figure 4-6: Nominal pile bearing resistance estimated using the Gates Equation versus that estimated with CAPWAP.

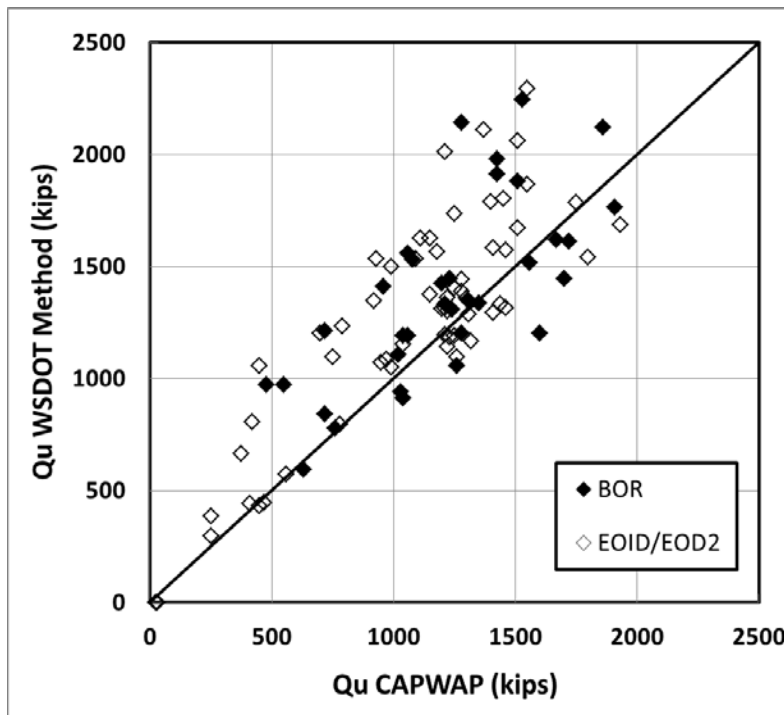


Figure 4-7: Nominal pile bearing resistance estimated using the WSDOT Equation versus that estimated with CAPWAP.

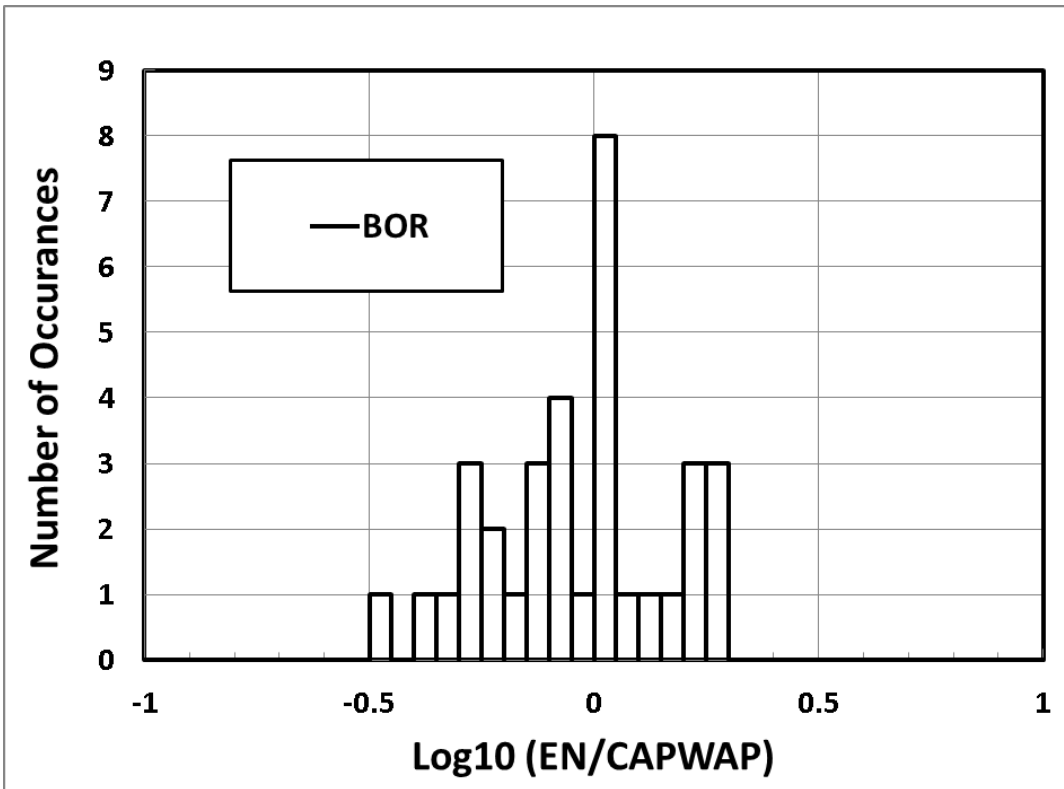
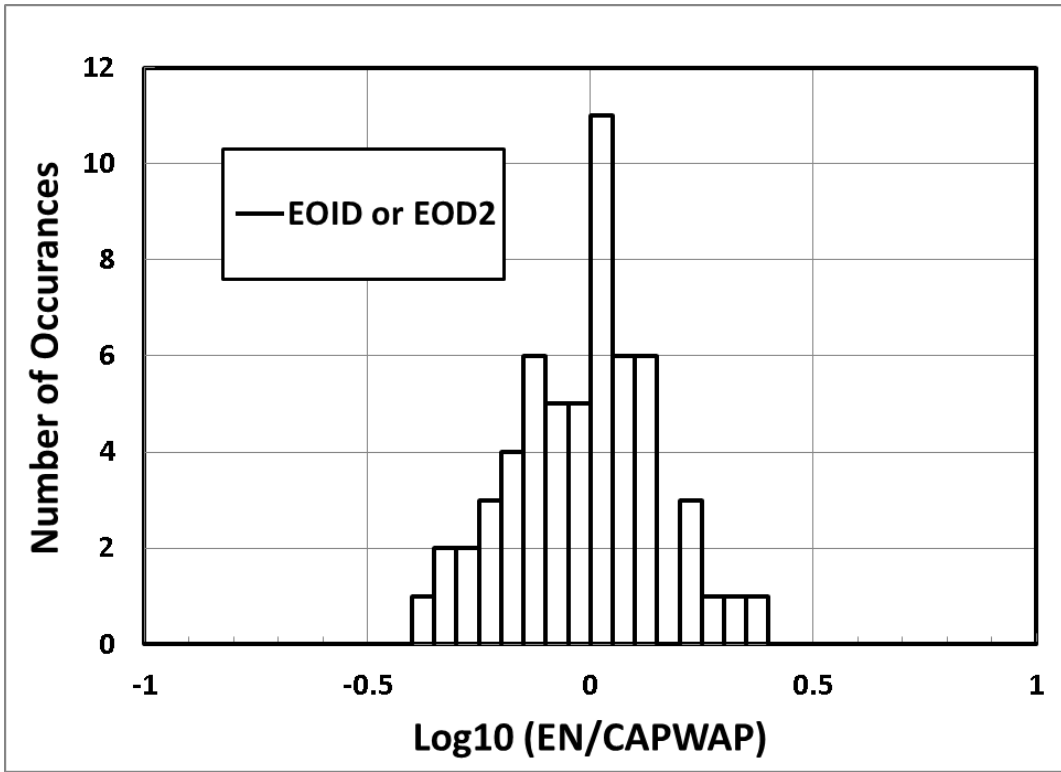


Figure 4-8: Histograms for comparison between the results of the Engineering News Method and CAPWAP analysis at End of Driving and Beginning of Restrike.

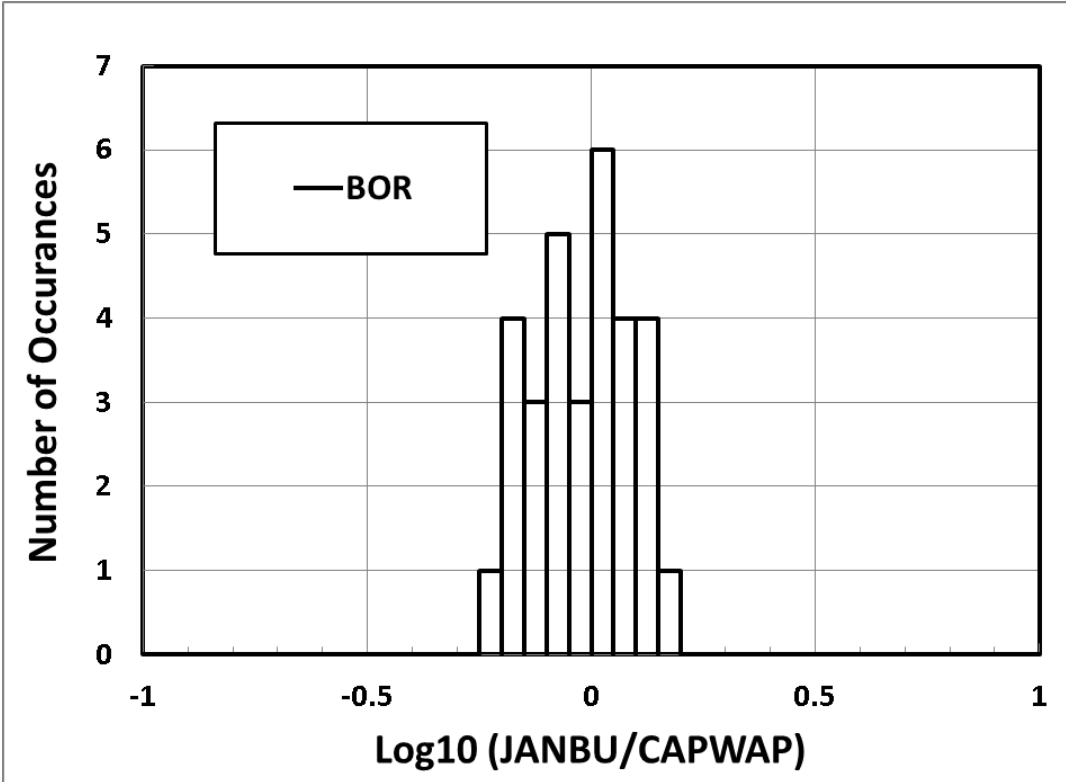
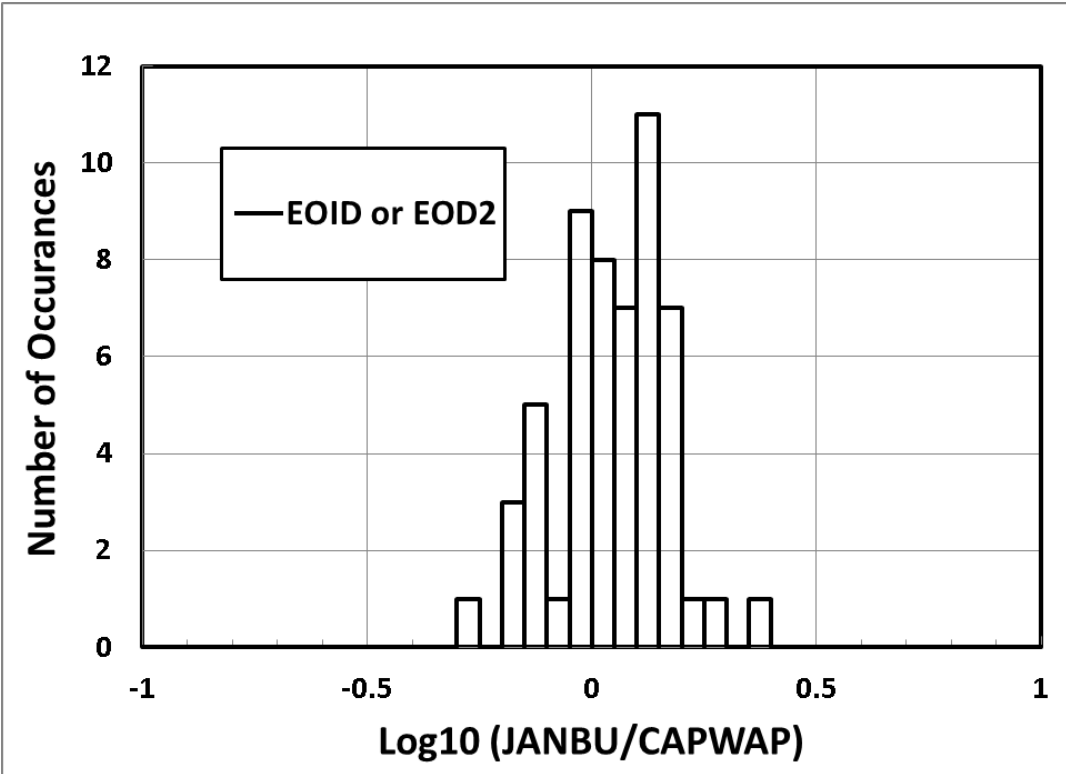


Figure 4-9: Histograms for comparison between the results of the Janbu Method and CAPWAP analysis at End of Driving and Beginning of Restrike.

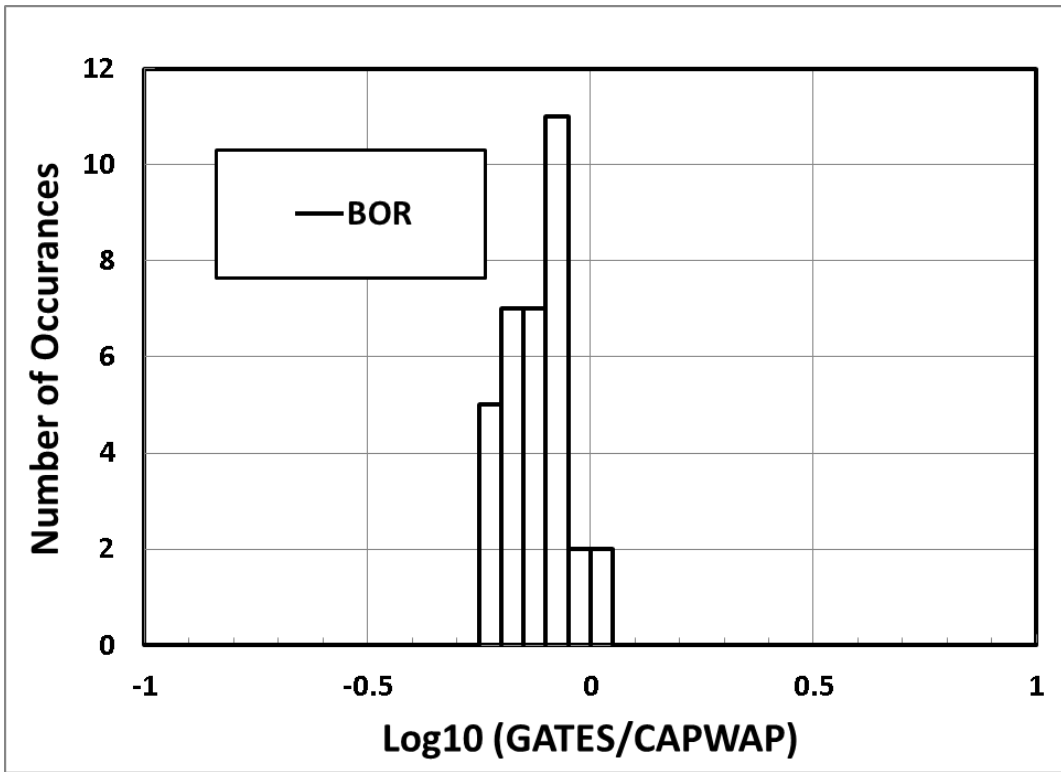
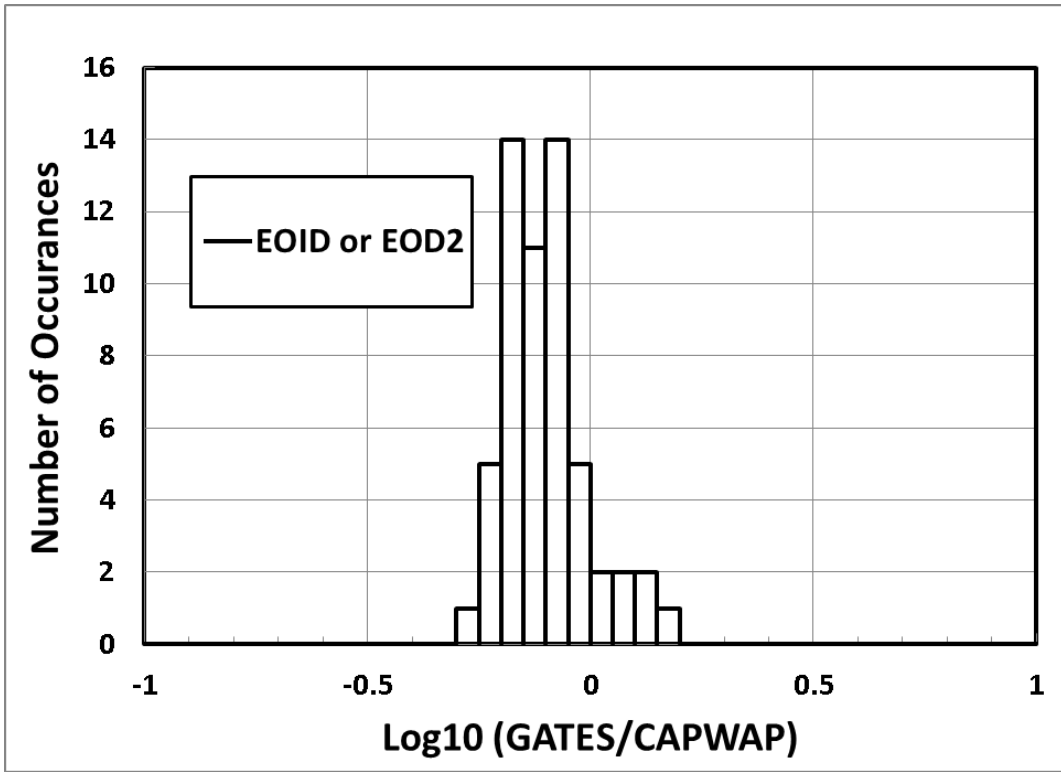


Figure 4-10: Histograms for comparison between the results of the Gates Equation and CAPWAP analysis at End of Driving and Beginning of Restrike.

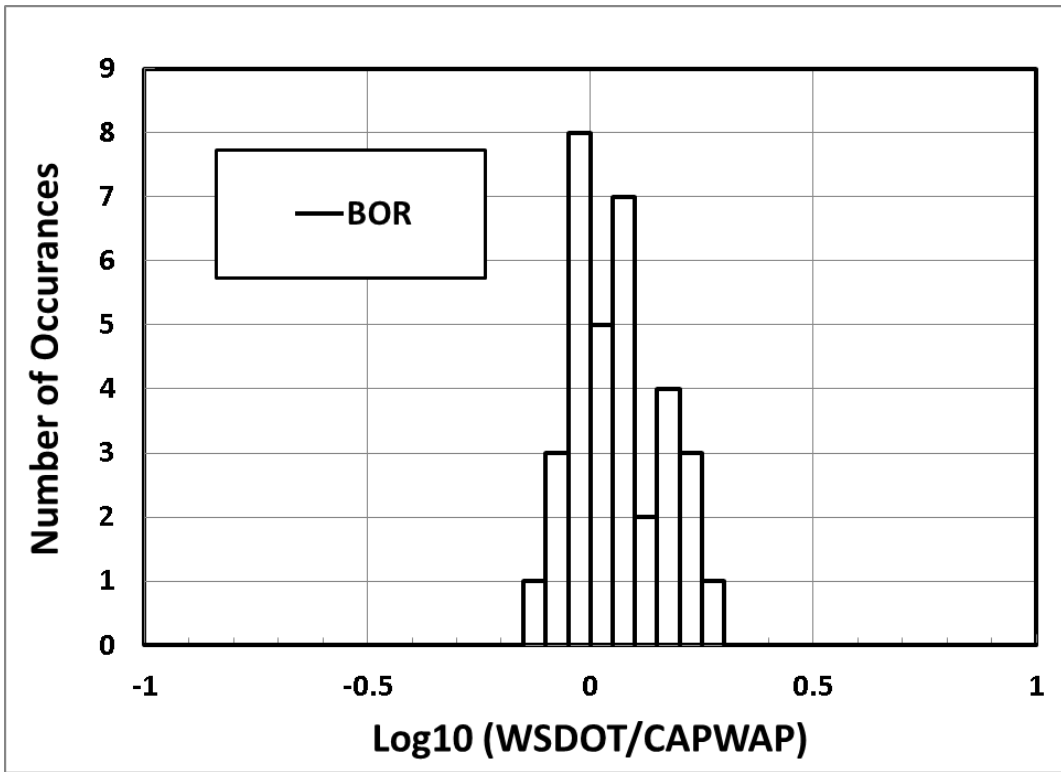
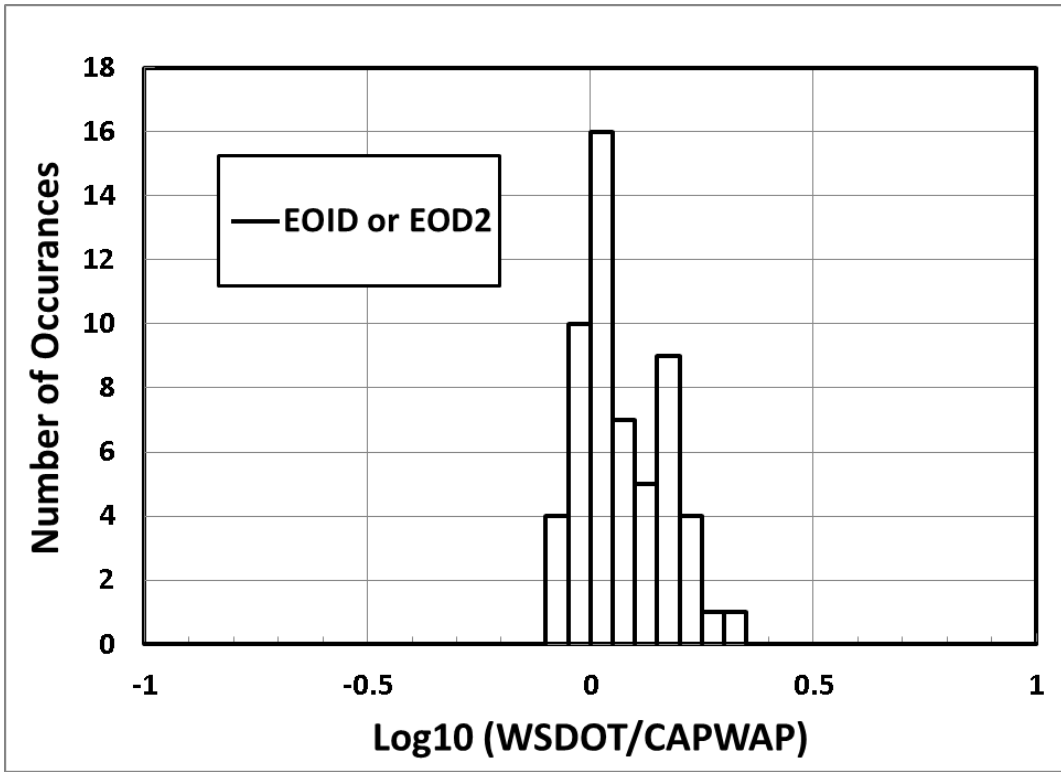


Figure 4-11: Histograms for comparison between the results of the WSDOT Equation and CAPWAP analysis at End of Driving and Beginning of Restrike.

## **5.0 EXAMPLE APPLICATION FOR DEEP FOUNDATION ANALYSIS**

### **5.1 INTRODUCTION TO THE CASE STUDY AND CLASS A PREDICTION**

The results of high strain dynamic testing (PDA) and analysis (CAPWAP) from 32 project sites in Alaska have been used in the development of the proposed empirical procedure for estimating unit shaft resistance and unit toe resistance for open-ended steel pipe piles. This CAPWAP-based method is intended to supplement the well-documented methods of analysis with the goal of reducing uncertainty in estimates of soil resistance and required pile lengths for ADOT&PF projects. The proposed practice-oriented method has been purposely developed to be similar to the Effective Stress Method commonly used in deep foundation design for bridge applications. In order to demonstrate the application of the proposed method a case study has been selected and the soil resistance determinations provided in a step-by-step manner following as outlined in Chapter 3 of this report. The Hyder Causeway Trestle replacement project in coastal, southeastern Alaska has been selected for this application.

The Hyder Causeway Trestle project (Hyder) provides a very timely and practical case study, as well as a Class A prediction of shaft resistance and toe resistance estimation procedures developed in this investigation. Both the CAPWAP-based method and the Effective Stress method were used prior to construction to estimate the pile capacity as a function of embedment depth before the pile driving. Shortly after the predictions were made pile driving was initiated at Hyder. Foundation support for the new trestle included 30, 24-inch diameter steel pipe piles with conical tips (closed-ended) driven into young, very loose, deltaic deposits of sand with gravel (SP), gravel with sand (GP), and silty sand (SM-SP). Pile embedment depths varied between approximately 92 feet and 161 feet. Dynamic testing and analysis (PDA and CAPWAP) were performed on 29 piles for the following conditions:

1. End of Initial Driving (EOID) tests on four piles.
2. Beginning of Restrike (BOR) tests on 29 piles, with waiting periods ranging from 1 day to 33 days between EOID and BOR.
3. Of the 29 piles tested for BOR, 12 were tested in a second BOR test conducted between 8 and 30 days after the first BOR test (total of 9 to 48 days after EOID).

The Hyder project provides the most extensive collection of PDA data and CAPWAP results in the ADOT&PF archives, adding 29 piles to the 68 in the database. The CAPWAP results from Hyder were not used to refine or amend the recommendations provided in Chapter 3 as incorporation of the data for 29 piles (45 PDA tests total) from this one site would skew the trends of the statewide database. A comparison between the field test results and the Class A predictions are provided as follows.

### **5.2 SITE INVESTIGATION AND PRELIMINARY FOUNDATION DESIGN AT HYDER**

The preliminary structural foundation engineering and foundation geology reports for the Hyder Causeway Trestle replacement project were completed in 2008 (ADOT&PF, 2008a, b). The causeway replaces an existing wooden trestle and provides access to a seaplane dock (Figure 5-1).

The preliminary design was conducted for a concrete bulb-T girder trestle resulting in unfactored dead loads plus live load estimated as 300 kips per pile, with factored dead loads plus live load of approximately 450 kips per pile. As described by ADOT&PF (2008a), the use of a soil/pile resistance factor of 0.65 with PDA/CAPWAP construction monitoring results in required nominal pile capacity of 700 kips per pile. Using a wave equation capacity determination during construction and associated resistance factor ( $\phi_r = 0.50$ ), the nominal pile capacity would need to be about 900 kips per pile.

Preliminary pile capacity estimates were made in 2008 using the FHWA program DRIVEN 1.2 (Mathias and Cribbs, 1998) with standard soil parameters for the cohesionless soils encountered at the site. These initial analyses were performed for three piling options: HP 14x117, 24-inch diameter closed-ended pipe pile, and 30-inch diameter closed-ended pipe pile. On the basis of the preliminary analyses the embedment lengths for the three pile types were estimated as 130 feet, 105 feet, and 90 feet, respectively.

During this stage of design (2008) two important recommendations were made by ADOT&PF engineers based on the geotechnical investigations and experience in the loose deltaic soil deposits:

1. *“Because of the loose soil conditions, it is recommended that careful monitoring be performed during construction to limit the potential for the piles “running” during installation.”*
2. *“PDA/CAPWAP will be used to confirm that the ultimate capacity has been achieved.”*

The existence of deep deposits of loose cohesionless soils and the potential for construction-related issues were identified, with recommendations in place for monitoring and dynamic testing during production pile driving.

Construction of the Hyder Causeway Trestle replacement (Figure 5-2) was initiated in late June 2012 with dynamic testing of piles conducted through the end of August 2012. Low pile driving resistance was experienced with correspondingly low soil resistance computed by CAPWAP analyses. This project provided a valuable opportunity to evaluate the inherent variability of soil resistance and CAPWAP results at one project site, and to highlight the strengths and limitations of the proposed CAPWAP-based procedures for estimating the axial capacity of single piles.



**Figure 5-1: Hyder Causeway Trestle and Harbor Island (Photo courtesy Andrew Banas, Robert Miner Dynamic Testing, Inc.).**



**Figure 5-2: Construction on the Hyder Causeway Trestle project (Photo courtesy Bruce Brunette, ADOT&PF).**

### **5.3 ESTIMATION OF AXIAL ULTIMATE BEARING RESISTANCE FOR PILES AT THE HYDER PROJECT SITE**

The following example provides an application for the analysis procedures provided in Chapter 3. The project-specific background and data used in this exercise have been drawn from ADOT&PF reports (2008a, b). The steps provided in Chapter 3 are highlighted and the trends of shaft resistance determined by several methods are plotted for comparison. The proposed CAPWAP-Based method for estimating unit shaft resistance (developed for open-ended piles) has been applied for the closed-ended piles used at Hyder due to the extensive program PDA testing completed on the project. The trends in soil resistance provided by the CAPWAP analyses provide useful data from which to assess the influence of pile toe condition (open versus closed end). The Hyder results are compared to the CAPWAP-Based methods with, and without, empirical adjustments for the closed-ended pile configuration.

#### **STEP 1: Classify the soil deposits based on the depositional environment and post-depositional stress history.**

The project site is located along the margins of the Salmon River delta in the Portland Canal fjord. The location of the existing trestle and the morphology of the delta are shown in the aerial image of the site (Figure 5-3). The following description of the site geology is taken from the Foundation Geology Report (ADOT&PF, 2008b):

*Hyder is located approximately 75 miles east of Ketchikan, Alaska, near the head of the Portland Canal fjord. The Salmon River in Alaska and the Bear River in British Columbia form large deltas at the head of the canal; with less than ¼ mile separating their intertidal zones. The two river valleys and the canal are steep-sided glacial-scoured geomorphic features. The recent geologic history of the region is one of cycles of glaciation followed by seawater inundation and slow rising of land due to isostatic rebound. During interglacial periods the Salmon and Bear rivers have deposited large amounts of alluvial sediments into their respective river valleys and deltas. The project site is located on the intertidal region of the Salmon River delta.*

*As a result of the past geologic events all or some of the following types of sediments could have been deposited; river alluvium (silt to boulders), beach deposits (preexisting material reworked by wave action), glacial deposits (till, moraines, outwash, erratics and drop stones) and marine sediments (silt, clay and marine organics). These sediments may be interbedded, reflecting cycles of glacial advance and retreat, subsequent seawater inundation and isostatic rebound. Bedrock was not encountered during the test drilling; the depth to bedrock in the immediate project area is unknown.”*

The soil deposits are classified in the boring logs as interlayered “Glacial Outwash/Delta Lobe” to the maximum depth of the borings at 141 feet to 161 feet. These are generally categorized for the sake of the proposed CAPWAP-Based Method as Site Class 1.

#### **STEP 2: Review the boring logs to establish soil layers and the location of the groundwater table.**

The native soils have been logged as predominantly sand with gravel, sand with silt, and gravel with sand. The site is located in the intertidal zone and is inundated twice daily. The water level is at or near the surface and groundwater is assumed to fluctuate in response to the tidal cycle.

### **STEP 3: Review particle gradation analyses.**

Seventy-five sieve analyses were completed to evaluate the particle size distribution of the sand and gravel deposits. Of the 75 specimens, only 13 had less than 40% by weight particles smaller than the #4 sieve (4.75 mm), and only 6 had less than 30% by weight sand-size particles or smaller. These tests confirmed the silty and gravelly nature of the sands, and suggest the sandy gravels appear to be matrix controlled (i.e., the engineering properties are governed by the sand matrix).

### **STEP 4: Compute the Vertical Effective Stress versus Depth.**

The vertical effective stress at 2-foot depth intervals was computed using a spreadsheet formulation. The groundwater table was assumed to be at the ground surface. The soil profile at boring TH-2 was used as the basis for the geostatic stress computation.

### **STEP 5: Develop plots of SPT $(N_1)_{60}$ versus Depth in soils that do not contain appreciable gravel or cobbles.**

Three water rotary borings were advanced to depths of 141 feet to 161 feet. Standard Penetration Tests were performed in two of the borings to a maximum depth of 120 feet. The SPT's were conducted using an autohammer with 140-lb hammer falling 30-in, and a 2.0-foot long, 2.0-in OD split-spoon sampler used without liners. The SPT N-values were adjusted to  $(N_1)_{60}$  values and the trend with depth is provided in Figure 5-4. No correction for sampler liner or fines content has been made for this plotting. The Modified Penetration Test was also used at the site; however, this data is not plotted for this example exercise.

The low SPT  $(N_1)_{60}$  values indicate the potential for very low unit shaft resistance. This is particularly evident at TH-2, where the average  $(N_1)_{60}$  value is approximately 5 bl/ft to Elevation -110 feet.



**Figure 5-3:** Aerial image showing the Salmon River delta and Hyder Causeway Trestle, Hyder, Alaska (GoogleEarth, 2012).

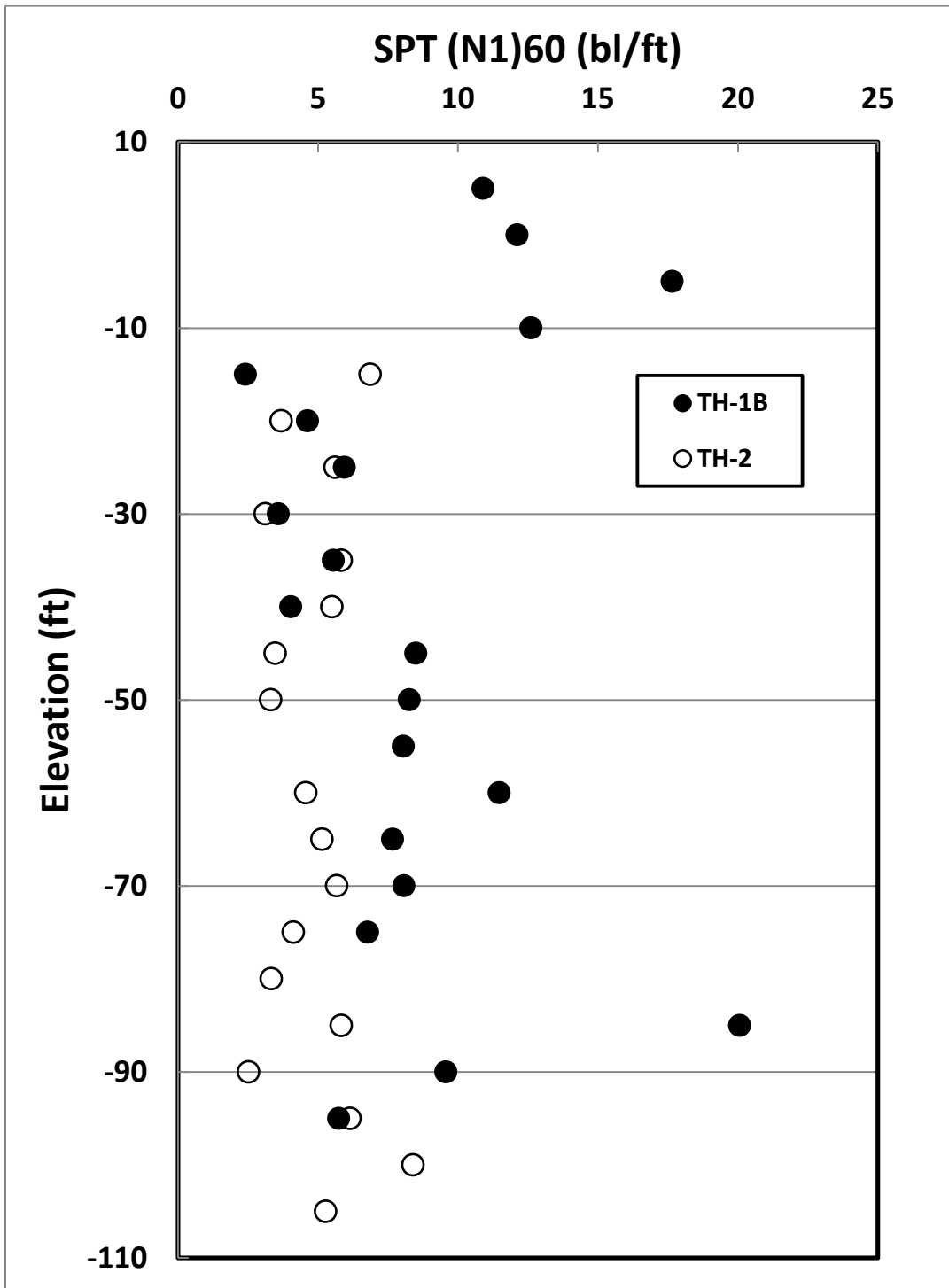


Figure 5-4: Trend of corrected SPT penetration resistance,  $(N_1)_{60}$ , versus elevation.

### **STEP 6: Review the trends of DOT&FP Friction Penetrometer with Depth.**

Two ADOT&PF Friction Penetrometer soundings were made at the site. The logs have been reviewed to screen for loose soils that could potentially result in very low unit shaft resistance values for steel pipe piles. A portion of one of the soundings (P-2) provided in Figure 5-5 demonstrates the low penetration resistance of the sandy deposits. The overall trend of penetration resistance to a depth of 150 ft can be simply approximated as;

$$N_{\text{ADOT}} \text{ (bl/ft)} \approx (0.50 \text{ to } 0.60) \cdot z \text{ (ft)}$$

This relationship indicates the potential for very low unit shaft resistance, which is consistent with the geologic environment, cohesionless soil deposits, and stress history of the soils (interpreted to be normally- to lightly-overconsolidated).

The results of the simple screening made on the basis of the ADOT&PF Friction Penetrometer are supported by the low corrected SPT N-values and indicate the potential for low to very low unit shaft resistance in these deposits. The  $(N_1)_{60}$  values are generally less than 10 bl/ft, extending to an elevation of -110 ft.

### **STEP 7: Evaluation of Unit Shaft Resistance.**

The unit shaft resistance has been evaluated using three methods to highlight the differences inherent in practice-oriented approaches to estimating unit shaft resistance mobilized along pipe piles in loose cohesionless soils. The three methods were: DRIVEN 1.2 (Norlund Method), the proposed CAPWAP-Based method, and the Effective Stress method. In light of the loose nature of the cohesionless deposits, lower bound  $\beta$ -coefficients (Table 3-1) were used in the Effective Stress method. The shearing resistance of the sandy gravel deposits was assumed to be controlled by the sand matrix, therefore, the  $\beta$ -coefficient was selected as representative of a predominantly sandy soil. An extremely low  $\beta$ -value of 0.1 was also applied for the sake of comparison.

### **STEP 8: Compute the Unit Shaft Resistance ( $f_s$ ) for each soil layer.**

The unit shaft resistance was computed on 5-foot depth intervals using the CAPWAP-Based method and Effective Stress method. The procedures provided in Chapter 3 were applied for computing  $f_s$  from the vertical effective stress and the respective unit shaft resistance coefficients ( $\beta, f_s/\sigma_v'$ ). A limiting maximum unit shaft resistance of 1.7 kips/ft<sup>2</sup> was applied.

The shaft resistance mobilized along each 5-foot section was then computed as the product of the unit shaft resistance ( $f_s$ ) and the external area of the 24-inch diameter pipe pile ( $\pi \cdot D \cdot 5\text{-ft}$ ).

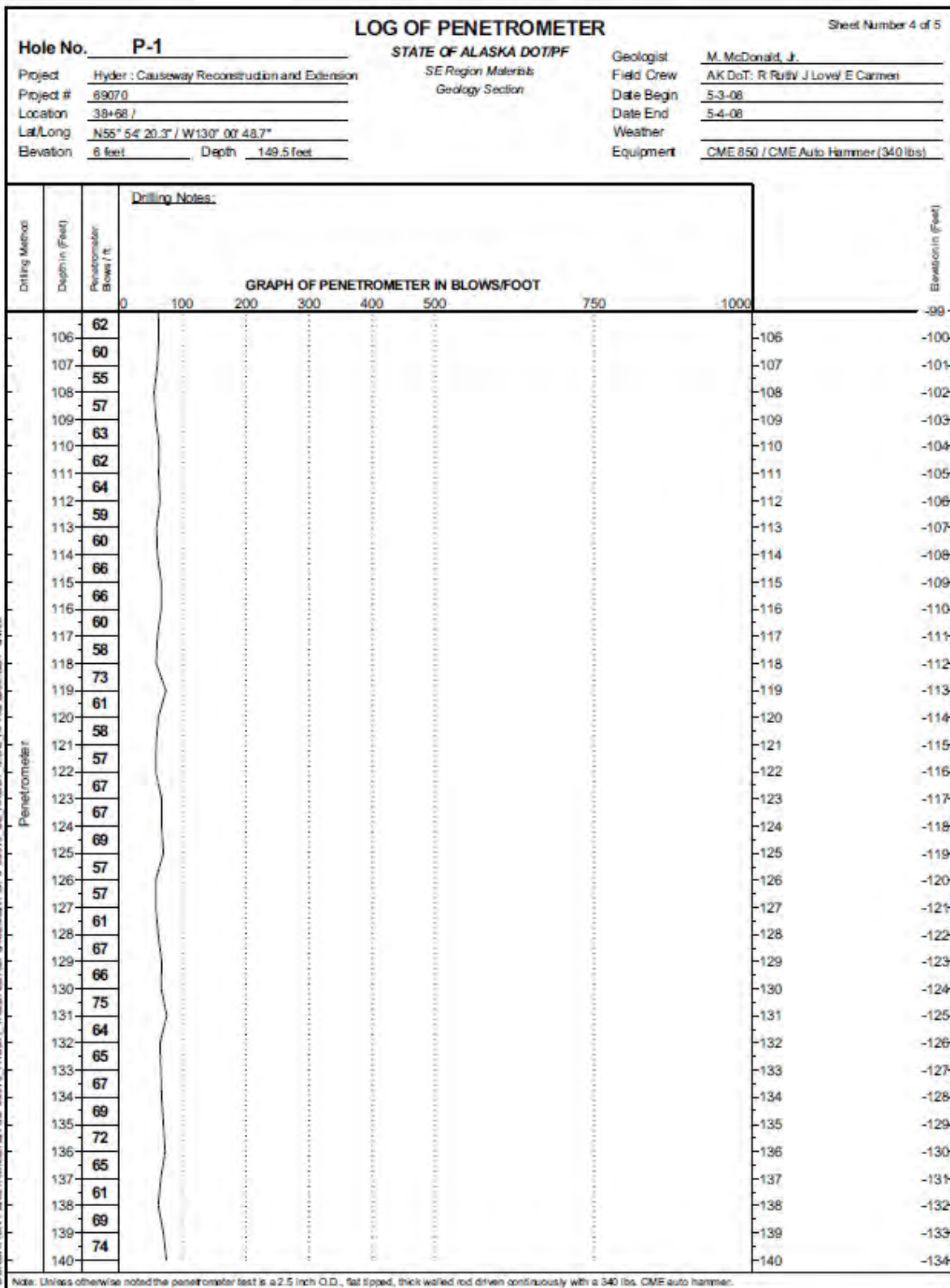


**Figure 5-5: Trend of Friction Penetrometer resistance versus depth.**

## **STEP 9: Compute the cumulative shaft resistance for the pile embedment of interest.**

The trends of cumulative shaft resistance versus pile embedment depth were computed using the three methods listed in Step 7. An additional trend was also computed using the Effective Stress method with a  $\beta$ -coefficient of 0.1, which represents a very approximate “mean – 1 standard deviation” relationship based on the CAPWAP database. It should be noted that lower values were observed at several sites in the database. Therefore, this does not represent the lowest bound possible for pipe piles in these soils. The four trends are provided in Figure 5-6 and demonstrate significant differences resulting from the various procedures. The recent compilation of CAPWAP data has helped to bracket the likely range of unit shaft resistance values and increased confidence in the pile embedment depths required to achieve design shaft resistance.

As a check on the computed shaft resistance, a case history from the database was selected for comparison. The criterion for selection of a representative project was based on the similarity of the: geologic history (depositional environment and stress history), soil types, and pile type(s). Of the 32 projects represented in the database, the Gustavus Causeway Replacement project was selected. The ADOT&PF Foundation Report (1998) provides the following background on the Gustavus site:

*“Gustavus lies on the north shore of Icy Passage at the mouth of the Salmon River, 48 air miles northwest of Juneau in the St. Elias Mountains... Quaternary surficial sediments typically consist of sandy intertidal, beach and marine deposits. Littoral drift is responsible for most erosion/deposition at this site.*

*Gustavus dock is located near the mouth of the Salmon River in the intertidal zone of Icy Passage and crossed a broad expanse of intertidal surficial sands that are exposed at low tide.”*

The soils at the Gustavus site are predominantly sand, sand with silt, and sand with occasional gravel. The penetrations resistances measured using both the ADOT&PF Friction Penetrometer and the SPT were very low, similar to the trends exhibited at the Hyder Causeway Trestle project. The average unit shaft resistance computed from CAPWAP analyses using PDA data obtained at BOR for three piles at the Gustavus site (Golder Associates, 2009) is plotted against the proposed PDA-Based method in Figure 5-7. The trends are in reasonable agreement and the CAPWAP-Based method is interpreted to provide a good first-order estimation of the unit shaft resistance for steel pipe piles in the soils at both the Gustavus and Hyder project sites.

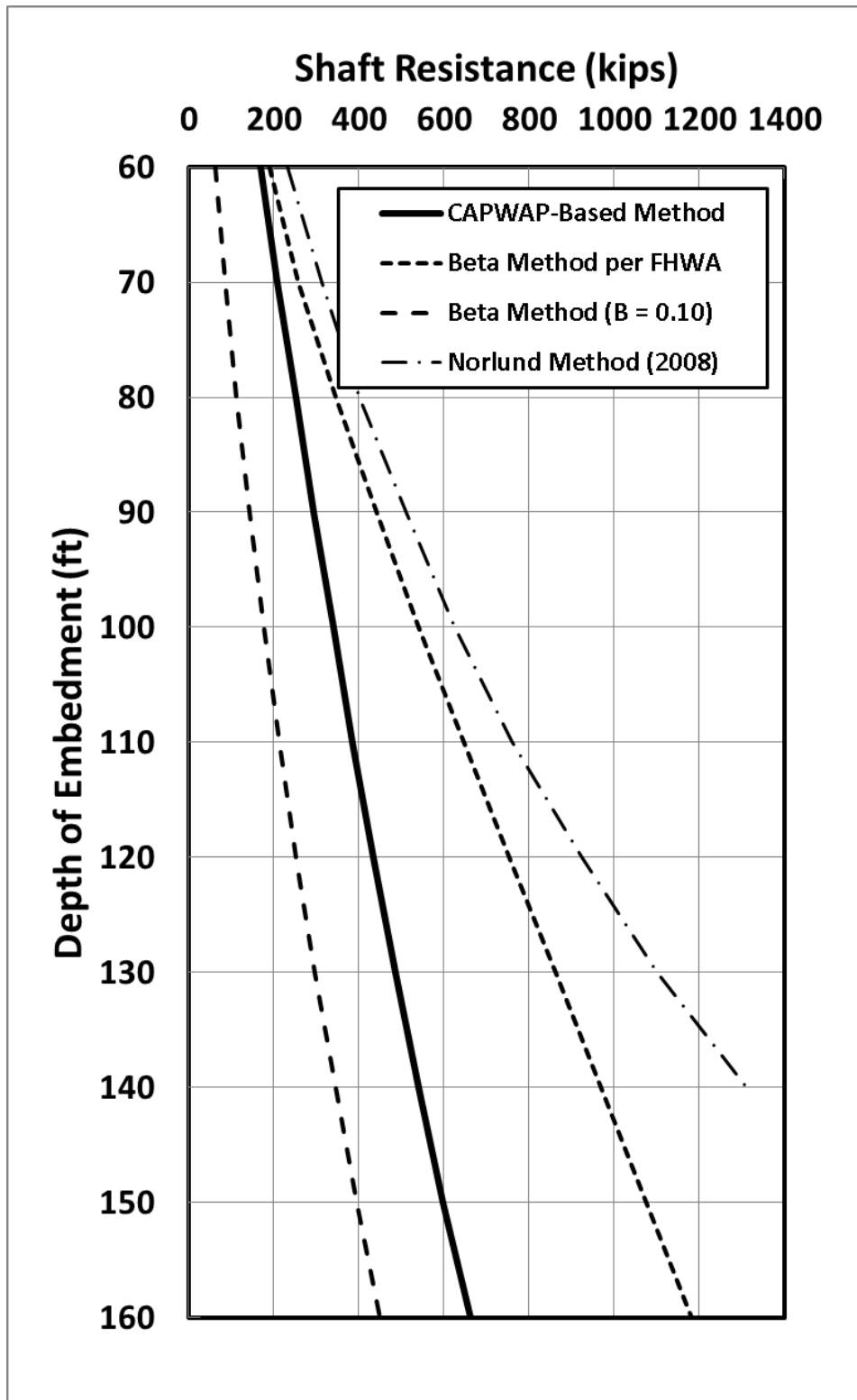


Figure 5-6: Trends of cumulative shaft resistance with embedment depth for a 24-inch diameter steel pipe pile.

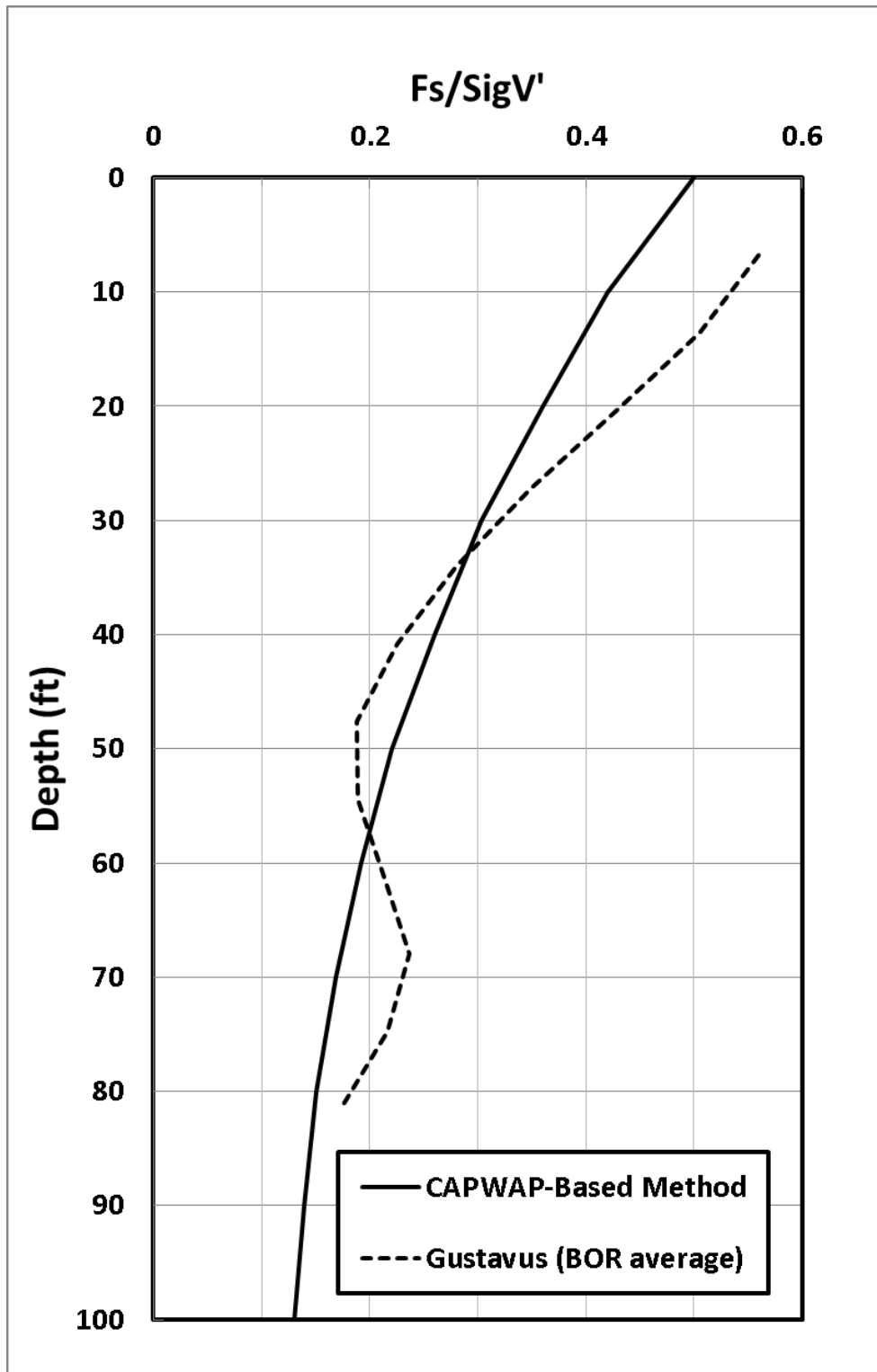


Figure 5-7: Trends of stress-normalized unit shaft resistance with pile embedment depth for dynamic load tests (BOR) on 3 piles at the Gustavus Causeway Trestle project and the proposed CAPWAP-Base method.

### **STEP 10: Compute the unit toe resistance ( $q_t$ ).**

The unit toe resistance was estimated using both the Effective Stress Method and a likely lower-bound approximated using the CAPWAP-Based method. For the former method, the lower bound  $N_t$  coefficient for sand of 30 (Table 3-1) was applied, resulting in a unit toe resistance ( $q_t = N_t \cdot \sigma_v'$ ) that varied from 168 to 269 kips/ft<sup>2</sup> at depths of 100 and 160 feet, respectively. These values are substantially greater than recommended maximum limits for loose sand. The limiting unit toe resistance for loose sand with a  $\phi'$  value of 30° could be as low as 15 kips/ft<sup>2</sup> (Meyerhoff, 1976, in Hannigan et al, 1997).

The projects documented in the database all involved open-ended pipe piles. Given the depths of embedment it is assumed that a semi-rigid, yielding plug developed in almost all cases. Neither the dynamic or static behavior of the plug was quantified in this investigation. For this example, the “equivalent unit toe resistance” computed from CAPWAP analyses is not directly applicable due to the closed-end conical tips that were employed. The use of the “equivalent unit toe resistance” based on PDA/CAPWAP data should yield a lower bound value of  $q_t$  for close-ended pipe piles. For the sake of comparison, the equivalent  $q_t$  values for 24-inch diameter, open-ended pipe piles at the Gustavus site ranged from 11 to 39 kips/ft<sup>2</sup> for pile embedment of 63 to 90 feet, respectively.

The following insight regarding the possible pile configuration provided in the dynamic testing report (Golder Associates, 2009) may additionally influence the comparison between the Gustavus and Hyder Causeway projects:

*“Based on information provided by ADOT & PF site personnel, the 24-inch diameter vertical piles were installed generally-open ended. Some of the piles were reported to have an internal plate at about 80 feet from the pile tip. The internal steel plate is about 1 inch thick with two stiffeners welded on top of the internal plate.”*

The Golder report states that an internal plate was used in one of the three piles (B13-W), 79.8 feet from the pile tip.

Based on a review of the equivalent  $q_t$  values in the database for pile diameters of 24-inch to 36-inch and end bearing in sand to silty sand, a value of 20 kips/ft<sup>2</sup> was selected for this example. This value was increased for the close-ended condition by a factor of 1.3 based on limited PDA data from other regions and observations made by Paik and others (2003), resulting in a unit toe resistance ( $q_t$ ) of 26 kips/ft<sup>2</sup>.

### **STEP 11: Compute the ultimate toe resistance ( $R_t$ ).**

The ultimate toe resistance is estimated to range from approximately 45 to 85 kips for a 24-inch diameter closed-ended pipe pile.

### **STEP 12: Consideration of plug development.**

The piles were driven closed-ended, therefore, the soil plug is not considered. Had open-ended pipe piles been used then the likelihood of plug development could have been assessed using empirical guidelines on the embedment depth required for plug development (i.e., pile penetration/pile diameter ratios per Hannigan et al, 1997, or the DRIVEN 1.2 Manual, 1998). If pile penetration is greater than roughly 20 to 35 times the pile diameter then the

CAPWAP-Based estimation procedure for  $q_t$  could be used, with a consistency check made using the Effective Stress Method or DRIVEN. The embedded pile lengths at Hyder ranged from roughly 90 feet to 160 feet (penetration to pile diameter ratios of 45 to 80), therefore, the difference in toe resistance between open- and close-end pipe piles may be relatively small in the loose sandy soils.

### **STEP 13: Compute the ultimate pile capacity ( $Q_u$ ).**

Given the initial design requirement of an ultimate axial resistance of 700 kip, the goal in this example problem is to determine the minimum allowable pile embedment. If a toe resistance of 65 kips is assumed, then the required shaft resistance would be 635 kips and the minimum pile embedment using the CAPWAP-Based method would be roughly 155 feet. This is compared to the preliminary estimate of 105 feet made in 2008, and roughly 110 feet based on the Effective Stress method using lower bound values of  $\beta$  and a limiting maximum unit shaft resistance of 1.7 kips/ft<sup>2</sup>.

### **STEP 14: Compute the allowable design load ( $Q_a$ ).**

The Foundation Engineering report (ADOT&PF, 2008a) provides the soil/pile resistance factors defined in AASHTO (2009) for LRFD design of deep foundations. The factors are functions of the type of pile capacity analysis performed (i.e., PDA/CAPWAP analysis, wave equation analyses, and static analysis methods). The axial capacity of 700 kips was provided in this case after the application of the soil/pile resistance factor of 0.65 assuming field construction monitoring with PDA and subsequent CAPWAP analysis.

This example has been presented to highlight the procedures and uncertainties associated with estimating the minimum required pile embedment for a prescribed ultimate pile capacity. The CAPWAP-Based method has been established from a large statewide database of PDA data, therefore, it is anticipated that for deep foundation applications in soil profiles similar to those making up the majority of the cases in the database the computed pile embedment lengths will provide reasonable agreement to project-specific PDA data and CAPWAP analyses.

For project applications involving the use of the CAPWAP-Based method and Effective Stress method to estimate pile capacities, dynamic monitoring and analysis (PDA/CAPWAP) are still recommended to confirm capacities, with the benefit of allowing for lower factor of safety or soil/pile resistance factors in LRFD-based design.

## **5.4 COMPARISON OF ESTIMATED SOIL RESISTANCE AND CAPWAP ANALYSES AT HYDER**

The design example outlined in Section 5.3 was completed prior to the initiation of pile driving on the Hyder Causeway Trestle project. The subsequent collection of CAPWAP analyses for 45 PDA measurements on 29 piles provides the opportunity to examine site-specific trends in pile behavior, assess variability in soil resistance across the site, and critically evaluate the practice-oriented static analysis methods for estimating soil resistance and pile capacity. The direct comparison of soil resistance estimates made prior to construction with the results of the PDA/CAPWAP analyses are provided as follows.

### 5.4.1 Shaft Resistance

The results of CAPWAP analyses for both first and second BOR tests have been reviewed for trends in the unit shaft resistance as a function of depth (consistent with the database) and the total shaft resistance at full embedment for each pile. The total shaft resistance determined by CAPWAP analyses for 16 piles is plotted in Figure 5-8 along with the trends provided by the CAPWAP-Based methods and Effective Stress method. It is again noted that the  $\beta$ -coefficients used for the Effective Stress procedure were the lower-bound values for sand as provided by Hannigan and others (1997, 2006). The 16 cases are for piles that were tested only once at BOR. The approximate time intervals between EOID and BOR for each pile test are provided in the figure and demonstrate the trend of increasing shaft resistance with time between 1 and 33 days.

In addition to the 16 piles that were tested at one BOR condition, 12 piles were tested at two BOR intervals, which further demonstrated influence of soil set-up on the shaft resistance. The time intervals between the first and second BOR test ranged from 8 to 30 days, thereby providing total intervals between EOID and BOR2 of as much as 48 days. The comparison of CAPWAP analyses and the predicted trends in total shaft resistance for these 12 cases is provided in Figure 5-9.

The CAPWAP analyses for the BOR tests at Hyder provide the following insights pertaining to the estimation of shaft resistance for the conditions on this project:

- The trend of total shaft resistance with depth provided by the CAPWAP-Based method is in very good agreement with the CAPWAP analyses for BOR cases conducted within roughly 1 to 5 days after EOID. This time interval is consistent with the majority of the cases represented in the database (median time between EOID and BOR 72 hours). The very favorable comparison of estimated and measured total shaft resistance for pile embedment depths between 90 feet and 160 feet provides a useful validation in this depth range.
- The increase in shaft resistance with time from EIOD is apparent in Figures 5-8 and 5-9. While there is a general trend in the CAPWAP results towards the shaft resistance provided by the Effective Stress method (using lower bound  $\beta$ -coefficients for the sandy soils) for EOID-BOR intervals greater than 30 days, the variability in the data do not allow for the development of time-dependent contour intervals for total shaft resistance.
- It is apparent for the conditions at Hyder that a reliance on CAPWAP results for BOR at time intervals less than roughly 6 to 8 days after EOID would yield conservative shaft resistance and pile capacity.
- Relatively minor increases in shaft resistance with time over 19 to 25-day intervals were observed for 5 piles (Figure 5-9).
- The development of time-dependent soil set-up factors for refining the CAPWAP-Based method is recommended. This issue is addressed in Section 5.5.

### 5.4.2 Toe Resistance

Toe resistance estimates made using CAPWAP have been provided for the 29 BOR1 tests and 12 additional BOR2 tests. The computed toe resistance values from CAPWAP analyses were divided by the cross sectional area of the pile resulting in the “equivalent” unit toe resistance, consistent with the procedure used in the database for the open-ended pipe piles. The difference in the pile configuration between the cases in the databases and the Hyder project (i.e., open-ended versus closed-end conical tip) is acknowledged and this comparison is provided to demonstrate the general applicability of the CAPWAP-Based procedure.

The range in “equivalent” unit toe resistance at Hyder is 13 to 29 kip/ft<sup>2</sup>, with a median value of 22.3 kip/ft<sup>2</sup>. This compares very well with the estimate of 26 kip/ft<sup>2</sup> made on the basis of the database and adjustment for closed-end pile. This case history highlights the utility of the database and benefit of supplementing the results of standard analyses with a range of likely toe resistance based on accumulated project experience with similar piles and soil deposits. The total toe resistance assumed in Section 5.3 was 65 kips, compared to the median value of roughly 70 kips computed with CAPWAP at Hyder.

The following observations were made from the CAPWAP results at Hyder:

- The median unit toe resistance of 22.3 kips/ft<sup>2</sup> at the embedment depths of interest at Hyder correspond to  $N_t$ -coefficients in the range of 2.5 to 4.5, significantly less than the values commonly recommended as lower-bound values for sand in the Effective Stress method.
- There is no clear depth-dependent trend in toe resistance with depth on this project. This covers pile embedment depths of roughly 90 to 160 feet in soils that are fairly uniform in this depth range.
- No trend in toe resistance with time after EOID was evident.
  - Five piles showed significant increase in toe resistance between BOR1 and BOR2 with “set-up” factors of 1.2 to 2.5.
  - Three piles exhibited a decrease in toe resistance between BOR1 and BOR2. This was likely due to high blow counts at BOR2 and possibly the failure to mobilize full toe resistance.

### 5.5 TIME-DEPENDENT SHAFT RESISTANCE AND SOIL SET-UP FACTORS

The extensive CAPWAP analyses performed for the Hyder Causeway Trestle project demonstrated the increase in shaft resistance with time after EOID and provide useful data for estimating soil set-up factors for the sandy soils at the project site. Investigations of time-dependent changes in shaft resistance in sandy and silty soil deposits similar to those at Hyder provide soil set-up factors ranging from 0.8 to 2.0 (e.g., Allen, 2005; Axelsson, 2002; Fellenius et al, 1998; Hannigan et al, 1997, 2006; Lee et al, 2010; Merrill et al, 1999). This range is evaluated with data from Hyder as well as cases from the statewide database.

The PDA testing at Hyder provides trends for shaft resistance measured as long as 48 days after EOID. The results of CAPWAP analyses performed on four piles for BOR1 and BOR2 conditions have been evaluated as a simple ratio of ( $R_s/R_{s,EOID}$ ) versus time since EOID, where;

$R_s$ : The total shaft resistance of the pile at the time of the BOR test  
 $R_{s,EOID}$ : The total shaft resistance of the pile at End of Initial Driving

The relationship of ( $R_s/R_{s,EOID}$ ) with time is plotted in Figure 5-10, where the time at EOID is arbitrarily taken as 0.1 days. The increase in total shaft resistance with time can be simply expressed as;

$$R_s/R_{s,EOID} = 1.0 + 0.24 \cdot \log(T/T_{EOID}) \quad (5-1)$$

where;

$R_s$  and  $R_{s,EOID}$ : As previously defined  
T: Time between EOID and the period of interest, in days  
 $T_{EOID}$ : Time at the End of Initial Driving, defined as 0.1 days

This simple formulation follows investigations by Axelsson (2002) and Lee and others (2010). The data obtained at Hyder are supplemented with CAPWAP results from the statewide database. The CAPWAP analyses at Hyder support a soil set-up factor between EOID and T of 100 days of roughly 1.5 to 1.7. The trend in the statewide data is weak reflecting the influence of variable soil deposits in the database and the limited length of time between EOID and BOR (maximum of 7.5 days). The trend in set-up with time provided by Equation 5-1 is tentatively recommended for use on projects with conditions similar to those experienced on the Hyder project (pile size and length, soil deposits, soil density). It is recommended the resulting estimates of shaft resistance should be compared to the trends in the database and checking using standard procedures for static analysis calibrated for regional use in Alaska.

## 5.6 CONCLUSIONS PERTAINING TO THE CASE STUDY AT HYDER

The breadth of the CAPWAP analyses performed on the Hyder Causeway Trestle replacement project has provided an extremely useful case study for aspects of axial pile analysis including: unit shaft and toe resistance in very loose to loose deposits of sand and gravel, the influence of soil matrix on the engineering behavior of gravelly soils, pile driveability, variability of CAPWAP results for adjacent piles in fairly uniform soil deposits, and time effects and soil set-up. The CAPWAP results graphically presented in Figures 5-8 through 5-10 support the use, and suggest possible refinements, for static analysis procedures for estimating shaft resistance in cohesionless soils. Similar guidance is provided for bracketing the range of toe resistance in these soil deposits.

The pipe piles used at Hyder were fabricated with conical tips, therefore, driven as close-ended displacement piles. The statewide database is comprised entirely of open-ended pipe piles. Unit toe and shaft resistances in sand have been shown to be significantly greater for closed-ended piles than for open-ended piles due to soil displacement, soil densification, and changes in lateral geostatic stress during driving (e.g., Paik et al, 2003). The use of close-ended piles at Hyder highlights two aspects of the project relative to the statewide database: (i) possibly greater shaft and toe resistance anticipated associated with closed-ended pipe piles, and (ii) the lower shaft and toe resistance expected due to the very loose nature of the sandy soils along the entire length of embedment of the piles. The very loose nature of the sandy deposits at Hyder indicate the

normalized unit shaft resistance and/or  $\beta$ -coefficient could be as low as 0.1 to 0.15 based on cases in the database and other project sites. These low values were not obtained in CAPWAP analyses suggesting the closed-ended displacement piles were advantageous in the loose sands. These effects are considered to be partially offsetting; however, the net influence was not evaluated in this investigation and the direct comparison of the Hyder results with the database has been provided.

The following observations pertaining to the Hyder case study are highlighted:

1. The median unit toe resistance of approximately 22 kip/ft<sup>2</sup> obtained from the CAPWAP analyses at Hyder is consistent with the range of values in the statewide database for piles in similar soil deposits. No influence of pile toe condition was evident in direct comparisons with the database.
2. The trend of shaft resistance with depth at Hyder measured in BOR tests 1 to 5 days after EOID is also consistent with the average trend established in the statewide database.
3. CAPWAP analyses of PDA data obtained up to 48 days after initial driving support the assertion that reliance on BOR results obtained less than roughly 6 to 9 days after EOID can yield soil resistances that are significantly less than long-term, static values. This is an important consideration on smaller projects where time constraints preclude longer waiting times for BOR tests.
4. The BOR data obtained at Hyder support general estimates for the increase in shaft resistance with time for closed-ended pipe piles. The application for open-ended piles in similar soils is considered a reasonable approximation for long piles ( $D/B > 30$ ) in which plug formation is assumed.



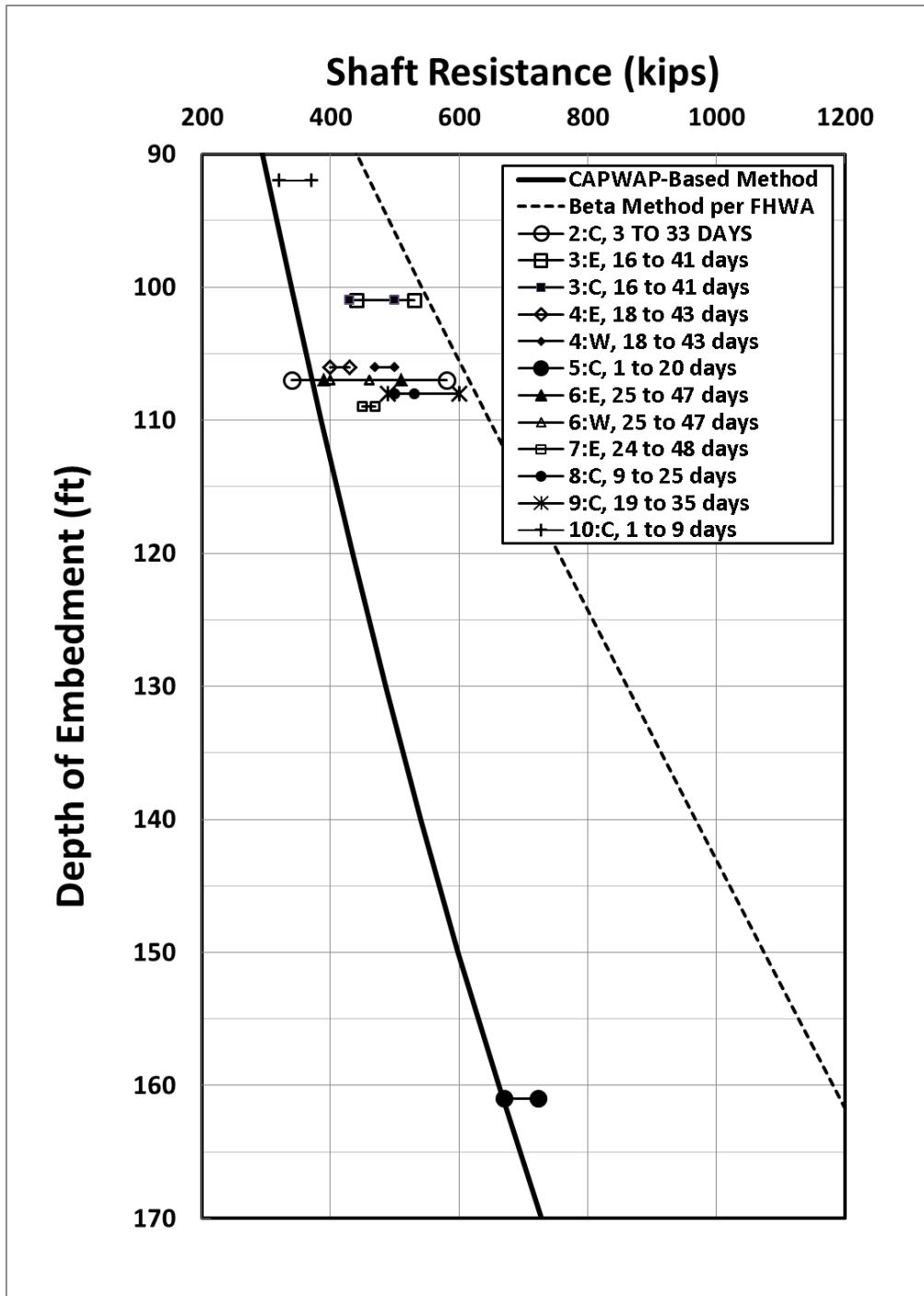


**Figure 5-9: Comparison of computed trends in total shaft resistance with embedment depth with the results of CAPWAP analyses for 12 piles tested for BOR conditions at two time intervals. The approximate time intervals between EOID and BOR1, and EOID and BOR2 are indicated in the legend.**

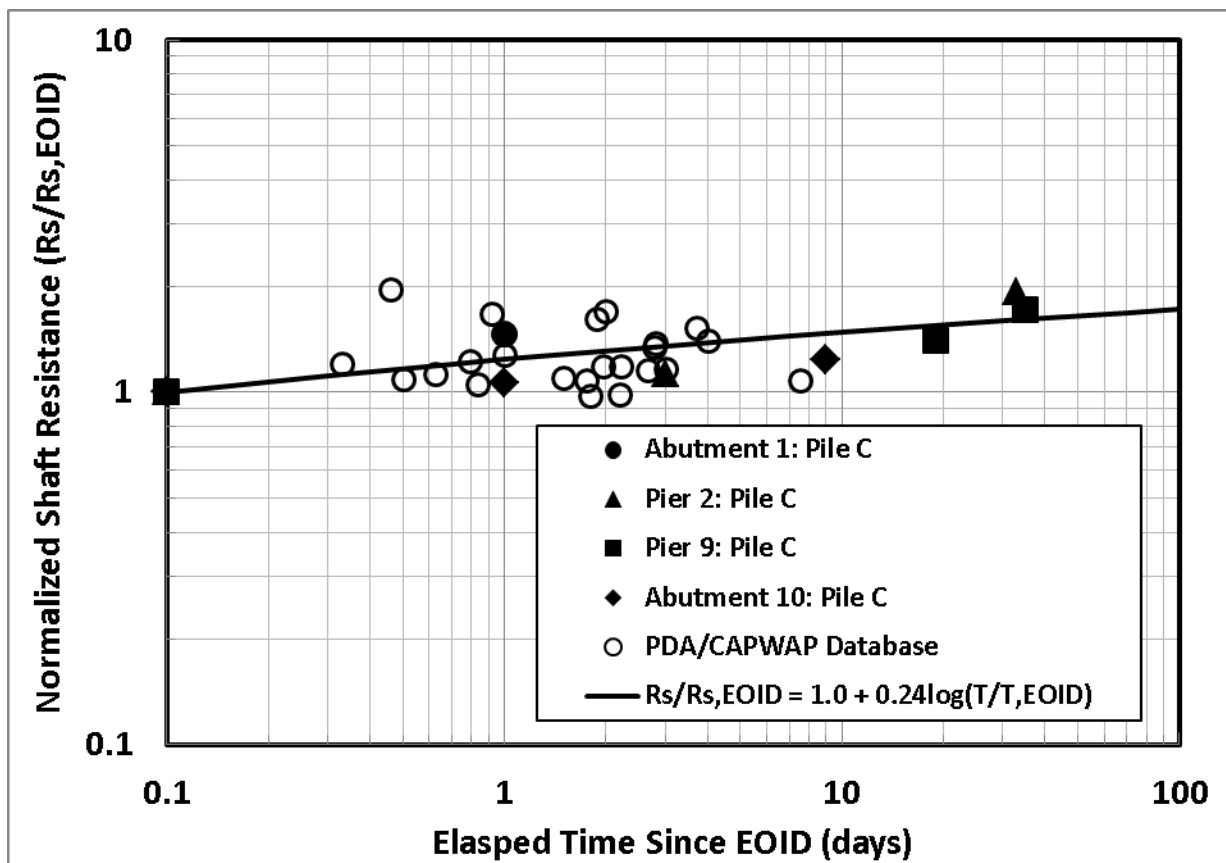


Figure 5-10: Trends of cumulative shaft resistance with embedment depth for a 24-inch diameter steel pipe pile.

## 6.0 RECOMMENDATIONS FOR FUTURE RESEARCH

Examination of the collected CAPWAP analyses in light of the supporting geologic, geotechnical, and construction information at 34 sites broadly located throughout the State of Alaska has revealed trends in the static axial capacity that will contribute to refined estimates for steel pipe piles in cohesionless soils based on both static analyses and dynamic formulas on future ADOT&PF projects. The primary goals of this investigation have been: (1) to calibrate existing static analysis methods and dynamic pile capacity formulas using high strain dynamic load test data (PDA) and analysis (CAPWAP) on projects throughout the State of Alaska, (2) to develop a static axial pile capacity estimation method based on trends in the accumulated results of CAPWAP analyses, and (3) to highlight the range of uncertainty associated with the various methods for estimating soil resistance (shaft and toe) applied for pipe piles. The project focused on providing practice-oriented procedures for pre-construction, static analysis and for dynamic analysis using pile driving records. The tasks associated with these project goals have illuminated additional considerations for deep foundation design, and highlighted knowledge gaps with respect to deep foundation performance during driving as well as long-term static loading, particularly for large diameter pile piles (diameter  $\geq$  48-inch).

On the basis of this investigation, considerations associated with the application of the proposed methods for ADOT&PF bridge projects, and numerous discussions with engineering practitioners in Alaska the following topics and issues warrant consideration for future research:

1. The recommendations developed in this investigation could be extended for applications involving: (i) closed-ended steel pipe piles, and (ii) steel H-piles for which enhanced estimates of unit shaft resistance and unit toe resistance are needed. In the case of the latter, a limited PDA/CAPWAP database could be developed from the ADOT&PF records. This would benefit from additional data for H-piles driven into sandy soils obtained from other regions.
2. Issues involving running of piles in very loose cohesionless soils have been identified as a problem on several ADOT&PF projects. In some of these cases, the axial pile capacity tested at EIOD increases at a very slow rate with pile embedment indicating that exceptionally long piles are required. This subset of cases in the database should be evaluated to develop screening methods for this situation, for estimating the possible rate of increase of shaft resistance with time after driving, and for providing recommendations for optimal pile type and size for these conditions.
3. The recommendations in this report are entirely based on the results of high strain dynamic load testing. This may result in systematic biases relative to long-term, static axial pile behavior. Additional research on the following topics are recommended for common ADOT&PF deep foundation applications: (i) time-dependent increase in pile capacity (*set-up*) beyond the roughly 3 to 14 days that was common for the large diameter piles in this investigation, (ii) unit end bearing of the larger diameter piles ( $D \geq 42$  inches) in situations where dynamic plug behavior during driving may result in lower bound toe resistance estimates using CAPWAP, (iii) influence of factors such as ram weight relative to nominal capacity, hammer size and velocity at impact, pile driving characteristics (set), and toe quake on the computed pile resistance.

4. The prevalence of the “problematic” soils encountered by the ADOT&PF suggests that a load test program involving dynamic and static load testing of various pile types would be extremely beneficial. Optimally, several of the pile types predominantly used by the ADOT&PF would be driven at a site with laterally uniform soil deposits confirmed with thorough geotechnical characterization thereby allowing for side by side comparison of the efficiency of the various piles. Well-instrumented piles would be monitored during driving, restrike after several days and perhaps several months later to assess the time-dependent changes in shaft and toe resistance. While “set-up” is commonly assumed to be minor in silt- and sand-rich cohesionless soils, a set-up factor of 1.7 was supported by pile testing at the Hyder project site. In addition, the observed running of long piles in these soils during driving suggests that the time-dependent increase in shaft resistance is worth investigating.

A static load test program on instrumented piles would support a variety of practical investigations including:

- (i) Relative pile resistance of open- and close-ended pipe piles
  - (ii) Static and dynamic soil plug behavior
  - (iii) Efficiency of internal plates for increasing pile capacity
  - (iv) Application of neutral plane concepts in these loose soils
  - (v) Residual stresses in piles after driving
  - (vi) Calibration of Wave Equation Analyses
  - (vii) Validation of load and resistance factors for AASHTO-based design
5. The very low “equivalent” unit toe resistances observed during dynamic testing of large diameter pipe piles should be evaluated for static loading conditions. Pertinent aspects of dynamic and static plug behavior were not addressed in this investigation. Potentially significant increases in the end bearing may be demonstrated with additional investigation and long-term, static data. This could be thoroughly evaluated during the static load test program previously recommended.

## 7.0 REFERENCES

ADOT&PF (1998). Foundation Report, Gustavus Causeway Replacement Project No. BR-0003 (53), Southeast Region, Alaska Department of Transportation and Public Facilities December.

ADOT&PF (2007a). Alaska Geological Field Investigations Guide, Alaska Department of Transportation and Public Facilities, effective March 2007, available at: [http://www.dot.state.ak.us/stwddes/desmaterials/mat\\_geology/pop\\_geotechman.shtml](http://www.dot.state.ak.us/stwddes/desmaterials/mat_geology/pop_geotechman.shtml)

ADOT&PF (2007b). Alaska Geotechnical Procedures Manual, Alaska Department of Transportation and Public Facilities, effective May 2007, available at: [http://www.dot.state.ak.us/stwddes/desmaterials/mat\\_geology/assets/pdf/geotechman/geotechmanual\\_all\\_07.pdf](http://www.dot.state.ak.us/stwddes/desmaterials/mat_geology/assets/pdf/geotechman/geotechmanual_all_07.pdf)

ADOT&PF (2008a). Preliminary Structural Foundation Engineering Report, Hyder Causeway Trestle (Project No. 69070), Alaska Department of Transportation and Public Facilities, Southeast Region Geotechnical Section, Juneau, Alaska, dated August 8, 2008.

ADOT&PF (2008b). Foundation Geology Report, Hyder Causeway Trestle (Project No. 69070), Alaska Department of Transportation and Public Facilities, Southeast Region Geotechnical Section, Juneau, Alaska, dated August 21, 2008.

Allen, T.M. (2005). "Development of the WSDOT Pile Driving Formula and Its Calibration for Load and Resistance Factor Design (LRFD)," Final Research Report WA-RD 610.1, Washington State Department of Transportation, 45 p., available at: <http://www.wsdot.wa.gov/research/reports/fullreports/610.1.pdf>

Allen, T.M. (2007). "Development of New Pile-Driving Formula and Its Calibration for Load and Resistance Factor Design," Transportation Research Record No.2004, Transportation Research Board, National Academies, Washington, D.C., p. 20 – 27.

API (1993). Recommended Practice for Planning, Designing and Constructing Fixed Offshore Platforms – Working Stress Design," API Recommended Practice 2A-WSD (RP 2A-WSD), 20<sup>th</sup> edition, American Petroleum Institute, Washington, D.C., 191 p.

AASHTO (2009). *AASHTO Bridge Design Specification, 2009 Interim Revision*, American Association of State Highway Transportation Officials, Washington, DC.

Axelsson, G. (2002). "A Conceptual Model of Pile Set-Up for Driven Piles in Non-cohesive Soil," *Proc. Deep Foundations 2002*, ASCE, 64 – 79.

Bhushan, K. (2004). "Design & Installation of Large Diameter Pipe Piles for LAXT Wharf," *Proc. Current Practices and Future Trends in Deep Foundations*, J.A. DiMaggio and M. H. Hussein (eds), ASCE Geo-Institute, Geotechnical Special Publication No. 125, 370-389.

Bowles, J.E. (1996). Foundation Analysis and Design, 5<sup>th</sup> edition, The McGraw-Hill Companies, Inc., 1173 p.

Charles, J.A., and Watts, K.S. (1980). "The influence of confining pressure on the shear strength of compacted rockfill," *Geotechnique*, 30(4), 353 – 367.

Duncan, J.M. (2004). "Friction angles for sand, gravel, and rockfill," notes of a lecture presented at the Kenneth L. Lee Memorial Seminar, Long Beach, CA, April 28.

Duncan, J.M., Horz, R.C., and Yang, T.L. (1989). *Shear Strength Correlations for Geotechnical Engineering*, Dept. of Civil Engineering, Virginia Tech, Blacksburg, VA, 100 p.

Fellenius, B.H. (1996). *Basics of Foundation Design*, BiTech Publishers, Richmond, B.C., Canada, 134 p.

Fellenius, B.H., Riker, R.E., O'Brien, A.O., and Tracy, G.R. (1998). "Dynamic and static testing in a soil exhibiting set-up," *Jrnl. of Geotechnical Engineering*, ASCE, 115(7), 984 – 1001.

Fellenius, B.H., and Altaee, A. (2001). "Pile Dynamics in Geotechnical Practice – Six Case Histories," *International Deep Foundation Congress*, ASCE Geotechnical Special Publication No. 116, O'Neill and Townsend (eds.), Vol. 2, 619 – 631.

Fragazy, R.J., Argo, D., and Higgins, J.D. (1989). "Comparison of Formula Predictions with Pile Load Tests," Transportation Research Record No. 1219; *Geotechnical Engineering 1989*, p. 1 – 12, Transportation Research Board, National Research Council, Washington, D.C.

Gerwick, B.C. (2004). "Pile Installation in Difficult Soils." *Jrnl. Geotechnical and Geoenvironmental Engineering*, ASCE, 130(5), 454 – 460.

Golder Associates (2009). *Dynamic Testing and Analysis of Piles, Causeway Replacement, Gustavus, Alaska*, Golder Associates report No. 093-95267 dated July 20, 2009.

Hannigan, P.J., Goble, G.G., Thendean, G., Likins, G.E., and Rausche, F. (1997a). *Design and Construction of Driven Pile Foundations*, FHWA-HI-97-013, U.S. Dept. of Transportation, FHWA, Workshop Manual – Volume 1. Available at:  
[http://www.fhwa.dot.gov/engineering/geotech/library\\_arc.cfm?pub\\_number=42](http://www.fhwa.dot.gov/engineering/geotech/library_arc.cfm?pub_number=42)

Hannigan, P.J., Goble, G.G., Thendean, G., Likins, G.E., and Rausche, F. (1997b). *Design and Construction of Driven Pile Foundations*, FHWA-HI-97-013, U.S. Dept. of Transportation, FHWA, Workshop Manual – Volume 2. Available at:  
[http://www.fhwa.dot.gov/engineering/geotech/library\\_arc.cfm?pub\\_number=42](http://www.fhwa.dot.gov/engineering/geotech/library_arc.cfm?pub_number=42)

Hannigan, P., Goble, G. Likins, and F. Rausche (2006). *Design and Construction of Driven Pile Foundations, Volumes 1 and 2*. FHWA-NHI-05-042/042, National Highway Institute, Federal Highway Administration, U.S. Department of Transportation, Washington, DC. 2006.

Janbu, N. (1956). "Guide to the solution of some foundation engineering problems," Publication 16, Norwegian Geotechnical Institute, also in; Bruun, P. (1981). *Port Engineering*, 3<sup>rd</sup> edition, Gulf Publishing Co., Houston, TX, Appendix C, Part 1; Pile Foundations.

Lee, W., Kim, D., Salgado, R., and Zaheer, M. (2010). "Setup of driven piles in layered soil," *Soils and Foundations*, 50(5), 585 – 598.

Likins, G., and Rausche, F. (2004). "Correlations of CAPWAP with static loads," *Proc. 7<sup>th</sup> International Conf. on the Application of Stress Wave Theory to Piles*, Malaysia, 153 – 165.

Mathias, D., and Cribbs, M. (1998). "DRIVEN 1.0: A Microsoft Windows Based Program for Determining Ultimate Vertical Static Pile Capacity," Publication No. FHWA-SA-98-074, U.S. Dept. of Transportation, FHWA, available at:  
<http://www.fhwa.dot.gov/engineering/geotech/software/sa98074.pdf>

Merrill, K.S., Korri, K., and Miner, R.F. (1999). "Installation and Evaluation of Driven Steel Pipe Piles in Alaska Soils using the Pile Driving Analyzer," *Proceedings of the Tenth International Conference on Cold Regions Engineering*, Zufelt J. E. (Ed.), p. 717-730, American Society of Civil Engineers, Reston, VA.

Miner, R. (2012). Personal communication on CAPWAP and unit pile resistances (shaft and toe), Robert Miner Dynamic Testing, Inc., Manchester, WA.

Morgano, C.M., White, B.A., and Allin, R.C. (2008). "Dynamic testing in sensitive & difficult soil conditions," *Proc. Stress Wave 2008; 8<sup>th</sup> International Conf. on Application of Stress Wave Theory to Piles, Science, Theory and Practice*, Santos, J.A. (ed.), Lisbon, Portugal, 135 – 138.

Paik, K., Salgado, R., Lee, J., and Kim, B. (2003). "Behavior of Open- and Close-Ended Piles Driven into Sands," *Jrnl. of Geotechnical and Geoenvironmental Engineering*, ASCE, 129(4), 296 – 306.

Paikowsky, S.G., Birgisson, B., McVay, M., Nguyen, T., Kuo, C., Beacher, G., Ayyub, B., Stenersen, K., O'Malley, K., Chernauskas, L., and O'Neill, M. (2004). Load and Resistance Factor Design (LRFD) for Deep Foundations, NCHRP Report 507, Transportation Research Board, Washington, D.C., available at:  
[http://onlinepubs.trb.org/onlinepubs/nchrp/nchrp\\_rpt\\_507.pdf](http://onlinepubs.trb.org/onlinepubs/nchrp/nchrp_rpt_507.pdf)

Poulos, H.G., and Davis, E.H. (1980). Pile Foundation Analysis and Design, John Wiley & Sons Publishers.

Prakash, S., and Sharma, H.D. (1990). Pile Foundations in Engineering Practice, John Wiley & Sons Publishers, 734 p.

Rausche, F., Goble, G.G., and Likins, G.E. (1985). "Dynamic Determination of Pile Capacity," *Jrnl. of Geotechnical Engineering*, ASCE, 111(3), 367 – 383.

Rausche, F., Nagy, M., and Likins, G. (2008). "Mastering the art of pile testing," *Proc. Stress Wave 2008; 8<sup>th</sup> International Conf. on Application of Stress Wave Theory to Piles, Science, Theory and Practice*, Santos, J.A. (ed.), Lisbon, Portugal, 19 - 32.

Rausche, F., Nagy, M., Webster, S., and Liang, L. (2009). "CAPWAP and Refined Wave Equation Analyses for Driveability Predictions and Capacity Assessment of Offshore Pile Installations," *Proc. ASME 28<sup>th</sup> Conf. on Ocean, Offshore and Artic Engineering, OMAE2009*, Honolulu, Hawaii, Paper OMAE2009-80163, 1 – 9.

Rausche, F., Likins, G., Liang, L., and Hussein, M. (2010). "Static and Dynamic Models for CAPWAP Signal Matching," *Art of Foundation Engineering Practice*, Hussein, M.H., Anderson, J.B., and Camp, W.M. (eds.), ASCE Geotechnical Special Publication No. 198,

Smith, T., Banas, A., Gummer, M., and Jin, J. (2011). "Recalibration of the GRLWEAP LRFD Resistance Factor for Oregon DOT," Final Report SPR 683, Oregon Department of Transportation, Research Section, Salem, Oregon, available at:  
[http://www.oregon.gov/ODOT/TD/TP\\_RES/docs/Reports/2011/GRLWEAP\\_LRFD.pdf?ga=t](http://www.oregon.gov/ODOT/TD/TP_RES/docs/Reports/2011/GRLWEAP_LRFD.pdf?ga=t)

Terzaghi, K., Peck, R.B., and Mesri, G. (1996). Soil Mechanics in Engineering Practice, 3<sup>rd</sup> edition, John Wiley & Sons, Inc., New York, NY, 549 p.

Tomlinson, M.J. (1995). Foundation Design & Construction, 6<sup>th</sup> Edition, Longman Scientific & Technical/John Wiley & Sons Publ., 536 p.

Tweedie, R., Clementino, R., and Law, D. (2009). "Comparison of static and high strain dynamic tests on driven steel piles at several industrial sites in Alberta," *Proc. GeoHalifax2009*, 214 - 221.

## **APPENDIX A:**

PDA Database

**PROJECT IDENTIFICATION AND REPORTING**

Database ID Number	Bridge Number	Site	Location	# Piles Tested	PDA Testing & Report	Report Date
					RMDT Report #	Report by Others
<b>PIPE PILES: Open-ended, non-tapered, and no internal plates</b>						
1	4 & 5	Ship Creek Trail, Phase II, Bridges 4 & 5	Anchorage	3	04F30	26-Nov-04
2						
3						
4	210	Willow Creek	Parks Highway	3	04F20	13-Aug-04
5a						
5b						
6						
7a	240	Little Sustina River, Parks Hwy MP 57 - 67	Houston	1	02F25	15-May-02
7b						
7c						
8a	317	Julius Creek, Parks Hwy MP 285	Nenana	1	07F20	20-Jun-07
8b						
9	543	Granite Creek Bridge, Glenn Hwy MP 61 - 67	Glenn Hwy	3	01F15	12-Jun-01
10a						
10b						
11						
12	596	Resurrection River, Seward Highway, MP 0 - 8	Seward Hwy	1	03F28	13-Dec-03
13	597	Resurrection River, Seward Highway, MP 0 - 8	Seward Hwy	2	03F28	13-Dec-03
14a	597	Resurrection River, Seward Highway, MP 0 - 8	Seward Hwy	2	03F28	13-Dec-03
14b	597	Resurrection River, Seward Highway, MP 0 - 8	Seward Hwy	2	03F28	13-Dec-03
14c	597	Resurrection River, Seward Highway, MP 0 - 8	Seward Hwy	2	03F28	13-Dec-03
15a	598	Resurrection River, Seward Highway, MP 0 - 8	Seward Hwy	1	03F28	13-Dec-03
15b	598	Resurrection River, Seward Highway, MP 0 - 8	Seward Hwy	1	03F28	13-Dec-03
15c	598	Resurrection River, Seward Highway, MP 0 - 8	Seward Hwy	1	03F28	13-Dec-03
16a	649	Christochina River (part 1)		1	05F16	20-Apr-05
16b						
17a	649	Christochina River (part 2)		1	05F16	20-Apr-05
17b						
18	655	Slana Slough	Tok Highway	1	data sheets	11-May-06
19a	656	Mabel Creek		1	data sheets	24-May-06
19b						
20a	671A	Kenai River Bridge - Sterling Hwy	Soldotna	2	05F18	25-Oct-06
20b						
21a						
21b						
22	865	Indian River Bridge Replacement	Sitka	2	07F09	23-Mar-07
23						
24a	700	International Airport Rd. & Minnesota Dr. Interchange	Anchorage	1		GRL996017 19-Oct-99
24b						
24c						
25a	1269	International Airport Rd. & Minnesota Dr. Interchange	Anchorage	1		GRL996017 19-Oct-99
25b						
25c						
26	1207	Lowe River Main - Dayville Rd		2	05F33	2-Feb-06
27						
28	1208	Lowe River Main - Dayville Rd		1	data sheets	7-Dec-05
29a	1308	Kouwegok Slough Bridge	Unalaklete	1	00F19	18-Apr-00
29b						
30a	1885	Knik River Bridge, Eklutna to Parks Hwy	Glenn Hwy	3		GRL916012 21-Oct-91
30b						
31a						
31b						
32a						
32b						
33a	1889	Matanuska River Bridge, Eklutna to Parks Hwy	Glenn Hwy	3		GRL916012/1 14-Jan-92
33b						
34a						
34b						
35a						
35b						
36	1904	Mendenhall River Pedestrian Bridge	Juneau	3	00F31	14-Sep-00
37						
38a						
38b						
39a	1913	Chena River Bridge, Parks Highway	Fairbanks	1		GRL946029 15-Aug-95
39b						
40a	1923	Lilly Creek Bridge, Whites Crossing (part 2)	Parks Hwy	1	02F18	8-Apr-02
40b						
41a	1923	Lilly Creek Bridge, Whites Crossing (part 3)	Parks Hwy	1	02F18	17-May-02
41b						
41c						
42a	1961	Portage Creek Bridge	Whittier	2		GRL976049 3-Feb-98
42b						
43						
44a	1962	Placer Creek Bridge	Whittier	2		GRL976010 26-Jun-98
44b						
44c						
45a						
45b						
46	1981	Geist Road - Thompson Drive Overhead	Fairbanks	9	04F32	13-Dec-05
47						
48						
49						
50						
51						
52						
53						
54a						
54b						
55a	2082	C St. Undercrossing EB O'Malley (2081/2082)	Anchorage	2	05F31	15-May-06
55b						
56a						
56b						
57	2209	Bragaw St. Overcrossing, Glenn Hwy	Anchorage	2	08F20	18-May-08
58a						
58b						
59a		48th Avenue & Boniface Extention U/C (MLK Jr. Bridge)	Anchorage	4	09F07	12-Jun-09
59b						
60a						
60b						
61						
62						
63		Gustavus Causeway (pier)	Gustavus	3		Golder Assoc 093-95267 20-Jul-09
64						
65						



APPENDIX A

**PILE CHARACTERISTICS**

Database ID Number	Database ID Number	Pile ID	Pile Type	Diameter	Wall Thickness	Full Length	Embedded Length	Cross Sectional Area of Pile Walls	Weight	End Condition	Steel Grade	Yield Strength	Elastic Modulus
				in	in	ft	ft	in^2	kips			ksi	ksi
1	1	Bridge 4, Abutment 3, Pile 4	PP	12.75	0.500	42.2	26	19.24	2.76	open	API 5L X60 (ASTM A252 Grade 2)	45	29000
2	2	Bridge 4, Pier 2, Pile 4	PP	18.00	0.562	46.5	30	30.79	4.87	open	API 5L X60 (ASTM A252 Grade 2)	45	29000
3	3	Bridge 5, Abutment 1, Pile 1	PP	12.75	0.500	31.0	23	19.24	2.03	open	API 5L X60 (ASTM A252 Grade 2)	45	29000
4	4	Pier 3, Pile 4	PP	42.00	0.750	107.0	97	97.19	35.39	open	ASTM A706M Grade 345	45	29000
5a	5a	Pier 2, Pile 7	PP	42.00	0.750	107.0	95.5	97.19	35.39	open	ASTM A706M Grade 345	45	29000
5b	5b	Pier 2, Pile 7	PP	42.00	0.750	110.0	96	97.19	36.38	open	ASTM A706M Grade 345	45	29000
6	6	Pier 2, Pile 4	PP	42.00	0.750	103.0	94	97.19	34.06	open	ASTM A706M Grade 345	45	29000
7a	7a	Pier 3, Pile 1	PP	36.00	0.750	160.0	145	83.06	45.22	open	API 5L x 52	52	29000
7b	7b	Pier 3, Pile 1	PP	36.00	0.750	160.0	145	83.06	45.22	open	API 5L x 52	52	29000
7c	7c	Pier 3, Pile 1	PP	36.00	0.750	160.0	146	83.06	45.22	open	API 5L x 52	52	29000
8a	8a	Abutment 1, Pile D	PP	18.00	0.750	125.0	116	40.64	17.29	open	5LX52	52	29000
8b	8b	Abutment 1, Pile D	PP	18.00	0.750	125.0	116	40.64	17.29	open	5LX52	52	29000
9	9	Pier 2, Pile 1	PP	30.00	1.00	86	59	91.11	26.66	open	API 5LX x 52	60	29000
10a	10a	Pier 2, Pile 3	PP	30.00	1.00	60	56	91.11	18.60	open	API 5LX x 52	60	29000
10b	10b	Pier 2, Pile 3	PP	30.00	1.00	88	77	91.11	27.28	open	API 5LX x 52	60	29000
11	11	Pier 2, Pile 4	PP	30.00	1.00	60	55	91.11	18.60	open	API 5LX x 52	60	29000
12	12	Pier 2, Pile 1	PP	48.00	1.00	179	166	147.65	89.94	open	API 5L x 52	52	29000
13	13	Abutment 3, Pile 1	PP	48.00	1.00	119	107	147.65	59.79	open	API 5L x 52	52	29000
14a	14a	Abutment 3, Pile 2	PP	48.00	1.00	119	107	147.65	59.79	open	API 5L x 52	52	29000
14b	14b	Abutment 3, Pile 2	PP	48.00	1.00	177	167	147.65	88.93	open	API 5L x 52	52	29000
14c	14c	Abutment 3, Pile 2	PP	48.00	1.00	177	167	147.65	88.93	open	API 5L x 52	52	29000
15a	15a	Abutment 1, Pile 1	PP	48.00	1.00	119	106	147.65	59.79	open	API 5L x 52	52	29000
15b	15b	Abutment 1, Pile 1	PP	48.00	1.00	178	170	147.65	89.43	open	API 5L x 52	52	29000
15c	15c	Abutment 1, Pile 1	PP	48.00	1.00	178	170	147.65	89.43	open	API 5L x 52	52	29000
16a	16a	Pier 1, Pile C	PP	36.00	0.825	75	64.5	91.17	23.27	open	API 5L x 52	52	29000
16b	16b	Pier 1, Pile C	PP	36.00	0.825	75	64.5	91.17	23.27	open			29000
17a	17a	Pier 8, Pile C	PP	36.00	0.825	75	70	91.17	23.27	open			29000
17b	17b	Pier 8, Pile C	PP	36.00	0.825	75	70	91.17	23.27	open			29000
18	18	Abutment 2, Pile D	PP	30.00	0.750	100	90.5	68.92	23.45	open			29000
19a	19a	Abutment 2, Pile F	PP	30.00	0.750	120	112	68.92	28.14	open			29000
19b	19b	Abutment 2, Pile F	PP	30.00	0.750	120	112	68.92	28.14	open			29000
20a	20a	Test Pile 1	PP	24.00	0.500	80	33	36.91	10.05	open			29000
20b	20b	Test Pile 1	PP	24.00	0.500	80	33	36.91	10.05	open			29000
21a	21a	Test Pile 2 (Pier 3, Pile 3)	PP	24.00	0.500	78	33	36.91	9.80	open			29000
21b	21b	Test Pile 2 (Pier 3, Pile 3)	PP	24.00	0.500	78	33	36.91	9.80	open			29000
22	22	Abutment 1, Pile 4	PP	24.00	0.500	105	79	36.91	13.19	open	API 5L GR X60-PS	52	29000
23	23	Abutment 2, Pile 5	PP	24.00	0.500	105	79	36.91	13.19	open	API 5L GR X60-PS	52	29000
24a	24a	Pier 3, Pile 1	PP	36.00	1.000	119	89.6	109.96	44.52	open	ASTM 709 Grade 50	50	29000
24b	24b	Pier 3, Pile 1	PP	36.00	1.000	119	89.6	109.96	44.52	open	ASTM 709 Grade 50	50	29000
24c	24c	Pier 3, Pile 1	PP	36.00	1.000	119	94	109.96	44.52	open	ASTM 709 Grade 50	50	29000
25a	25a	Pier 2, Pile 4	PP	48.00	1.000	79	64	147.65	39.69	open	ASTM 709 Grade 50	50	29000
25b	25b	Pier 2, Pile 4	PP	48.00	1.000	99	90	147.65	49.74	open	ASTM 709 Grade 50	50	29000
25c	25c	Pier 2, Pile 4	PP	48.00	1.000	138	114	147.65	69.34	open	ASTM 709 Grade 50	50	29000
26	26	Pier 2, Pile 4	PP	48.00	1.000	120	108	147.65	60.29	open			29000
27	27	Abutment 1, Pile 1	PP	48.00	1.000	120	110	147.65	60.29	open			29000
28	28	Abutment 1, Pile 4	PP	48.00	1.000	132	122	147.65	66.32	open			29000
29a	29a	Pier 2, Pile 1	PP	30.00	1.000	157	128	91.11	48.67	open	API 5LX x 52	60	29000
29b	29b	Pier 2, Pile 1	PP	30.00	1.000	157	128	91.11	48.67	open	API 5LX x 52	60	29000
30a	30a	Pier 2, F-2	PP	48.00	0.800	120	99	118.63	48.44	open	ASTM A252	50	29000
30b	30b	Pier 2, F-2	PP	48.00	0.800	120	99	118.63	48.44	open	ASTM A252	50	29000
31a	31a	Pier 5, E-3	PP	48.00	1.000	145	113	147.65	72.85	open	ASTM A252	50	29000
31b	31b	Pier 5, E-3	PP	48.00	1.000	145	113	147.65	72.85	open	ASTM A252	50	29000
32a	32a	Pier 8, F-2	PP	48.00	0.800	120	91	118.63	48.44	open	ASTM A252	50	29000
32b	32b	Pier 8, F-2	PP	48.00	0.800	120	91	118.63	48.44	open	ASTM A252	50	29000
33a	33a	Pier 2, Pile A-2	PP	48.00	0.800	120	101	118.63	48.44	open	ASTM A252	50	29000
33b	33b	Pier 2, Pile A-2	PP	48.00	0.800	120	106	118.63	48.44	open	ASTM A252	50	29000
34a	34a	Pier 4, Pile E-3	PP	48.00	1.000	145	128	147.65	72.85	open	ASTM A252	50	29000
34b	34b	Pier 4, Pile E-3	PP	48.00	1.000	145	131	147.65	72.85	open	ASTM A252	50	29000
35a	35a	Pier 6, Pile A-2	PP	48.00	0.800	120	101	118.63	48.44	open	ASTM A252	50	29000
35b	35b	Pier 6, Pile A-2	PP	48.00	0.800	120	106	118.63	48.44	open	ASTM A252	50	29000
36	36	Abutment 3, Pile N	PP	30.00	0.625	99	94	57.68	19.43	open	A36 Grade 50	50	29000
37	37	Abutment 3, Pile S	PP	30.00	0.625	98	94	57.68	19.23	open	A36 Grade 50	50	29000
38a	38a	Pier 2, Pile N	PP	48.00	0.750	134	118	111.33	50.76	open	A36 Grade 50	50	29000
38b	38b	Pier 2, Pile N	PP	48.00	0.750	134	119	111.33	50.76	open	A36 Grade 50	50	29000
39a	39a	Pier 3	PP	42.00	0.750	138	120	97.19	45.64	open	ASTM 252 GR2		29000
39b	39b	Pier 3	PP	42.00	0.750	138	120	97.19	45.64	open	ASTM 252 GR2		29000
40a	40a	Pier 3, Pile 1	PP	48.00	1.000	139	102	147.65	69.84	open	API 5L x 52	52	29000
40b	40b	Pier 3, Pile 1	PP	48.00	1.000	139	103	147.65	69.84	open	API 5L x 52	52	29000
41a	41a	Pier 2, Pile 7	PP	48.00	1.000	176	129	147.65	88.43	open	API 5L x 52	52	29000
41b	41b	Pier 2, Pile 7	PP	48.00	1.000	176	130	147.65	88.43	open	API 5L x 52	52	29000
41c	41c	Pier 2, Pile 7	PP	48.00	1.000	176	130	147.65	88.43	open	API 5L x 52	52	29000
42a	42a	TP1 - Abutment A1-2	PP	42.00	0.750	159	147	97.19	52.59	open	API-5LX	42	29000
42b	42b	TP1 - Abutment A1-2	PP	42.00	0.750	159	147	97.19	52.59	open	API-5LX	42	29000
43	43	TP2 - Abutment A1-1	PP	42.00	0.750	159	132	97.19	52.59	open	API-5LX	42	29000
44a	44a	Abutment 1, Left Pile	PP	42.00	0.750	134	112	97.19	44.32	open	API-5LX	42	29000
44b	44b	Abutment 1, Left Pile	PP	42.00	0.750	134	112	97.19	44.32	open	API-5LX	42	29000
44c	44c	Abutment 1, Left Pile	PP	42.00	0.750	134	116	97.19	44.32	open	API-5LX	42	29000
45a	45a	Abutment 2, Right Pile	PP	42.00	0.750	134	124	97.19	44.32	open	API-5LX	42	29000
45b	45b	Abutment 2, Right Pile	PP	42.00	0.750	134	124	97.19	44.32	open	API-5LX	42	29000
46	46	Abutment 1, Pile 1	PP	36.00	0.750	114.5	98	83.06	32.36	open			29000
47	47	Abutment 1, Pile 4	PP	36.00	0.750	130	112	83.06	36.74	open			29000
48	48	Pier 2, Pile 1	PP	36.00	0.750	69	52	83.06	19.50	open			29000
49	49	Pier 2, Pile 4	PP	36.00	0.750	87.6	71	83.06	24.76	open			29000
50	50	Pier 2, Pile 5	PP	36.00	0.750	69	53	83.06	19.50	open			29000
51	51	Pier 3, Pile 1	PP	36.00	0.750	105	79	83.06	29.68	open			29000
52	52	Pier 3, Pile 2	PP	36.00	0.750	101.2	79	83.06	28.60	open			29000
53	53	Pier 3, Pile 3	PP	36.00	0.750	76	58	83.06	21.48	open			29000
54a	54a	Abutment 4, Pile 4	PP	36.00	0.750	86	67	83.06	24.31	open			29000
54b	54b	Abutment 4, Pile 4	PP	36.00	0.750	86	67	83.06	24.31	open			29000
55a	55a	Pier 2, Pile A (2081)	PP	42.00	0.875	80	60	113.05	30.77	open			29000
55b	55b	Pier 2, Pile A (2081)	PP	42.00	0.875	80	60	113.05	30.77	open			29000
56a	56a	Pier 2, Pile D (2082)	PP	42.00	0.875	80	60	113.05	30.77	open			29000
56b	56b	Pier 2, Pile D (2082)	PP	42.00	0.875	80	60	113.05	30.77	open			29000
57	57	Location 1	PP	36.00	1.000	79.5	57	109.96	29.75	open	API 5L		

HAMMER CHARACTERISTICS							
Database ID Number	Hammer Type	Configuration	Ram Weight	Anvil/Helmet Weight	Cushion Material	Maximum Rated Energy	Maximum Stroke
		Open-ended Closed-ended	kip	kip		kip-ft	ft
1	Delmag D15	0	3.3			27.9	10.8
2	Delmag D30	0	6.6			59.7	9.5
3	Delmag D30	0	6.6			59.7	9.5
4	Delmag D46-32	0	10.1			113	11.2
5a	Delmag D46-32	0	10.1			113	11.2
5b	Delmag D46-32	0	10.1			113	11.2
6	Delmag D46-32	0	10.1			113	11.2
7a	Delmag D46-32	0	10.1			107	10.6
7b	Delmag D46-32	0	10.1			107	10.6
7c	Delmag D46-32	0	10.1			107	10.6
8a	Delmag APE D30-32	0	6.6	1.2		70	11.2
8b	Delmag APE D30-32	0	6.6	1.2		70	11.2
9	ICE 220 Hydraulic	hydraulic	22			88	4.0
10a	ICE 220 Hydraulic	hydraulic	22			88	4.0
10b	ICE 220 Hydraulic	hydraulic	22			88	4.0
11	ICE 220 Hydraulic	hydraulic	22			88	4.0
12	Delmag D62-22	0	13.66			152	11.2
13	Delmag D62-22	0	13.66			152	11.2
14a	Delmag D62-22	0	13.66			152	11.2
14b	Delmag D62-22	0	13.66			152	11.2
14c	Delmag D62-22	0	13.66			152	11.2
15a	Delmag D62-22	0	13.66			152	11.2
15b	Delmag D62-22	0	13.66			152	11.2
15c	Delmag D62-22	0	13.66			152	11.2
16a	APE D62-22	0	13.66			152	11.2
16b	APE D62-22	0	13.66			152	11.2
17a	APE D62-22	0	13.66			152	11.2
17b	APE D62-22	0	13.66			152	11.2
18	Delmag D46-32	0	10.1			110	11.2
19a	Delmag D46-32	0	10.1			110	11.2
19b	Delmag D46-32	0	10.1			110	11.2
20a	ICE I36	0	7.9			91	12.1
20b	ICE I36	0	7.9			91	12.1
21a	ICE I36	0	7.9			91	12.1
21b	ICE I36	0	7.9			91	12.1
22	APE D50-32	0	11			116	13.1
23	APE D50-32	0	11			116	13.1
24a	ICE 120-S15	0	15	10.3	4" thick nylon disk	132.5	8.8
24b	ICE 120-S15	0	15	10.3	4" thick nylon disk	132.5	8.8
24c	ICE 120-S15	0	15	10.3	4" thick nylon disk	132.5	8.8
25a	ICE 120-S15	0	15	10.3	4" thick nylon disk	132.5	8.8
25b	ICE 120-S15	0	15	10.3	4" thick nylon disk	132.5	8.8
25c	ICE 120-S15	0	15	10.3	4" thick nylon disk	132.5	8.8
26	D100-13	0	22.04			245.93	11.2
27	D100-13	0	22.04			245.93	11.2
28	APE D100	0	22.04			245.93	11.2
29a	Delmag D46-32	0	10.14	9	3.5" (material?)	114	11.2
29b	Delmag D46-32	0	10.14	9	3.5" (material?)	114	11.2
30a	Delmag D80-23	0	17.6	9	3.5" (material?)	197	11.2
30b	Delmag D80-23	0	17.6	9	3.5" (material?)	197	11.2
31a	Delmag D80-23	0	17.6	9	3.5" (material?)	197	11.2
31b	Delmag D80-23	0	17.6	9	3.5" (material?)	197	11.2
32a	Delmag D80-23	0	17.6	9	3.5" (material?)	197	11.2
32b	Delmag D80-23	0	17.6	9	3.5" (material?)	197	11.2
33a	Delmag D80-23	0	17.6	9	3.5" (material?)	197	11.2
33b	Delmag D80-23	0	17.6	9	3.5" (material?)	197	11.2
34a	Delmag D80-23	0	17.6	9	3.5" (material?)	197	11.2
34b	Delmag D80-23	0	17.6	9	3.5" (material?)	197	11.2
35a	Delmag D80-23	0	17.6	9	3.5" (material?)	197	11.2
35b	Delmag D80-23	0	17.6	9	3.5" (material?)	197	11.2
36	Juntlan HHK 7A	hydraulic	15.4			62	4.0
37	Juntlan HHK 7A	hydraulic	15.4			62	4.0
38a	Juntlan HHK 7A	hydraulic	15.4			62	4.0
38b	Juntlan HHK 7A	hydraulic	15.4			62	4.0
39a	Delmag D46-32	0	10.14			113	10.6
39b	Delmag D46-32	0	10.14			113	10.6
40a	Delmag D46-32	0	10.14			107	10.6
40b	Delmag D46-32	0	10.14			107	10.6
41a	Delmag D46-32	0	10.14			107	10.6
41b	Delmag D46-32	0	10.14			107	10.6
41c	Delmag D46-32	0	10.14			107	10.6
42a	Delmag D46-32	0	10.14			113	11.2
42b	Delmag D46-32	0	10.14			113	11.2
43	Delmag D46-32	0	10.14			113	11.2
44a	Delmag D46-32	0	10.14			113	11.2
44b	Delmag D46-32	0	10.14			113	11.2
44c	Delmag D46-32	0	10.14			113	11.2
45a	Delmag D46-32	0	10.14			113	11.2
45b	Delmag D46-32	0	10.14			113	11.2
46	Delmag D62-22	0	13.67			152.5	11.2
47	Delmag D62-22	0	13.67			152.5	11.2
48	Delmag D62-22	0	13.67			152.5	11.2
49	Delmag D62-22	0	13.67			152.5	11.2
50	Delmag D62-22	0	13.67			152.5	11.2
51	Delmag D62-22	0	13.67			152.5	11.2
52	Delmag D62-22	0	13.67			152.5	11.2
53	Delmag D62-22	0	13.67			152.5	11.2
54a	Delmag D62-22	0	13.67			152.5	11.2
54b	Delmag D62-22	0	13.67			152.5	11.2
55a	Delmag D62-54	0	13.7			161	13.2
55b	Delmag D62-54	0	13.7			161	13.2
56a	Delmag D62-54	0	13.7			161	13.2
56b	Delmag D62-54	0	13.7			161	13.2
57	Delmag D62-22	0	13.7	10.9		153	12.0
58a	Delmag D62-22	0	13.7	10.9		153	12.0
58b	Delmag D62-22	0	13.7	10.9		153	12.0
59a	APE D30-32	0	6.6			73.7	13.0
59b	APE D30-32	0	6.6			73.7	13.0
60a	APE D30-32	0	6.6			73.7	13.0
60b	APE D30-32	0	6.6			73.7	13.0
61	APE D30-32	0	6.6			73.7	13.0
62	APE D30-32	0	6.6			73.7	13.0
63	Vulcan 06	ECH	6.5			19.5	3.0
64	Vulcan 512	ECH	12.0			60	5.0
65	Vulcan 512	ECH	12.0			60	5.0

APPENDIX A

DRIVING DATA											
Database ID Number	ADOT Driving Records	Noted Hammer Operation	Saximeter Blow Rate (average)	Estimated Stroke (average)	Driving at EOID or EOR		Driving at BOR		PDA Testing	Time Between EOID & BOR	
					Consistent	Erratic	Average Blows/min	ft			in/blow
1	no	erratic	n/a	n/a	1.71	7			0	n/a	
2	no	erratic	n/a	n/a	1	12			0	n/a	
3	no	consistent	47.2	6.16	0.3	40			0	n/a	
4	no	consistent	39.9	8.75	0.076	158			0	n/a	
5a	no	consistent	39.9	8.75	0.071	170			0	n/a	
5b	no	consistent	40.5	8.48			0.056	216	1	48	
6	no	consistent	39.2	9.07			0.047	258	1	48	
7a	no	consistent	40.0	8.70	0.099	121			0	n/a	
7b	no	consistent	42.0	7.86			0.143	84	1	44	
7c	no	consistent	41.3	8.14	0.059	204			2	n/a	
8a	no	consistent	42.5	7.67	0.429	28			0	n/a	
8b	no	consistent		9.00			0.250	48	1	22	
9	yes	consistent	n/a	4.0			0.040	300	1	520	
10a	yes	consistent	n/a	4.0	0.522	23			0	n/a	
10b	yes	consistent	n/a	4.0	0.364	33			0	n/a	
11	yes	consistent	n/a	4.0	0.122	98			0	n/a	
12	no	consistent	36.2	10.69	0.109	110			0	n/a	
13	no	consistent	38.8	9.27	0.273	44			0	n/a	
14a	no	consistent	40.1	8.66	0.197	61			0	n/a	
14b	no	consistent	36.7	10.39	0.129	93			0	n/a	
14c	no	consistent	37.4	9.99			0.125	96	1	9	
15a	no	consistent	38.8	9.27	0.235	51			0	n/a	
15b	no	consistent	38.1	9.62	0.103	116			0	n/a	
15c	no	consistent	37.4	9.99			0.128	94	1	23.5	
16a	no	consistent	37.1	10.16			0.035	341	1	120	
16b	no	consistent	37.2	10.11	0.110	109			2	n/a	
17a	no	consistent	36.0	10.81	0.171	70			0	n/a	
17b	no	consistent							1	67	
18	no	consistent	39.3	9.02	0.130	92			0	n/a	
19a	no	consistent	39.0	9.17	0.044	274			0	n/a	
19b	no	consistent							1	72	
20a	no	consistent	35.5	11.13	0.100	120			0	n/a	
20b	no	consistent		8.20			0.119	101	1	20	
21a	no	consistent	36.2	10.69	n/a	n/a			0	n/a	
21b	no	consistent		8.10			0.077	156	1	11	
22	no	consistent	39.6	8.88			0.111	108	1	48	
23	no	consistent	39.6	8.88			0.111	108	1	48	
24a	yes	consistent	39.1	9.12	0.226	53			0	n/a	
24b	yes	consistent		8.3			0.207	58	1	52.5	
24c	yes	consistent	39.1	9.12	0.203	59			2	n/a	
25a	yes	consistent	44.0	7.14	0.100	120			0	n/a	
25b	yes	consistent	44.0	7.14	0.115	104			0	n/a	
25c	yes	consistent	39.8	8.79	0.064	187			2	n/a	
26	no	consistent		9.84	0.200	60			0	n/a	
27	no	consistent		9.64	0.245	49			0	n/a	
28	no	consistent		9.44	0.235	51			0	n/a	
29a	no	consistent	37.2	10.11	0.067	180			0	n/a	
29b	no	consistent		9.80			0.067	180	1	27	
30a	yes	consistent		10.00	0.261	46			0	n/a	
30b	yes	consistent		11.20			0.245	49	1	53	
31a	yes	consistent		10.70	0.194	62			0	n/a	
31b	yes	consistent		11.50			0.200	60	1	15	
32a	yes	consistent		10.00	0.400	30			0	n/a	
32b	yes	consistent		9.70			0.364	33	1	8	
33a	yes	consistent		9.20			0.400	30	1	18	
33b	yes	consistent		9.40	0.353	34			2		
34a	yes	consistent		9.80			0.167	72	1	14	
34b	yes	consistent		10.50	0.162	74			2		
35a	yes	consistent		9.70			0.343	35	1	18	
35b	yes	consistent		9.40	0.324	37			2		
36	no	consistent	22	4.01			0.333	36	1	48	
37	no	consistent	24	4.01			0.333	36	1	48	
38a	no	consistent	44	4.01	0.245	49			0	n/a	
38b	no	consistent	variable	4.01			0.143	84	1	89	
39a	no	consistent		11.00	0.129	93			0	n/a	
39b	no	consistent		10.00			0.077	156	1	24	
40a	no	consistent		10.50	0.231	52			0	n/a	
40b	no	consistent		9.30			0.250	48	1	12	
41a	yes	consistent		8.90	0.136	88			0	n/a	
41b	yes	consistent		8.80			0.125	96	1	97	
41c	yes	consistent		9.00	0.167	72			2	n/a	
42a	yes	consistent		10.60	0.050	240			0	n/a	
42b	yes	consistent		9.60			0.042	289	1	65	
43	yes	consistent		10.50	0.053	228			0	n/a	
44a	yes	consistent		10.10	0.156	77			0	n/a	
44b	yes	consistent		9.50			0.143	84	1	19	
44c	yes	consistent		10.00	0.067	180			2	n/a	
45a	yes	consistent		10.40	0.041	290			0	n/a	
45b	yes	consistent		9.40			0.040	300	1	45	
46	no	consistent		8.38	0.214	56			0	n/a	
47	no	consistent		9.10			0.111	108	1	?	
48	no	consistent		8.80			0.250	48	1	?	
49	no	consistent		9.40			0.063	192	1	?	
50	no	consistent		9.00	0.194	62			0	n/a	
51	no	consistent		8.85	0.261	46			0	n/a	
52	no	consistent		9.44	0.250	48			0	n/a	
53	no	consistent		9.05	0.174	69			0	n/a	
54a	no	consistent		8.92			0.033	360	1	?	
54b	no	consistent		8.85	0.033	360			2	n/a	
55a	no	consistent		9.10	0.211	57			0	n/a	
55b	no	consistent							1	67	
56a	no	consistent		9.10	0.203	59			0	n/a	
56b	no	consistent							1	47	
57	no	consistent		9.80	0.128	94			0	n/a	
58a	no	consistent		10.1	0.150	80			0	n/a	
58b	no	consistent		9.80			0.188	64	1	64	
59a	no	consistent		7.02	0.286	42			0	n/a	
59b	no	consistent					0.286	42	1	42	
60a	no	consistent		7.37	0.353	34			0	n/a	
60b	no	consistent					0.333	36	1	36	
61	no	consistent		10.19	0.128	94			0	n/a	
62	no	consistent		9.14	0.300	40			0	n/a	
63	no	consistent		3.0	0.121	99			0	n/a	
64	no	consistent		5.0	0.400	30			0	n/a	
65	no	consistent		5.0	0.200	60			0	n/a	

APPENDIX A

AXIAL CAPACITY ESTIMATION BY PDA

Database ID Number	CASE METHOD				CAPWAP RESULTS														Penetrometer Diameter, Hammer Weight, Fall Height	Notes			
	EMX (avg max)	CSX (avg max)	RMX (max)	Damping Factor	Avg Energy Transfer	Energy Transfer Ratio	Evidence of Pile Damage based on PDA Data	Computed Soil Resistance (EOD/EOD2)			Computed Soil Resistance (BOR)			Recommended Soil Resistance based on BOR Data and Rt Considerations			Toe Quake	Shaft Quake			Equivalent Unit Toe Resistance	ADOT Penetrometer Average over 4B above and below Pile Tip	ADOT Penetrometer Average over 2B below Pile Tip
								Total	Shaft	Toe	Total	Shaft	Toe	Total	Shaft	Toe							
	kip-ft	ksi	kips		kip-ft		kips	kips	kips	kips	kips	kips	kips	kips	kips	kips	kips	inch			inch	kips/ft^2	blows/ft
1	7.4	8			n/a	0.27	no	30	10	20							1.20	0.10	22.6	no data	no data	n/a	
2	15.0	14			n/a	0.25	no	26	15	11							0.60	0.10	6.2	no data	no data	n/a	
3	16.0	27	366	RX6	16	0.27	no	250	110	140							0.30	0.10	157.9	no data	no data	n/a	
4	41.0	23	1190	RX7	39	0.36	no	1320	1020	300							0.10	0.10	31.2	no data	no data	n/a	
5a	37.0	24	1240	RX7	39	0.33	no	1230	810	420							0.10	0.10	43.7	>600	>600	2.5/340 lb/30 in	
5b	38.0	23	1290	RX7	39	0.34	no				1600	1380	220	1800	1380	420	0.12	0.10	43.7	>600	>600	2.5/340 lb/30 in	
6	39.0	23	1340	RX7	39	0.35	no				1210	880	330	1210	880	330	0.12	0.10	34.3	>600	>600	2.5/340 lb/30 in	
7a	45.0	21.4	1020	RX6	46.1	0.42	no	1260	860	400							0.19	0.10	56.6	= 350	= 500	2.5/340 lb/30 in	
7b	42.0	21.1	940	RX6	39.6	0.39	no				1040	840	200	1225	840	385	0.18	0.10	54.5	= 350	= 500	2.5/340 lb/30 in	
7c	45.0	21.8	1030	RX6	48.9	0.42	no	1220	850	370							0.21	0.10	52.3	= 350	= 500	2.5/340 lb/30 in	
8a	22.7	22	430	RX5	22.9	0.32	no	450	270	180							0.22	0.10	101.9	= 75	= 65	2.5 in/??	
8b	29.0	29	670	RX5	33.0	0.41	no				630	450	180	630	450	180	0.20	0.10	101.9	= 75	= 65	2.5 in/??	
9	66.0	23	1800	RX8	66.0	0.75	no				1530	750	780	1530	750	780	0.12	0.10	158.9	>600	>600	64mm/155kg/0.76m	
10a	64.0	22	1000	RX8	64.0	0.73	no	700	165	535							0.32	0.11	109.0	>600	>600	64mm/155kg/0.76m	
10b	63.0	23	1050	RX8	63.0	0.72	no	920	430	490							0.40	0.10	99.8	>600	>600	64mm/155kg/0.76m	
11	65.0	21	1220	RX8	65.0	0.74	no	1400	300	1100							0.30	0.10	224.1	>600	>600	64mm/155kg/0.76m	
12	69.0	23	1160	RX7	69.0	0.45	no	1750	1630	120							0.16	0.10	9.5	= 200	= 220	64mm/155kg/0.76m	
13	62.0	22	730	RX7	62.0	0.41	no	790	410	380							0.23	0.10	30.2	= 65	= 70	64mm/155kg/0.76m	
14a	45.0	19	820	RX7	45.0	0.30	no													= 65	= 70	64mm/155kg/0.76m	
14b	67.0	22	1040	RX7	67.0	0.44	no	1510	1410	100							0.20	0.10	8.0	= 110	= 120	64mm/155kg/0.76m	
14c	71.0	23	1070	RX7	71.0	0.47	no				1670	1480	190	1670	1480	190	0.19	0.10	15.1	= 110	= 120	64mm/155kg/0.76m	
15a	58.0	21	890	RX7	58.0	0.38	no													= 80	= 80	64mm/155kg/0.76m	
15b	66.0	23	1140	RX7	66.0	0.43	no	1150	1000	150							0.20	0.10	11.9	= 105	= 110	64mm/155kg/0.76m	
15c	68.0	25	1370	RX7	68.0	0.45	no				1720	1520	200	1720	1520	200	0.17	0.10	15.9	= 105	= 110	64mm/155kg/0.76m	
16a	69.0	29.7	1753	RX6	69.0	0.45	no				1860	1560	300	2075	1560	515	0.12	0.10	72.9	no data	no data	64mm/155kg/0.76m cobbles/boulders (high end bearing)	
16b	67.0	30.4	1722	RX6	67.0	0.44	no	1930	1415	515							0.10	0.10	72.9	no data	no data	64mm/155kg/0.76m cobbles/boulders (high end bearing)	
17a	64.0	27.7	1274	RX6	64.0	0.42	no	1110	960	150							0.24	0.10	21.2	no data	no data	64mm/155kg/0.76m cobbles/boulders (high end bearing)	
17b			1679	RX6			no				1550	1320	230	1550	1320	230	0.24	0.10	32.5	no data	no data	64mm/155kg/0.76m cobbles/boulders (high end bearing)	
18	38.0	22.7	960	RX6	38.0	0.35	no	950	700	250							0.24	0.10	50.9	> 600	> 600	2.5/340 lb/30 in	
19a	51.0	26.1	1382	RX6	51.0	0.46	no	1220	910	310							0.12	0.10	63.2	> 600	> 600	2.5/340 lb/30 in	
19b	51.9		976	RX6	51.9	0.47	no				1210	1060	150	1370	1060	310	0.116	0.10	63.2	> 600	> 600	2.5/340 lb/30 in	
20a	37.7	24.5	760	RX8	37.7	0.41	no	750	580	170							0.33	0.10	54.1	= 105	= 110	64mm/155kg/0.76m	
20b	29.0	23	787	RX6	29.0	0.32	no				760	610	150	780	610	170	0.14	0.10	54.1	= 105	= 110	64mm/155kg/0.76m	
21a	39.0	25	799	RX6	39.0	0.43	no	620	330	290							0.33	0.10	92.3	= 160	= 200	64mm/155kg/0.76m	
21b	34.0	28	857	RX6	34.0	0.37	no				720	650	70	940	650	290	0.30	0.10	92.3	= 160	= 200	64mm/155kg/0.76m	
22	62.0	32	1230	RX8	62.0	0.53	no				1060	220	840	1060	220	840	0.28	0.10	267.4	>600	>600	2.5/340 lb/30 in	
23	64.0	32	1140	RX8	64.0	0.55	no				1040	260	780	1040	260	780	0.23	0.10	248.3	>600	>600	2.5/340 lb/30 in	
24a	67.0	23	1210	RX4	67.0	0.51	no	1250	1100	150							0.30	0.10	21.2	>600	>600	2.5/340 lb/30 in assumed N (no data - high skin friction)	
24b	60.0	22	1110	RX4	60.0	0.45	no				1240	1090	150	1240	1090	150	0.12	0.10	21.2	>600	>600	2.5/340 lb/30 in assumed N (no data - high skin friction)	
24c	69.0	23.5	1240	RX4	69.0	0.52	no	1280	1135	145							0.22	0.10	20.5	>600	>600	2.5/340 lb/30 in assumed N (no data - high skin friction)	
25a	38.0	16.8	1140	RX4	38.0	0.29	no	1440	1240	200							0.12	0.10	15.9	>600	>600	2.5/340 lb/30 in assumed N (no data - high skin friction)	
25b	42.0	17.9	1030	RX4	42.0	0.32	no	1410	1340	70							0.15	0.10	5.6	>600	>600	2.5/340 lb/30 in assumed N (no data - high skin friction)	
25c	49.0	18.2	1400	RX4	49.0	0.37	no	1450	1300	150							0.20	0.10	11.9	>600	>600	2.5/340 lb/30 in assumed N (no data - high skin friction)	
26	82	22.6	1592	RX6	82	0.33	no	1550	1350	200							0.25	0.10	15.9	= 120	= 150	2.5/340 lb/30 in	
27	97	24.8	1450	RX6	97	0.39	no													= 120	= 110	2.5/340 lb/30 in	
28	89	23.6	1357	RX6	89	0.36	no	1370	1060	310							0.27	0.10	24.7	= 75	= 70	2.5/340 lb/30 in	
29a	43	21	1220	RX7	43	0.38	no	1280	880	400							0.05	0.10	81.5	>600	>600	64mm/155kg/0.76m	
29b	47	24	1140	RX7	47	0.41	no				1310	950	360	1350	950	400	0.20	0.10	81.5	>600	>600	64mm/155kg/0.76m	
30a	77	28	1250	?	77	0.39	no	1249	949	300							0.19	0.10	23.9	= 135	= 160	2.5/340 lb/30 in	
30b	77-109	31	1700	?	93	0.47	no				1425	1125	300	1425	949	300	0.26	0.13	23.9	= 135	= 160	2.5/340 lb/30 in	
31a	60	22	1300	?	60	0.30	no	1210	860	350							0.15	0.09	27.9	= 120	= 130	2.5/340 lb/30 in	
31b	67	25	1350	?	67	0.34	no				1280	970	310	1320	970	350	0.15	0.09	27.9	= 120	= 130	2.5/340 lb/30 in	
32a	67	24	1050	?	67	0.34	no	930	740	190							0.24	0.16	15.1	= 70	= 70	2.5/340 lb/30 in	
32b	65	25	1080	?	65	0.33	no				1080	890	190	1080	890	190	0.20	0.15	15.1	= 70	= 70	2.5/340 lb/30 in	
33a	58	23	900	?	58	0.29	no				960	884	76	1034	884	150	0.11	0.05	11.9	= 100	= 110	2.5/340 lb/30 in	
33b	62	23	930	?	62	0.31	no	990	840	150							0.20	0.05	11.9	= 130	= 140	2.5/340 lb/30 in	
34a	56	19	1450	?	56	0.28	no				1425	1120	305	1425	1120	305	0.16	0.07	24.3	= 400	> 400	2.5/340 lb/30 in	
34b	60	21	1550	?	60	0.30	no	1509	1308	202							0.14	0.07	16.1	= 400	> 400	2.5/340 lb/30 in	
35a	66	25	1100	?	66	0.34	no				1060	980	80	1111	980	131	0.12	0.07	10.4	= 220	= 235	2.5/340 lb/30 in	
35b	67	26	1110	?	67	0.34	no	1090	959	131							0.14	0.06	10.4	= 270	= 300	2.5/340 lb/30 in	
36	39	22	510	RX5	39	0.63	no				480	440	40	480	440	40	0.09	0.09	8.1	= 120		2.5in/340lb/30in	
37	50	26	590	RX5	50	0.81	no				550	470	80	550	470	80	0.13	0.07	16.3	= 120		2.5in/340lb/30in	
38a	30	12	460	RX3	30	0.48	no	450	425	25							0.10	0.06	2.0	no data	no data	n/a	
38b	41	18	800	RX5	41	0.66	no				720	650	70	720	650	70	0.09	0.07	5.6	no data	no data	n/a	
39a	52	25.3	950	RX5	52	0.46	no	1200	800</														

APPENDIX A

**AXIAL CAPACITY BY VARIOUS DYNAMIC FORMULAE**

Database ID Number	GATES EQUATION		JANBU EQUATION				ENR/NAVFAC DM 7.2 EQUATION					WSDOT Equation		
	Stroke	Ru	(WHL)/(Aes*2)	Wp/Wr	Ku (from chart)	Qu	(Wp+Wh)/Wr	Set	Qall	FS	Qu	Feff Constant	Rn	(Rn) * (Set-Up Factor) for EOD Data
	ft	kips				kips			in/blow	kips	2.25	kips		kips
1	n/a		#VALUE!	0.837	n/a		0.837	1.71	#VALUE!	2.25		0.41	#VALUE!	
2	n/a		#VALUE!	0.738	n/a		0.738	1.00	#VALUE!	2.25		0.41	#VALUE!	
3	6.16	391.45	3.62	0.308	2.6	625.849	0.308	0.30	203.401	2.25	457.652	0.41	386.004	501.80
4	8.75	907.84	83.71	3.504	11.7	1192.78	3.504	0.08	414.363	2.25	932.317	0.41	1166.44	1516.37
5a	8.75	922.96	96.90	3.504	12.5	1201.24	3.504	0.07	419.64	2.25	944.191	0.41	1183.93	1539.11
5b	8.48	955.98	155.93	3.602	15.0	1233.21	3.602	0.06	411.973	2.25	926.94	0.41	1203.42	1203.42
6	9.07	1029.59	222.86	3.373	18.0	1313.19	3.373	0.05	477.442	2.25	1074.25	0.41	1331.48	1331.48
7a	8.70	850.28	85.46	4.477	12.9	824.207	4.477	0.10	321.345	2.25	723.03	0.41	1096.97	1426.07
7b	7.86	731.96	37.22	4.477	8.9	749.572	4.477	0.14	268.956	2.25	605.15	0.41	913.035	913.03
7c	8.14	923.40	227.34	4.477	20.5	818.364	4.477	0.06	324.703	2.25	730.58	0.41	1142.89	1485.76
8a	7.67	392.53	4.21	2.619	3.5	405.098	2.801	0.43	142.904	2.25	321.53	0.41	431.611	561.09
8b	9.00	524.73	14.51	2.619	5.6	509.143	2.801	0.25	224.1	2.25	504.22	0.41	592.937	592.94
9	4.00	1038.15	257.80	1.212	15.5	1703.23	1.212	0.04	1091.9	2.25	2456.77	0.7	2244.81	2244.81
10a	4.00	508.74	1.06	0.845	1.9	1065.26	0.845	0.52	283.077	2.25	636.92	0.7	1200.64	1560.83
10b	4.00	583.16	3.19	1.240	3.0	968	1.240	0.36	360.921	2.25	812.07	0.7	1347.42	1751.64
11	4.00	807.53	19.19	0.845	5.2	1658.46	0.845	0.12	791.193	2.25	1780.18	0.7	1789.94	2326.92
12	10.69	1099.65	73.85	6.584	13.5	1189.69	6.584	0.11	380.484	2.25	856.09	0.41	1785.11	2320.64
13	9.27	790.40	6.81	4.377	4.9	1136.49	4.377	0.27	356.304	2.25	801.68	0.41	1233.58	1603.65
14a	8.66	838.64	12.23	4.377	5.9	1222.37	4.377	0.20	372.716	2.25	838.61	0.41	1256.86	1633.92
14b	10.39	1038.89	50.75	6.510	11.6	1138.01	6.510	0.13	363.931	2.25	818.84	0.41	1670.96	2172.24
14c	9.99	1025.10	52.01	6.510	11.7	1120.24	6.510	0.13	351.864	2.25	791.69	0.41	1618.93	1618.93
15a	9.27	826.90	9.15	4.377	5.3	1217.88	4.377	0.24	376.122	2.25	846.27	0.41	1284.14	1669.38
15b	9.62	1051.47	73.51	6.547	13.5	1129.15	6.547	0.10	346.653	2.25	779.97	0.41	1625.52	2113.17
15c	9.99	1019.70	50.15	6.547	11.5	1115.98	6.547	0.13	349.014	2.25	785.28	0.41	1611.16	1611.16
16a	10.16	1362.63	457.89	1.703	off chart		1.703	0.04	1350.87	2.25	3039.45	0.41	2122.13	2122.13
16b	10.11	1064.12	46.53	1.703	7.8	1929.1	1.703	0.11	984.57	2.25	2215.28	0.41	1684.35	2189.66
17a	10.81	985.80	20.53	1.703	5.6	1846	1.703	0.17	864.244	2.25	1944.55	0.41	1624.93	2112.41
17b														
18	9.02	810.31	38.60	2.322	7.8	1074.95	2.322	0.13	502.648	2.25	1130.96	0.41	1070.19	1391.24
19a	9.17	1048.30	417.37	2.786	off chart		2.786	0.04	574.339	2.25	1292.26	0.41	1360.7	1768.91
19b														
20a	11.13	848.72	94.59	1.272	10.5	1004.55	1.272	0.10	773.751	2.25	1740.94	0.41	1095.35	1423.95
20b	8.20	683.98	49.38	1.272	7.8	838.818	1.272	0.12	526.643	2.25	1184.95	0.41	777.046	777.05
21a	10.69		1.240	n/a			1.240	n/a		2.25				
21b	8.10	755.60	113.47	1.240	11.2	891.289	1.240	0.08	636.899	2.25	1433.02	0.41	842.847	842.85
22	8.88	877.39	111.79	1.199	11.2	942.205	1.199	0.11	845.935	2.25	1903.35	0.41	1189.77	1189.77
23	8.88	877.39	111.79	1.199	11.2	942.205	1.199	0.11	845.935	2.25	1903.35	0.41	1189.77	1189.77
24a	9.12	873.49	14.34	2.968	5.75	1260.81	3.655	0.23	462.185	2.25	1039.92	0.41	1402.09	1822.72
24b	8.30	850.85	15.63	2.968	6.0	1203.5	3.655	0.21	435.016	2.25	978.79	0.41	1306.53	1306.53
24c	9.12	901.05	17.77	2.968	6.1	1323.02	3.655	0.20	480.892	2.25	1082.01	0.41	1441.79	1874.33
25a	7.14	947.09	28.45	2.646	6.9	1862.09	3.333	0.10	494.227	2.25	1112.01	0.41	1334.27	1734.55
25b	7.14	914.55	26.77	3.316	7.3	1525.38	4.003	0.12	415.275	2.25	934.37	0.41	1292.8	1680.65
25c	8.79	1173.94	148.60	4.622	16.2	1522.09	5.309	0.06	443.168	2.25	997.13	0.41	1801.48	2341.92
26	9.84	1165.93	21.88	2.736	6.3	2065.46	2.736	0.20	915.931	2.25	2060.84	0.41	2295.81	2984.55
27	9.64	1088.13	14.30	2.736	5.5	1892.88	2.736	0.24	819.608	2.25	1844.12	0.41	2132.71	2772.52
28	9.44	1088.42	16.68	3.009	6.0	1768.49	3.009	0.24	776.032	2.25	1746.07	0.41	2110.99	2744.28
29a	10.11	1014.56	197.29	4.800	19.0	970.798	5.688	0.07	322.533	2.25	725.70	0.41	1389.41	1806.23
29b	9.80	997.56	191.32	4.800	18.6	961.665	5.688	0.07	312.773	2.25	703.74	0.41	1347.36	1347.36
30a	10.00	962.96	12.99	2.752	5.3	1527.55	3.264	0.26	599.426	2.25	1348.71	0.41	1736.58	2257.56
30b	11.20	1044.42	16.51	2.752	5.8	1665.32	3.264	0.24	690.127	2.25	1552.79	0.41	1978.67	1978.67
31a	10.70	1089.54	24.51	4.139	7.8	1496.9	4.651	0.19	571.859	2.25	1286.68	0.41	2010.25	2613.33
31b	11.50	1122.96	24.67	4.139	7.8	1556.92	4.651	0.20	608.653	2.25	1369.47	0.41	2142.59	2142.59
32a	10.00	838.35	5.53	2.752	3.9	1353.85	3.264	0.40	484.609	2.25	1090.37	0.41	1533.01	1992.91
32b	9.70	851.53	6.49	2.752	4.1	1374.09	3.264	0.36	494.844	2.25	1113.40	0.41	1531.05	1531.05
33a	9.20	800.03	5.08	2.752	3.8	1278.32	3.264	0.40	445.84	2.25	1003.14	0.41	1410.37	1410.37
33b	9.40	845.14	6.67	2.752	4.2	1339.28	3.264	0.35	487.09	2.25	1095.95	0.41	1497.06	1946.18
34a	9.80	1081.57	30.28	4.139	8.0	1552.32	4.651	0.17	546.045	2.25	1228.60	0.41	1910.96	1910.96
34b	10.50	1131.22	34.27	4.139	8.6	1590.14	4.651	0.16	589.25	2.25	1325.81	0.41	2061.16	2679.50
35a	9.70	868.43	7.29	2.752	4.3	1389.58	3.264	0.34	510.209	2.25	1147.97	0.41	1558.23	1558.23
35b	9.40	869.04	7.90	2.752	4.5	1360.28	3.264	0.32	508.512	2.25	1144.15	0.41	1534.92	1995.39
36	4.01	487.31	4.74	1.262	3.2	694.733	1.262	0.33	268.786	2.25	604.77	0.7	970.373	970.37
37	4.01	487.31	4.69	1.249	3.2	694.733	1.249	0.33	269.533	2.25	606.45	0.7	970.373	970.37
38a	4.01	540.55	6.15	3.296	4.3	703.708	3.296	0.24	214.972	2.25	483.69	0.7	1058.33	1375.83
38b	4.01	633.62	18.08	3.296	6.4	810.521	3.296	0.14	261.398	2.25	588.15	0.7	1212.11	1212.11
39a	11.00	909.57	47.23	4.501	9.6	1080.54	4.501	0.13	385.196	2.25	866.69	0.41	1313.03	1706.94
39b	10.00	977.04	120.82	4.501	14.6	1083.45	4.501	0.08	384.802	2.25	865.81	0.41	1335.59	1335.59
40a	10.50	754.55	9.35	6.887	7.3	758.416	6.887	0.23	231.579	2.25	521.05	0.41	1085.86	1411.61
40b	9.30	687.15	7.05	6.887	6.3	718.491	6.887	0.25	200.911	2.25	452.05	0.41	941.333	941.33
41a	8.90	796.57	28.73	8.721	10.2	778.593	8.721	0.14	178.981	2.25	402.71	0.41	1048.87	1363.53
41b	8.80	809.58	33.80	8.721	10.9	785.897	8.721	0.13	178.987	2.25	402.72	0.41	1058.09	1058.09
41c	9.00	759.47	19.45	8.721	8.8	746.673	8.721	0.17	175.712	2.25	395.35	0.41	1011.1	1314.43
42a	10.60	1107.02	349.25	5.186	25.5	1011.61	5.186	0.05	378.069	2.25	850.66	0.41	1541.02	2003.33
42b	9.60	1088.95	458.64	5.186	25.5	1103.23	5.186	0.04	347.585	2.25	782.07	0.41	1444.58	1444.58
43	10.50	1089.68	312.22	5.186	24.5	990.823	5.186	0.05	372.777	2.25	838.75	0.41	1511.71	1965.22
44a	10.10	825.41	28.87	4.371	7.6	1037.62	4.371	0.16	345.469	2.25	777.30	0.41	1153.28	1499.27
44b	9.50	816.26	32.31	4.371	7.6	1064.7	4.371	0.14	332.223	2.25	747.50	0.41	1107.45	1107.45
44c	10.00	1008.71	156.19	4.371	15.7	1162.55	4.371	0.07	402.604	2.25	905.86	0.41	1374.86	1787.32
45a	10.40	1138.28	421.64	4.371	29.0	1054.56	4.371	0.04	440.838	2.25	991.89	0.41	1565.95	2035.74

## **APPENDIX B:**

PDA Database Revisions December 23, 2012

Dynamic Pile Testing Database

[http://www.dot.state.ak.us/stwddes/research/assets/pdf/PDA\\_DB\\_121223.xlsx](http://www.dot.state.ak.us/stwddes/research/assets/pdf/PDA_DB_121223.xlsx)